Intrinsic Physiology and Experience-Dependent Plasticity of the Zebra Finch Caudal Mesopallium

Andrew N Chen

Bethesda, Maryland

Bachelor of Arts, Neuroscience

Johns Hopkins University, 2013

A Dissertation presented to the Graduate Faculty of the University of Virginia

in the Candidacy for the Degree of Doctor of Philosophy

Neuroscience Graduate Program, Department of Psychology

University of Virginia

December 2018

Abstract

Auditory processing is a complex task that relies on a hierarchical relay of information from the periphery to central regions of the nervous system. Intrinsic physiological properties of neurons in the auditory system allow it process spectrotemporal information for behavioral purposes such as sound localization and perception. Songbirds and humans hold parallels in the manner in which they use their auditory system for vocal communication. They both require early song and speech experience taught by a tutor to properly learn to sing or speak. Changes in the brain occur during these early life critical periods, which ultimately develop the neural circuitry for perceiving natural communication signals. In songbirds, the caudal mesopallium (CM) is a key auditory area in the learning and processing of conspecific vocalizations. In chapter 2, I investigate the intrinsic properties of neurons in CM to understand what physiological and morphological correlates give rise to its auditory processing capabilities. We found that neurons in CM have a diversity of firing patterns that are associated with various physiological and morphological correlates. Phasic-spiking neurons fire one or few action potentials to depolarizing stimuli, whereas tonic-spiking neurons fire sustained trains of action potentials. Phasic-spiking activity is regulated by a low-threshold, outward rectifying current. Phasic-spiking neurons are tuned to better follow rapid temporal modulations

present in birdsong, whereas tonic-spiking neurons better entrain low frequency modulations, suggesting that intrinsic properties of CM neurons are specialized for processing specific auditory information. In chapter 3, I detail the experience-dependent transient emergence of phasic excitability during the song memorization phase of the sensory acquisition period of song learning. Depriving birds of normal colony-rearing experiences resulted in an abolishment of phasic responses during the age in which phasic excitability normally emerges in colony-reared birds. Phasic excitability was not able to be induced in birds that had been initially deprived of auditory experience, and passive membrane properties were altered even before phasic excitability normally emerges. The work presented in this dissertation lays the foundational groundwork for understanding the intrinsic neural correlates and plasticity of auditory perception in the songbird auditory system.

Acknowledgements

Thanks to Dan Meliza for being my mentor over these many years, it was an honor to be part of your growing lab. Thank you to Dave Hill, Alev Erisir, Mark Beenhakker, and Ali Güler for being an incredibly supportive committee, and Peter Brunjes for being my co-mentor. I cannot think of a better group of people with which to have shared my work.

Thanks to my mom, dad, and sister for dealing with my insanity. My stubbornness in perseverance is a quality that only this family could have imprinted on me.

Thanks to Trinity and Vega for being the best dogs.

Table Of Contents

Chapter 1: Introduction

The auditory system is essential for human behavior, mediating the ability to quickly locate sounds and for vocal communication. Arguably one of the most distinguishing traits of humans, learning to speak and understand spoken language is a vital component of social behavior. This trait is shared with songbirds, in which auditory processing is important for decoding information to recognize birdsong from other vocalizations and sounds. Auditory processing transforms sound waves from the environment into neural activity, propagating from the periphery into cortical brain regions. Information becomes more refined and complex as distinct regions along the auditory pathway process auditory signals, starting from sound localization in the hindbrain to recognizing distinct features essential for intraspecies communication. Distinct intrinsic properties of neurons in auditory regions influence the capability for the auditory system to process increasingly complex information. In both humans and songbirds, early experience with speech and song are paramount in developing these vocal communication skills. Experience helps shape the neural circuitry and cell-intrinsic dynamics in the auditory system to acquire vocal production and perception. However, many questions still remain about understanding how the intrinsic properties of individual cells and activity-dependent plasticity contribute to auditory processing

Auditory processing is a challenging task that requires the transformation of external stimuli into relevant information. Experience-dependent changes in cell-intrinsic mechanisms allow the brain to process and perceive specific aspects of auditory signals that are particularly salient for behavior. This chapter will provide a brief review on the songbird auditory system, explore how early experience shapes auditory perception, and review the contributions of intrinsic cell dynamics to auditory processing in subcortical and cortical levels. In Chapter 2, I investigate the intrinsic cellular dynamics of CM to understand how they contribute to the function of this key step in the auditory processing pathway. In Chapter 3, these findings led me to explore the experience-dependent intrinsic plasticity that gives rise to these cellular dynamics through interaction with acoustic and social qualities of the environment. The findings presented in this dissertation provide further insight into how early experience shapes the intrinsic physiology of neurons for auditory perception.

Songbirds as a Model Organism

Songbirds are a strong model organism for investigating auditory processing. In most songbird species including the widely used zebra finch, males will sing as a way to convey fitness, attract mates and mark territory (Doupe and Kuhl, 1999; Woolley, 2012). The function and spectrotemporal acoustics of

their songs are well-defined, but perhaps the most interesting aspect of songbirds is that they learn their songs in a manner very similar to how humans learn how to speak. This presents an intriguing basis of investigating auditory processing with potential translational relevance to humans.

The process of birdsong learning shares many parallels with human speech learning. There are two phases of learning: sensory and sensorimotor. First, in the sensory phase after birth, birds are exposed to the song of a male tutor's song. This forms a representation of the tutor song which will be used as a template for song learning in the future. When the bird reaches a juvenile state and is capable of producing vocalizations, they enter the sensorimotor phase where they attempt to recreate the tutor song on their own. During this process, the bird relies heavily on hearing the bird's-own song (BOS) to receive auditory feedback and compare it to the tutor song. This corrective and rehearsal process will last until adulthood where the song then becomes crystallized (Brainard and Doupe, 2002).

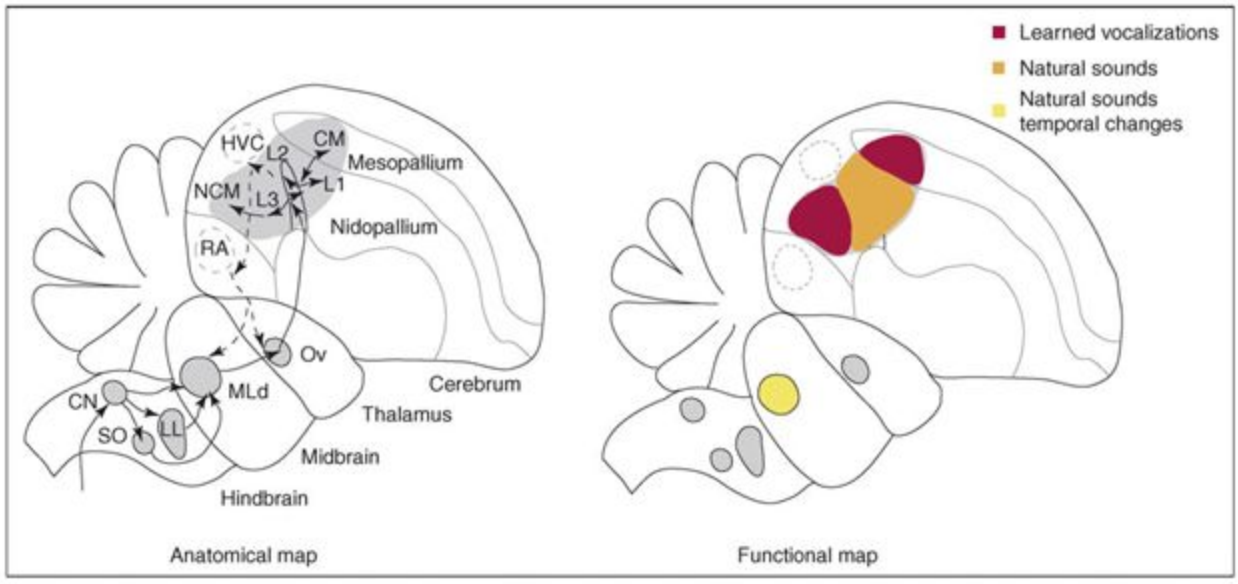

Figure 1 (adapted from Theunissen and Shaevitz, 2006). Sagittal illustration of the avian brain with auditory processing pathways highlighted. Feedforward projections are solid arrows, feedback projections are dashed arrows. CN, cochlear nucleus; SO, superior olive; LL, lateral lemniscus; MLd, dorsal lateral nucleus of the mesencephalon; Ov, ovoidalis; L1, L2, L3, Fields L1, L2, L3; CM, caudal mesopallium; NCM, nidopallium caudomedial; HVC (name proper); RA, robust nucleus of arcopallium.

Songbird Auditory Processing

Auditory processing goes through many stages along the ascending auditory pathway. Each of these stages builds on the previous to transform sound waves into neural activity containing salient information. The intrinsic dynamics of the neurons in these regions allow them to uniquely handle

auditory information with increasing complexity, and are shaped through experience. This section will provide a review of key areas in the songbird auditory pathway of the midbrain and cortical regions, and their respective functional properties. The auditory processing pathway begins in the periphery at the hair cells in the cochlea. Hair cell stereocilia are deflected back and forth in response to basilar membrane oscillations from incoming sound waves, opening mechanotransduction channels and creating depolarizations which then create action potentials that travel through the auditory nerve. In the cochlea, there is a tonotopic organization of frequency representations; high frequency sounds activate the base of the cochlea and low frequency sounds activate the apex of the cochlea. From here, signals are sent to the brainstem auditory nuclei such as the superior olive and cochlear nucleus. Decussation of fiber tracts also occurs at this level, creating a bilateral representation of sounds and allowing for sound localization (Kolb and Whishaw, 2005). Neurons in these areas then project to the auditory midbrain nucleus: the inferior colliculus (IC) in mammals, or the dorsal lateral nucleus of the mesencephalon in songbirds (MLd). Neurons in the midbrain send projections to the medial geniculate nucleus/body (MGN/MGB), the auditory thalamic nucleus, which is ovoidalas (Ov) in songbirds. Downstream of the thalamus is the primary auditory cortex (A1), where the perception of the auditory information can lead to relevant behavior. The equivalent

primary auditory cortical region in songbirds is made of Field L (Figure 1; Theunissen and Shaevitz, 2006).

Midbrain: MLd is the avian homologous correlate (Karten, 1967) of the inferior colliculus. Being fairly early within the auditory processing circuitry, MLd responds to a large variety of sounds such as pure tones (Schneider and Woolley, 2011), noise (Schneider and Woolley, 2011), heterospecific song, and conspecific song (Schneider and Woolley, 2010). Nonetheless, the midbrain remains an important nexus for auditory processing because of the diverse inputs it receives from lower nuclei such as the GABAergic and glycinergic projections from the lateral lemnisci (Pollak et al., 2003). A hallmark of MLd neurons is their lack of adaptation to repeated stimuli. Presenting zebra finch MLd neurons with repeated songs shows reliable responses, meaning that their response remain fairly static through multiple presentations. MLd neurons display a variety of response patterns to pure tones, grouped into two major groups: onset and ongoing. Ongoing response patterns have sub-variations such as primary-like, sustained, and long lasting, with onset responding cells having higher CF thresholds than ongoing responding cells. CF tuning curves also were diverse in MLd, ranging from narrow to wide, and multipeak. Intensity rate-coding in MLd could be classified into monotonic, low-saturation, and nonmonotonic (Woolley and Casseday, 2004).

MLd neurons also display gain modulation by excitatory or inhibitory sidebands. These sidebands exist in the extra-classical receptive field (eCRF) outside of a neuron's classical receptive field (CRF), a range of frequencies and intensities of pure tones that elicit a spiking response. As the name implies, eCRFs are frequencies and intensities that are outside of the CRF. When tones in the eCRF are played in conjunction with tones in a neuron's CRF, two things may happen depending on whether the eCRF is excitatory or inhibitory; excitatory eCRFs increase the firing rates while inhibitory eCRFs decrease firing rates (Schneider and Woolley 2011), thereby potentially sharpening frequency tuning in MLd neurons. This mechanism has been explored by blocking GABAergic and glycinergic receptors in IC of bats (Klug et al., 2002) and mice (Mayko et al., 2012), which decreases selectivity for vocalizations in both species, and showed an broadening of MLd tuning curves in mice (Xie et al., 2005; Mayko et al., 2012).

STRFs can also be used to model MLd neuron tuning properties (Schneider and Woolley, 2011; Woolley et al. 2009). Four functional groups of MLd neurons were classified based on STRF clustering: wideband, broadband, two-band excitatory, and narrowband-temporal. STRFs within MLd also are stimulus-selective, responding differently to song than to modulation-limited noise with similar intensity and frequency ranges as a song. The population responses to song within MLd behave synchronously

with lower response latencies and precise encoding to the temporal structure compared to noise of a song (Woolley et al., 2006), suggesting a temporal coding of song within the midbrain.

Auditory Thalamus

In songbirds the auditory thalamic nucleus is Ov. It receives projections from MLd in the midbrain and sits upstream of Field L. STRFs in Ov show selectivity for three major auditory stimuli: narrow-band (NB), broadband (BB), and frequency sweeps (FS). Interestingly, STRFs for FS were not found in the midbrain nucleus MLd and also higher in proportion than in the downstream Field L, suggesting that Ov does not follow the conventional thalamic relay nexus archetype, but rather may act as an intermediate processor in hierarchical processing (Amin et al., 2010). As mentioned previously, some response latencies from Ov are longer than latencies from Field L, which suggests that Ov's processing capabilities are made possible not only from feedforward connections but also from feedback connections. The feedback connections may contribute to the complexity of Ov's STRFs.

Avian Auditory Cortex and Hierarchical Organization

From Ov, projections make their way to the avian primary auditory cortex. The anatomy of the avian brain does not suggest the canonical mammalian six-layered neocortex with columns of interconnected cell bodies and axons

between layers, but rather appears as a collection of distinct, interconnected nuclei (Fortune and Margoliash, 1992; Vates et al., 1996). The Avian Brain Nomenclature Consortium revised the nomenclature used for describing the avian brain in 2002 (Reiner et al., 2004), standardizing the terminology used to more accurately reflects analogies and homologies to mammalian cortex (Dugas-Ford et al., 2012). This revision came after a long history of evidence that disproved the view of the avian brain as a mainly basal ganglia structure. Recent evidence (Wang et al., 2010) has emerged that demonstrates that the avian auditory forebrain possesses similar columnar organization (Wang et al., 2010) and supports a hypothesis of a hierarchical organization of the avian auditory forebrain which may share similar processing strategies to the neocortex. Biotinylated dextran amine (BDA) injections into auditory forebrain areas revealed that L2, L1, L3, and CM have their cell bodies and axons organized into narrow columns (Wang et al., 2010).

Additionally, L2a seems to correspond to layer 4 of mammalian primary auditory cortex based on the presence of small stellate granule cells and parvalbumin immunoreactive neuropils, commons features of layer 4 neurons (Wang et al., 2010; Douglas and Martin, 2004). The intrinsic circuitry within the Field L/CM complex also displays familiarities with the canonical neocortical layered structure. The same BDA tracings as described above revealed reciprocal connections from CM and L1 back onto L2a, L3, and other

areas in the auditory forebrain. If we adopt the neocortical view of the avian forebrain, CM/L1 can thought to be the superficial layers of neocortex: L2 being layer 4, and L3 representing a portion of deep cortical layers 5 and 6 (Figure 2). Based on its circuitry, L1 draws comparisons to layer 3 of mammalian primary auditory cortex; both regions send projections down to the intermediate archistriatum (Aivm) and layers 5/6 in their respective anatomies (Wang et al., 2010; Douglas and Martin, 2004). CM also projects onto a secondary auditory area, the caudomedial nidopallium (NCM). Within the avian forebrain, the representative regions for deeper cortical layers (Aivm and dorsal neostriatum) do not seem to be organized in the same columnar fashion. However, contralateral projections from Aivm to the Field L/CM complex as well as the presence of layer 5/6 markers seem to support its comparison to layers 5 and 6 (Harris et al., 2013).

Further evidence for a hierarchical organization of the avian auditory forebrain is supported by extracellular recording studies conducted in European starlings. Meliza and Margoliash (2012) demonstrated a general increase in motif selectivity in downstream connections within the forebrain circuitry. L1 and L2 showed the lowest amounts of selectivity while NCM and L3 showed highest levels of selectivity. Intermediate areas such as CLM and CMM showed varying levels of selectivity that were on average, in between L1/L2 and NCM/L3. Response latencies also increase from midbrain to

thalamus to pallium (Amin et al., 2010); however, some neurons within Field L have shorter latencies than some neurons in Mld and Ov. This evidence suggests the possibility for feedback connections from pallium onto lower brain areas.

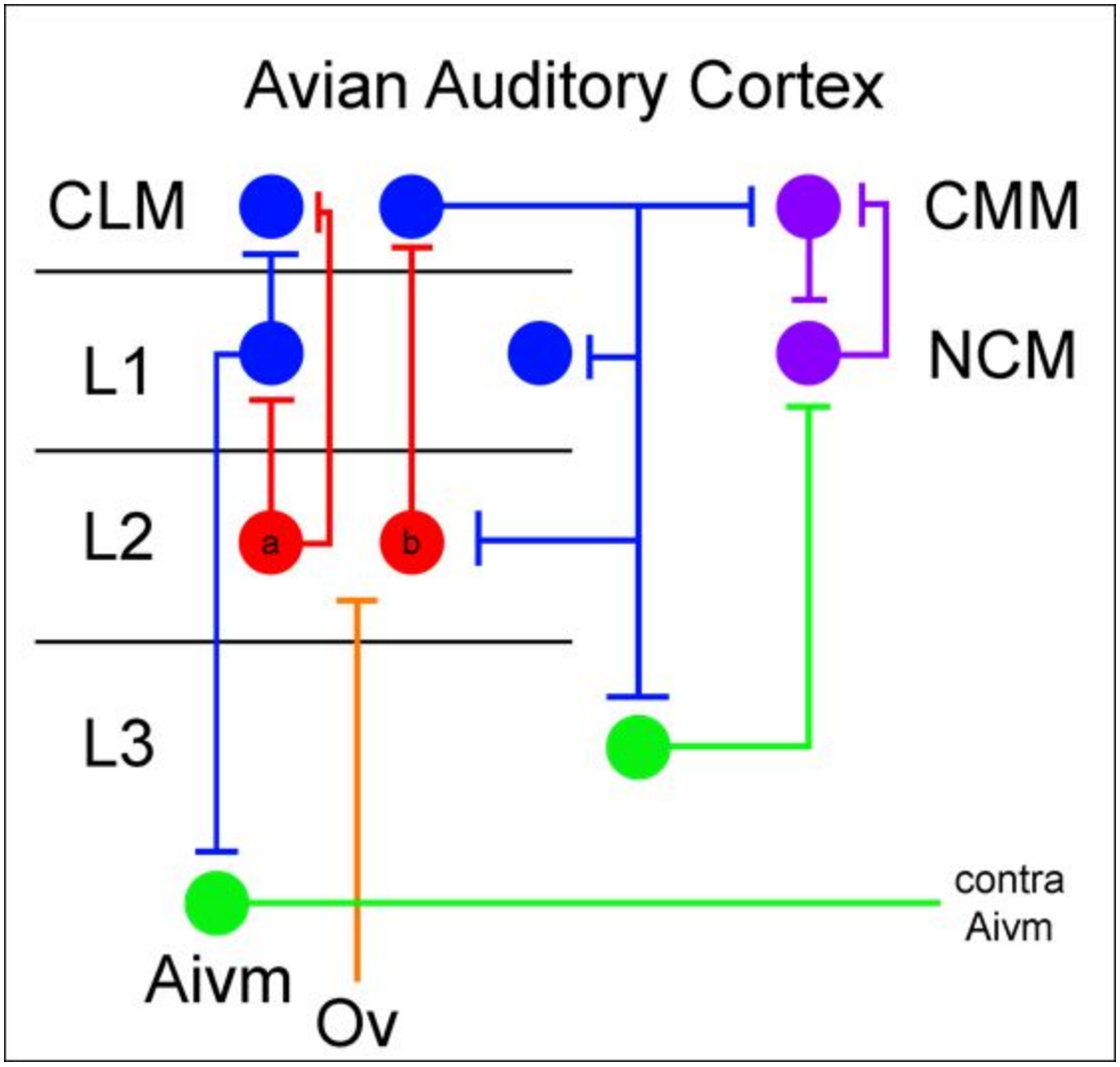

Figure 2. Schematic representation of avian auditory cortex connectivity. Thalamic input is highlighted in orange; intermediate layers in red;

superficial layers in blue; deep layers in green; secondary auditory areas in purple.

Field L

Field L is the downstream target of Ov (specifically L2, the thalamocortical region) (Karten, 1968; Wang et al., 2010) and is thought to be analogous to primary auditory cortex (Kim and Doupe 2011). Field L comprises 3 major areas: L1, L2, and L3 (Fortune and Margoliash, 1992). STRFs within Field L reflect the hierarchical organization of its subregions (Sen et al., 2001; Kim and Doupe, 2011). Various parameters of STRFs within Field L also reflect this organization, including delay between stimulus and response and sharpness of tuning. L2 is the primary thalamorecipient region, receiving projections from Ov. L1 primarily receives input from L2a, a sub-region of L2 (Vates et al., 1996). L2a STRFs indicate a sensitivity to more narrowband components of song (Sen et al., 2001). Interestingly another subregion of L2, L2b, displayed some more complex STRFs compared to L2a, even though both L2a and L2b receive inputs from Ov and considered to both be within early stages of auditory processing. As expected, areas that receive L2's projections and other higher order areas have increasingly complex STRFs that display sensitivity to broadband stimuli, frequency sweeps and have time-dependent frequency sensitivities.

Field L also displays topographic organization of STRFs in two separate axes (Kim and Doupe, 2011). STRFs in Field L change from spectrally narrowband to broadband sensitive in the mediolateral aspect, and temporally narrow to broad from L2 to L1/L3. The change in temporal band sensitivity from the L2 to L1/L3 provides further evidence for a hierarchical organization of these subregions, where more sensitivity to more spectrotemporally complex stimuli is present in higher order areas. And whereas the spectral band sensitivity in Field L as a whole changes from narrow to broad, STRFs in L2 are still comparatively narrower than STRFs in L1/L3, as indicated before by Sen and colleagues. (2001). Additionally, L2 neurons as a whole show narrow temporal tuning, with most of its variations in STRFs coming from changes in the spectral width dimension. L3 shows much more diversity in its STRF spatial organization, displaying broad sensitivity to temporal and spectral widths; L1 displays a mix of L2 and L3 clustering of STRFs (Kim and Doupe, 2011), again reinforcing the possibility for a sequential processing pattern in Field L that shares similarities with the neocortical processing circuitry.

Selective responses of Field L neurons to conspecific song is also modulated by early auditory exposure to vocalizations. A functional magnetic resonance imaging (fMRI) study investigated the effects of lack of adult song exposure in zebra finches by measuring blood oxygenation level differences (BOLD) (Maul et al., 2010). Isolated males displayed larger areas of activation to

sound presentations and also showed a lack of selectivity for conspecific song over tones compared to normal reared males. BOLD responses in isolated females interestingly were similar to adult song exposed males (but not raised within a social colony), potentially because female zebra finches do not sing.

Caudal Mesopallium

CM is an area of the avian auditory cortex (Fortune and Margoliash, 1992; Butler et al., 2011) that has seen more study in recent years. CM has two subdivisions known as caudolateral mesopallium (CLM) and caudomedial mesopallium (CMM), which can be delineated as two separate regions in the hierarchical processing circuit. CLM is thought to be a primary auditory area while CMM is proposed to be a secondary auditory area (Vates et al., 1996). There are not clear cytoarchitectonic distinctions between the two areas, and as such some studies will group these areas together. However in terms of connectivity, CLM is defined as receiving inputs from L2a whereas CMM does not. CMM receives major inputs from CLM and projects to NCM (Vates et al., 1996). Jeanne and colleagues (2011) showed through single-unit recordings that CMM neurons are more selective and encode more information about song components than CLM neurons. This suggests that CMM acts as a higher processing region than CLM, also supported by their respective connectivities (Vates et al., 1996; Wang et al., 2010).

Recent studies of CLM have suggested that it may be homologous to superficial layers of cortex, particularly layer 2 and 3 of neocortex (Wang et al., 2010). Similar to layers 2 and 3 of neocortex, there are extensive efferents of CM within itself (Vates et al., 1996; Avermann 2012). A gene expression study conducted by Atoji and colleagues (2014) investigated mRNA expression of cholecystokinin (CCK), a gene marker of mammalian neocortex layers 2 and 3. *In situ* hybridization of CCK mRNA in adult chicken brains found strong expression within the mesopallium. CLM in particular is a projection site of the auditory thalamorecipient region Field L2 and seems to be one of the first areas of the auditory forebrain involved in selectivity for invariant objects (Lu and Vicario, 2014).

The selective properties of CMM for conspecific song have also been studied. Higher order areas such as CMM and NCM are hard to characterize using STRFs (Sen et al., 2001; Sharpee et al., 2011). To measure selectivity in these areas, the distribution of neuronal responses is measured during presentation of a broad range of stimuli. Preference for forward played conspecific song over reverse played conspecific song was displayed by CMM as well as Field L neurons. This preference did not exist for forward played song versus songs where the order of syllables were reversed, suggesting that auditory forebrain neurons are tuned to respond to

conspecific song based on within syllable spectral-temporal modulations that are found within naturally occurring song (Theunissen et al. 2004; Janata and Margoliash, 1999; Amin et al., 2004). Extracellular recordings in CMM of European starlings revealed different neuronal populations within the area based on spike shape and selectivity. Responses of neurons were taken during presentations of starling song motifs. A large proportion of neurons showed a broad, shallow repolarization (wide-spiking) while a separate set showed a narrower depolarization phase and deeper, faster repolarizing phase similar to interneurons (narrow-spiking) (Meliza et al., 2010). Neuron selectivity was also quantified by taking into account the proportion of motifs a neuron would respond to. Narrow spiking neurons showed the least amount of selectivity and highest spontaneous firing rates, while broad spiking cells on average showed higher selectivity and lower spontaneous firing rates, opposite indicating that there may be a correlation between spike waveform and spontaneous firing rate. There also seemed to be a sub-populations within the wide-spiking neurons. A cluster of wide-spiking cells displayed a high selectivity index with low spontaneous firing rates while the remainder had lower selectivity and comparatively higher spontaneous firing rates. Properties of this lower selective broad-spiking population have yet to be investigated, but it is possible that they may represent a plastic population of cells that are naïve to song specific tuning.

CMM neurons also display preferences for familiar over unfamiliar stimuli. Gentner and Margoliash (2003) trained European starlings to discriminate between two songs in two-choice and go/no-go tasks. In the two-choice task, birds discriminated between two songs by pecking the correct port learned for each song. In the go/no-go task, birds learned to respond only to a specified song set (S+) amidst other unrewarded song sets (S-). CMM neurons displayed greater response magnitude to learned songs over unfamiliar songs; in addition, in the go/no-go paradigm, S+ songs elicited larger responses than S- songs. Meliza and Margoliash (2012) demonstrated as well that CMM neurons display selectivity for familiar motifs over unfamiliar motifs using similar behavioral paradigms. However, in another study by Gentner and colleagues (2004), *zenk* immediate early gene (IEG) expression in CMM was higher when European starlings learned to discriminate novel songs versus familiar songs during a 2-choice behavioral task. These biases highlight the potential for neuromodulatory and plasticity-based mechanisms within the auditory forebrain that can shape selectivity responses through learning. One such study demonstrated that CCK infusions into rat auditory cortex was able to potentiate synaptic strength during an audiovisual stimulus pairing, and that entorhinal-cortex-CCK-positive projections are one possibility for this neuromodulatory input (Li et al., 2014). Given that CCK mRNA has been found

within CM, it is possible that this mechanism may also be present in songbirds.

The Role of Early Auditory Experience on Perception

Song perception in songbirds is important for recognizing conspecifics, kin, and mates, and is shaped by early auditory experience. This experience is important for the memorization of songs early in life, and serves to guide the formation of the tutor template for vocal learning and influences neural coding of birdsong. In species in which females do not sing such as zebra finches, females also need to perceive song during mate selection or when identifying individuals (Hauber et al., 2010, Wooley, 2012).

On a broad scale, early auditory experience allows birds to form preferences for conspecific song over songs of other species (Braaten and Reynolds, 1999). There also seems to be an innate component to this behavioral preference, as birds raised in the presence of the songs of another species will still learn their conspecific song (Marler and Peters, 1977). In addition, zebra finches raised in the absence of conspecific song still show preferences to zebra finch song over starling and canary songs (Braaten and Reynolds, 1999). Conversely, when birds are cross-fostered with parents of another species results in no preference for conspecific song and higher attraction to the songs of the tutor species (Campbell and Hauber, 2009). Early song

exposure also shapes song perception for female zebra finches to form preferences for high-quality courtship songs (Chen et al., 2017). Females raised without exposure to song show no preference for normal song over abnormal, isolate song (Lauay et al., 2004). Closer investigations of the role of auditory experience on perception found that zebra finches raised without birdsong exposure have deficits in absolute pitch discrimination tasks. These perceptual deficits are exacerbated in zebra finches raised apart from all conspecifics after 35 days post-hatch, which show deficits in absolute and relative pitch discrimination, and in their ability to identify individual song notes (Sturdy et al., 2001).

The effects of early auditory experience on the auditory coding of vocalizations have also been studied on the level of neural circuits. Early experience influences information coding, which is the capacity of a neuronal response to encode information as a function of firing rates, change in firing rate over time, rate of change in firing rates, and response reliability, in the midbrain and Field L (Woolley, 2012). Cross-fostering juvenile zebra finches with Bengalese finches resulted in lower information coding for both conspecific and tutor-specific songs relative to normally raised zebra finches (Woolley et al., 2010). Furthermore, spike rates in L2a of normally raised zebra finches are higher overall for conspecific song over heterospecific songs, but this selectivity is not seen in birds cross-fostered with Bengalese

finches (Hauber et al., 2013). In starlings that have been reared without song exposure, Field L neurons show lower response selectivity, and an overall enlargement of song-selective regions, and that these functional changes are also a function of time in isolation (George et al., 2004). Similar experience-dependent effects have also been demonstrated in NCM and CMM. Neurons in NCM of starlings that have been raised in the absence of adult song also show deficits in response selectivity for song features than wild-caught starlings (George et al., 2010). In normally reared zebra finches, EGR1 levels after listening to high-quality courtship song is higher compared to levels after listening to non-courtship song, but this disparity is absent in birds that have not been developmentally exposed to birdsong. Interestingly, EGR1 responses in CMM were not affected by early song experience, and both normally reared and song-naive birds showed higher EGR1 levels for courtship song over non-courtship song. This has been speculated to be a result of NCM connections to other higher order areas involved in decision-making, whereas CMM does not (Chen et al., 2017).

Intrinsic Neuronal Physiology

The intrinsic physiology of individual neurons play a crucial role in information processing of sensory input. Onset-firing neurons in rat inferior colliculus are better able to encode high frequency stimuli compared to sustained firing neurons (Peruzzi et al., 2000). The precise firing of neurons

also encodes temporal information for sound localization. This temporal encoding allows animals such as barn owls to hunt mice using only auditory information (Konishi, 1973), and is the product of intrinsic morphological and physiological specializations. In chickens the cochlear nucleus magnocellularis (NM) is a region that encodes phase (Sullivan and Konishi, 1984), whose neurons are electrically compact due to their large cell bodies and short dendritic arbors (Carr et al., 2006). Physiologically, these neurons fire phasically with single to few action spikes at the onset of depolarizing stimuli. These phasically spiking neurons are functionally significant for their temporal precision which makes them effective at coincidence detection and phase locking (Svirskis et al., 2004; Huguet et al., 2017). In mammals and birds, this precise time-code needs to be interpreted in binaural processing regions, where coincidence detection in the hindbrain thereby encodes interaural time differences for sound localization, making it imperative for the time-code to be accurate for behaviors such as escaping threats or hunting prey.

It is also important to understand what gives cellular mechanisms rise to these physiologically distinct neurons. Pharmacological and modeling approaches have investigated what regulates spiking dynamics to give neurons their unique functional capabilities. Voltage-gated and calcium-dependent ion channels in the midbrain (Sivaramakrishnan and

Oliver, 2001) and hindbrain (Rothman and Manis, 2003, Iwasaki et al., 2008) are differentially expressed in these regions to shape intrinsic neuronal responses. Phase-locked time-coding neurons in mammalian cochlear nucleus derive their phase locking responses from a low-threshold K^+ conductance (LTC) and high-threshold K^+ conductance (HTC). The LTC is responsible for outward rectification and nonlinear current-voltage relationships at potentials near rest. Only large EPSPs produce spikes, and slower depolarizing events become shunted by the activation of outward rectification (Oertel, 1999). Manis and Marx demonstrated that blockade of LTC allows these neurons to fire multiple spikes, and are thought to be regulated by voltage-gated $K_V1.1$ and $K_V1.2$ potassium channels (1991). In MSO neurons, phasic responses are reliant on a low-threshold potassium current, and reducing the conductance of this current diminishes the neuron's sensitivity to coincidence (Svirskis et al., 2004). MNTB neurons with HTC display high frequency firing with fast spiking kinetics which leads to brief, quick action potentials that allows neurons to follow high-frequency stimuli. Abolishing this HTC via knockout of the $K_V3.1$ gene in mice leads to dysfunction of MNTB neurons' ability to follow high frequency stimulation (Macica et al., 2003).

A substantial amount of work has been put into studying the function and organization of songbird auditory areas, mainly in the scale of neuron

ensembles or selectivity of individual neurons. However, the intrinsic physiology of neurons that comprise these regions and how their functions contribute to auditory processing remains to be understood. In this dissertation, I focus on CM, a region with crucial implications for invariant representations of auditory categories. Although there is a large body of work that details the contribution of CM to auditory processing, up to this point the underlying properties of its neuronal building blocks and their individual contributions to this task remained elusive. This highlights the importance of investigating the cell-intrinsic properties of CM in order to fully understand its functional capacity and contributions to the auditory pathway.

Intrinsic Plasticity

Neuronal plasticity is a critical component in the formation of sensory circuits (Holtmaat and Svoboda, 2009; Levelt and Hübener, 2012) and learning (Hölscher, 1999). Much of the research exploring plasticity has been focused on structural and synaptic level dynamics (Fu and Zuo, 2011; Medini, 2014) such as synaptic scaling (Turrigiano, 2008). Intrinsic plasticity, on the other hand, is characterized by modifications to the inherent electrical properties of individuals neurons independent of synaptic strength (Schulz, 2006), though they are not mutually exclusive. Intrinsic plasticity is often characterized by changes in the expression of specific ion channels, which

affects overall excitability and capacity to generate action potentials often takes place through activity-dependent mechanisms, either for homeostatic purposes or memory storage (Zhang and Linden, 2003; Turrigiano, 2011).

Homeostatic intrinsic plasticity is a response to long-lasting stimulation or deprivation which alters intrinsic excitability to maintain a characteristic target level of activity and reliable neuronal encoding (Schulz, 2006; Ge et al., 2009). In cell cultures of rat visual cortical neurons, blockade of neuron activity using tetrodotoxin (TTX), which blocks voltage-gated sodium channels, leads to increased firing rates and decreased spike thresholds, indicating a compensatory and homeostatic increase in intrinsic excitability (Desai et al., 1999). Homeostatic intrinsic plasticity through up- or downregulation of various currents in response to artificially induced stimuli is also seen in the hippocampus and crustacean stomatogastric ganglion (Fan et al., 2005; Karmarkar and Buonomano, 2006; Haedo and Golowasch, 2006; Brager and Johnston, 2007). This homeostatic plasticity acts through modifications in ion channel density to alter the conductances of various currents (Desai et al., 1999).

Intrinsic plasticity has been explored in memory formation in the context of stimulus-associated behavioral learning tasks. In the *Helix* snail, classical conditioning pairing shell taps and air puffs with a conditioned response of

reflexive closure induced intrinsic physiological changes such as decreased spike threshold and increased resting membrane potential of interneurons involved in the closure reflex (Gainutdinov et al., 1998; Gainutdinov et al., 2000). This intrinsic plasticity is also observed in the sea hare *Aplysia*, in which a siphon tap (unconditioned stimulus) and tail shock (conditioned stimulus) are paired to induce the siphon withdrawal reflex (conditioned response). After conditioning, increases in synaptic strength are noted along with an increase in intrinsic excitability. Motor neurons involved in the siphon withdrawal reflex show an increase in input resistance and number of spikes evoked by either direct current stimulation or by siphon tap (Antonov et al., 2001). In mammals such as cats (Brons and Woody, 1980) and rabbits, changes in intrinsic excitability have also been noted in response to classical conditioning training, and persist in memory long term. Voltage-clamp recordings of pyramidal CA1 cells in the hippocampus of rabbits after trace eyeblink conditioning revealed an increased number of spikes evoked by depolarizing current stimulus and reduction in the amplitude of the calcium-sensitive potassium current which mediates afterhyperpolarization, eventually returning to pre-training levels after seven days (Disterhoft et al., 1986; Coulter et al., 1989; de Jonge et al., 1990). In addition, the same reduction in afterhyperpolarization was still seen in CA1 cells in the presence of TTX, indicating that these physiological changes were intrinsic and not as a result of input from other neurons (Sanchez-Andres and Alkon 1991; Power

et al., 2002). Interestingly, persistent changes in physiology due to intrinsic plasticity may reflect a form of non-declarative memory that primes circuits for learning (Zhang and Linden, 2003). When thirsty rats underwent an operant conditioning task to discriminate between two odors for a water reward, reductions in afterhyperpolarization and spike accomodation were seen in layer 2 pyramidal cells of the pyriform cortex (Saar et al., 1998; Saar et al., 2001; Seroussi et al., 2002). Similar to the changes observed in rabbits after behavioral conditioning, these changes only lasted about seven days post-training. However, when rats were trained on a second odor pair before the decay of the physiological changes, the acquisition period for subsequent discrimination tasks was much quicker. In the cerebellum, synaptic plasticity is accompanied by intrinsic plasticity in Purkinje cells (PC), which not only respond to conditioned stimuli with precisely timed patterns of activity (Belmeguenai et al., 2011; Johansson et al., 2014), suggesting that memory storage in PCs may extend beyond simply increasing or decreasing firing rates, and may be realized as adaptive responses to stimuli (Shim et al., 2018).

Sensory experience can also induce changes in intrinsic physiology. Synaptic and intrinsic plasticity changes were observed in *Xenopus* tadpoles after 4 hours of visual exposure to a visual motion stimulus in the form of flashing diodes. Synaptic depression occurred in the form of synthesis of polyamines that block calcium-permeable AMPA receptors that are typically involved in

the induction of potentiation. In addition, voltage-clamp recordings revealed an increase in voltage-dependent sodium currents, leading to increased evoked spikes. Interestingly, while these two outcomes seem to offset one another, background firing of tectal neurons was greatly decreased, suggesting that synaptic and intrinsic plasticity may play off one another to enhance processing by improving signal-noise ratio (Aizenman et al., 2002; Aizenman et al., 2003).

Studies have shown that lack of auditory experience can also affect intrinsic physiology in auditory cortex; intrinsic excitability can be increased through induced hearing loss (Kotak et al., 2005; Xu et al., 2007, Mowery et al., 2015). However, in visual cortex, visual deprivation elicits experience-dependent increases in layer 4 visual synaptic excitability, but does not induce changes in intrinsic excitability (Maffei et al., 2004). In contrast, plastic changes in intrinsic excitability were noted in cultured visual cortical pyramidal neurons after incubation in TTX to limit spiking activity (Desai et al., 1999), suggesting disparate compensatory mechanisms *in vivo* and *in vitro* for managing limited neuronal activity. Behaviorally and *in vivo* induced experience-dependent changes in the functionality and topographic structure of neural circuitry in auditory cortex reflect the statistics of sensory experience. Exposure to pulsed or continuous tones can lead to increased or decreased representation of those specific tones in primary

auditory areas in rats (Zhang et al., 2001; Zhou and Merzenich, 2008), and acoustic isolation from birdsong in European starlings can lead to broader selectivity in primary auditory neurons (Cousillas et al., 2004). However, little is known about the capacity for intrinsic physiology to undergo these experience-dependent plasticity modifications seen in functional changes that are reflective of the structure and quality of experience, rather than the quantity.

The findings presented in this dissertation identify cell-intrinsic mechanisms that provide the caudal mesopallium of songbirds the ability to uniquely process temporally complex natural auditory signals, and explore the dynamics of intrinsic plasticity and early experience in shaping the physiology of auditory neurons for this task.

Chapter 2: Phasic and Tonic Cell Types in the Zebra Finch Auditory Caudal Mesopallium

Abstract

The caudal mesopallium (CM) is a cortical-level area in the songbird auditory pathway where selective, invariant responses to familiar songs emerge. To characterize the cell types that perform this computation, we made whole-cell recordings from brain slices in juvenile zebra (*Taeniopygia guttata*) of both sexes. We found three groups of putatively excitatory neurons with distinct firing patterns. Tonic cells produced sustained responses to depolarizing step currents, phasic cells produced only a few spikes at the onset, and an intermediate group was also phasic but responded for up to a few hundred ms. Phasic cells had smaller dendritic fields, higher resting potentials, and strong low-threshold outward rectification. Pharmacological treatment with voltage-gated potassium channel antagonists 4-aminopyridine or α-dendrotoxin converted phasic to tonic firing. When stimulated with broadband currents, phasic cells fired coherently with frequencies up to 20-30 Hz, whereas tonic neurons were more responsive to frequencies around 0-10 Hz. The distribution of peak coherence frequencies was similar to the distribution of temporal modulation rates in zebra finch song. We reproduced these observations in a

single-compartment biophysical model by varying cell size and the magnitude of a slowly inactivating, low-threshold potassium current I_{LT}. These data suggest that intrinsic dynamics in CM are matched to the temporal statistics of conspecific song.

Introduction

In songbirds, one of the functions of the auditory system is to decode information about individual identity from song and other vocalizations. A key step in this process occurs in the caudal mesopallium (CM), which is part of the avian homologue of the auditory cortex (Dugas-Ford and Ragsdale, 2015). Ascending input to CM comes from field L (Wang et al., 2010), where responses are explained well by simple, linear receptive fields (Sen et al., 2001). Information about identity is present in field L, but it is implicitly encoded in the timing of activity across the population (Woolley et al., 2005). In CM, an explicit, sparse code begins to emerge: neurons respond selectively to a small number of conspecific song units and are more tolerant of background noise and production variability (Meliza et al., 2010; Meliza and Margoliash, 2012); selectivity is enhanced for familiar songs (Gentner and Margoliash, 2003; Jeanne et al., 2011); and receptive fields are complex and nonlinear (Sen et al., 2001; Calabrese and Woolley, 2015).

Cell-intrinsic mechanisms can contribute to the transformation of ascending sensory input (Llinás, 1988). Areas in the auditory hindbrain and midbrain, for example, contain multiple cell types with distinct morphological and biophysical properties that enhance coding for amplitude envelope modulations, periodicity, and other complementary acoustic features (Peruzzi et al., 2000; Carr and Soares, 2002; Rothman and Manis, 2003). Compared to the mammalian auditory cortex, little is known about the cell types in CM. Indeed, the large-scale architectures of the avian and mammalian telencephalon are so different that their evolutionary relationship has been a matter of significant dispute (Dugas-Ford and Ragsdale, 2015). Recent studies have identified parallels in connectivity, gene expression, and function (Wang et al., 2010; Jarvis et al., 2013; Calabrese and Woolley, 2015), supporting the hypothesis that many cell types have been conserved in birds, mammals, and other amniotes (Karten, 1967). According to this view, the mesopallium (of which CM is a part) is thought to correspond to layer 2/3 (Jarvis et al., 2013), but it is unknown whether it has similar intracellular physiology.

In this study, I used whole-cell recordings in zebra finch brain slices to identify cell types in CM. Our goals were to identify intrinsic biophysical mechanisms that might contribute to neural coding and to assess if CM neurons are similar to those in mammalian auditory cortex. The results

indicate that although CM contains cells that resemble the two major groups found in neocortex, narrow-spiking interneurons and broad-spiking principal cells (Harris and Shepherd, 2015), the broad-spiking cells in CM comprise three morphologically and physiologically distinct classes, none of which corresponds well with regular-spiking pyramidal neurons. Whereas regular-spiking responses to current steps are sustained, weakly adapting, and have consistent inter-spike intervals (Tateno et al., 2004; Huggenberger et al., 2009), all of the broad-spiking cells in CM were strongly adapting, and two of the cell types only responded at the onset of current injection. This intrinsic phasicness may enhance encoding of the fast temporal modulations found in zebra finch song.

Results

Phasic and Tonic Spiking Responses in CM

I examined the intrinsic physiology of juvenile zebra finch CM neurons by making whole-cell patch recordings in acute brain slices (Fig. 1A, B). Approximately 9% (n = 17) of the neurons were classified as narrow-spiking (NS). These neurons had narrow action potentials (mean width ± SD: 0.67 ± 0.15 ms), strong after-hyperpolarizations (AHPs; mean amplitude ± SD: 9.1 ± 4.5 mV; mean time to trough ± SD: 2.5 ± 0.6 ms), and short membrane time constants (mean ± SD: 16.9 ± 8.3 ms). Some NS cells could achieve high sustained firing rates with relatively little adaptation (Fig. 1C), but others

were strongly adapting. The other 91% of the cells (n = 169) had wide action potentials (1.43 ± 0.36 ms), shallow AHPs (amplitude: 2.1 ± 5.8 mV; time to trough: 4.6 ± 1.5 ms), low steady-state firing rates (Fig.1D-F), and longer membrane time constants (mean ± SD: 28.4 ± 10.3 ms). The spike shapes and passive physiological properties of these two groups resemble narrow-spiking interneurons and excitatory principal cells in the neocortex, respectively (Harris and Shepherd, 2015), but with some notable differences. In this study, I focused on the putatively excitatory, broad-spiking cells.

Broad-spiking neurons responded to injections of depolarizing current steps (1500-2000 ms) with sustained, phasic, and onset firing patterns. Some neurons produced multiple patterns of responses over the range of step sizes tested, and others produced only one. Sustained responses (Fig. 1D, middle left) continued throughout the depolarizing step, accommodating to maximum steady-state rates of 7.5 ± 6.5 Hz (mean ± SD). Decreases in rate were typically accompanied by decreases in spike height and increases in spike width. I termed this response type sustained rather than regular, because the accommodation was not described well by an exponential decay function, and steady-state firing rates were irregular (Fig. 1D, top right). The average coefficient of variation (CV) of inter-spike intervals during sustained firing was 1.30 ± 0.14. By comparison, step responses of regular-spiking neurons in cat visual cortex have a CV of less than 0.3 (Holt et al., 1996).

Phasic responses (Fig. 1D, top left, and 1E-F, both sweeps) ceased after about 10-100 ms. In some cases, spikes progressively broadened to several ms in duration as height and rate decreased to zero. In other cases, spike shape and rate were comparatively stable before firing abruptly terminated. After firing stopped, the membrane potential continue to fluctuate with broad oscillations and irregularly shaped spikelets. Onset responses consisted only of a single spike at the beginning of the current injection (Fig. 1F), sometimes followed by an after-depolarization or a failed spike. A few broad-spiking cells (n = 6) produced irregular, bursting firing patterns. These cells may be akin to intrinsic bursting or chattering cells of the superficial neocortex (Gray and McCormick, 1996; Huggenberger et al., 2009), but they were too rare in this preparation to be analyzed in more detail.

Overall, putative principal neurons were strongly accommodating. Some cells produced sustained responses at lower levels of current injection, but almost every cell (n = 146, 90%) became phasic with stronger currents. Fig. 1D shows an example of this pattern: for steps larger than 65 pA, the instantaneous firing rate continued to increase, but the steady-state rate decreased and eventually became zero. The current and voltage levels at which cells became phasic varied broadly. Many cells were phasic at all current levels (Fig. 1E), and some extreme cases only produced onset responses to all above-threshold currents (Fig. 1F). Although such onset firing is often

evidence of an unhealthy neuron or poor recording conditions, these neurons were able to spike repetitively and reliably to rapidly modulated currents (see Fig. 5), and thus are likely to be healthy exemplars of cells in which active, intrinsic mechanisms prevent repetitive firing to slowly varying inputs (Prescott et al., 2008). The electrophysiological properties of onset-only neurons were statistically indistinguishable from other phasic neurons, with the exception of spike height, which was 8.1 mV lower on average (LMM: $t_{14} = -2.4$, $p = 0.029$).

To quantify phasicness on a per-cell basis, I used the logarithm of the average response duration (*D*). This measure varied broadly across the population, falling into three groups (Fig. 2A). Tonic-spiking cells (TS; n = 112, 69%) like the neuron in Fig. 1D produced sustained responses at low levels of depolarization, but were usually phasic when stimulated strongly, leading to an average response duration of 1035 ± 517 ms (mean ± SD). Phasic-spiking cells (PS; n = 39, 24%) like the one shown in Fig. 1F showed complete, rapid accommodation (response duration: 10.9 ± 6.5 ms) at all levels of stimulation. Intermediate-spiking cells (IS; n = 12, 7%; Fig. 1E) also accommodated fully but over a longer timescale (88 ± 34 ms). Within TS neurons, I further quantified phasicness with the adaptation ratio (A), which ranged between 0.46 and 1.0 (mean ± SD: 0.87 ± 0.13) and was negatively correlated with *D*

(Pearson test: $r_{110} = -0.66$, $p < 0.001$). A was always 1.0 for PS and IS neurons, because they never displayed sustained firing.

Physiological and Anatomical Correlates of Phasic Excitability

Why do the putatively excitatory neurons in CM exhibit such a diversity of phasic and tonic firing patterns? I first examined whether phasic excitability was correlated with anatomical or passive physiological properties. More phasic neurons had higher resting potentials, shorter spikes, higher input resistances, and lower capacitances (Fig. 2B-E). The variations in input resistance and capacitance balanced each other such that membrane time constants did not covary significantly with response duration (Fig. 2F). In a number of recordings (n = 11), I filled cells with biocytin and reconstructed their morphologies (Fig. 2G). Cell bodies were small (mean diameter ± SD: 13.9 ± 5.4 μm), with irregular or triangular shapes. Dendritic arbors comprised 4-10 primary dendrites of similar caliber extending in all directions. Arbor size and complexity varied from simple unbranched fields only a few cell diameters across to highly branched, elaborate fields several hundred microns in diameter. PS and IS neurons had smaller and less complex arbors. Response duration was strongly correlated with total dendrite length and the number of bifurcations (Fig. 2G, insets), but not with soma surface area (LMM: $t_{2.2} = 2.6$, $p = 0.11$), suggesting that variation in C_m primarily reflects differences in dendritic elaboration.

To determine if phasicness was correlated with spatial location in CM, I used low-power images taken after recording to reconstruct approximate locations relative to the midline, the ventricle, and the ventral mesopallial lamina (LMV), which are the medial, superior, and inferior boundaries of CM. Although CM includes lateral (CLM) and medial (CMM) divisions, the boundary is not clearly defined, and I was unable to reliably locate cells in one or the other area. However, most of the reconstructed sites (n = 42/58, 76%) were over 1200 μm from the midline and were probably in CLM. There were no significant differences in the average location of the cell types along the mediolateral or superior-inferior axes (MANOVA: $F_{4,104} = 1.11$, $p = 0.35$) and no correlation between *D* and mediolateral (LMM: $t_{44} = -1.5$, $p = 0.14$) or superior-inferior location ($t_{44} = 1.4$, $p = 0.17$), so there was no evidence for any spatial segregation of cell types within CM. Although it is possible that some cells were recorded from the avalanche region of CM, which projects directly to HVC (Akutagawa and Konishi, 2010) and is involved in song learning (Roberts et al., 2017), the broad distribution of all three cell types indicates that they are a general characteristic of CM.

Ionic Mechanisms of Phasic Excitability

A qualitative inspection of spike waveforms suggested that phasic accommodation depends on more than one mechanism. When neurons were

strongly depolarized, spikes became progressively shorter and broader, and the troughs between spikes became increasingly shallow (e.g., Fig. 1D,E, top traces). This pattern is consistent with a buildup of sodium channel inactivation, or depolarization block (Tucker et al., 2012; Bianchi et al., 2012). The phasic responses exhibited by IS and PS neurons to weak currents, on the other hand, did not exhibit the same progressive changes in height and width. For example, the neuron shown in Fig. 1E stopped firing after about 500 ms of a 50 pA current even though spike height, spike width, and trough depth had stabilized. I also noted that the plateau voltages for PS and IS neurons tended to be lower than for TS neurons, around -60 mV, suggesting that a different mechanism involving an outward (hyperpolarizing) current caused these cells to stop firing.

To test this hypothesis, I investigated current-voltage (I-V) relationships over a range of depolarizing and hyperpolarizing currents. CM neurons had highly nonlinear I-V curves, with pronounced inward and outward rectification (Fig. 3A-D). Resting potentials were usually close to the steepest region of the I-V curves, and currents as small as 5-10 pA could evoke spikes (e.g., Fig. 3A). A dominant component of the inward rectification was a sag current with delayed activation at hyperpolarized potentials, and rebound spiking was common (e.g., Fig. 3A). Sag currents, as measured by the ratio of transient to steady-state voltage deflections, were stronger in tonic neurons (Fig. 3E).

However, after correcting for resting input resistance, total inward rectification had similar magnitude and activation voltage in all three cell classes, as indicated by overlap in the toes of the average I-V curves (Fig. 3F).

Outward rectification (OR) was prevalent throughout the population, with over 95% of cells (n = 155) showing more than a 50% decrease in input resistance at depolarized voltages. The magnitude of OR was similar in all three cell classes above -50 mV, but the activation voltage was lower in PS neurons, as indicated by the stronger curvature of the average I-V curve (Fig. 3F). The OR activation voltage V_{OR}, quantified as the point where the I-V slope was less than 50% of its maximum, was strongly correlated with response duration (Fig. 3G).

In the auditory midbrain and hindbrain, phasic neurons express low-threshold potassium currents (Carr and Soares, 2002), which could be the source of the OR seen in CM. To test this hypothesis, I applied synaptic and potassium-channel blockers in the bath (Fig. 4). Blocking fast synaptic excitation and inhibition did not significantly change *D* (Tukey test: z = 2.1, p = 0.13) or A (z = -0.94, p = 0.81), excluding the possibility that phasicness arises from recurrent inhibition. Application of 100 nM charybdotoxin, which blocks the B_K-type Ca^{2+}-activated potassium channel, also did not affect response phasicness (A: z = 0.092, p = 1.0; *D*: z = -0.12, p = 1.0). In contrast, 2

mM 4-AP, a broad blocker of voltage-gated potassium channels, caused PS and IS neurons to become regular-spiking (Fig. 4A). Across the population, 4-AP caused A to decrease (Fig. 4D) and *D* to increase (Fig. 4E). In most cases, these changes in global firing patterns were accompanied by small increases in spike width and by more uniform spike heights and thresholds (e.g., Fig. 4B), indicating that 4-AP did not strongly affect potassium currents responsible for the spike downstroke. Application of 100 nM α-dendrotoxin, a specific blocker of low-threshold $K_V1.1$, $K_V1.2$, and $K_V1.6$ potassium channels (Guan et al., 2007), caused responses to become faster and more regular (Fig. 4C), leading to a decrease in A (Fig. 4D). However, α-dendrotoxin did not lead to significant changes in *D* (Fig. 4E; $z = 1.7$, $p = 0.29$), suggesting that other 4-AP-sensitive channels also contribute to phasicness.

Phasic Neurons are Tuned to Higher Modulation Frequencies than Tonic Neurons

Phasic neurons are found throughout the early auditory system in mammals and birds, where they function as coincidence detectors and for processing rapidly modulated signals (Carr and Soares, 2002). Zebra finch song has broadband temporal modulations at rates up to 20-30 Hz (Singh and Theunissen, 2003), suggesting that phasicness in CM may be a specialization for processing rapid temporal structure in song. A prediction of this hypothesis is that phasic neurons will be more coherent with the

higher-frequency components of a complex driving current. In other words, because phasic neurons do not respond well to long depolarizations, I expect them to filter out low-frequency inputs but fire precisely and reliably to high-frequency signals. In contrast, I expect tonic neurons to more faithfully follow low-frequency inputs. To test this prediction, I calculated the coherence between broadband current stimuli and spiking output (Fig. 5). Neurons were injected with a 15-s waveform comprising small, fast oscillations superimposed on larger depolarizations and hyperpolarizations of varying duration. The mean frequency of the current was gradually increased over time to probe the maximum frequency at which spiking could follow the input, giving an overall spectral distribution with power at frequencies up to 100 Hz (Fig. 5A,B). Tonic and phasic neurons (including onset-only cells) responded to this current with robust and reliable spiking, though most neurons became less reliable near the end of the stimulus as the frequency increased.

Looking in the time domain, differences between PS and TS neurons were subtle. There was a tendency for TS neurons to respond throughout longer depolarizations, whereas PS neurons responded at onsets and offsets (e.g., Fig. 5A, right panels). Importantly, PS neurons were able to follow the high-frequency modulations in the signal, indicating that the putative I_{LT} current that prevents repetitive firing to long depolarizations can be

deactivated by brief hyperpolarizations. In the frequency domain, however, differences were more apparent. For example, in Fig. 5B, the power spectrum of the PS neuron was more strongly attenuated at low frequencies than the TS neuron. More significantly, the coherence spectrum of the PS neuron (Fig. 5C), which indicates how reliably the spiking output followed the current input, looked like a bandpass filter with a peak frequency of about 25 Hz and strong lowpass attenuation. The lowpass attenuation is consistent with PS neurons' inability to respond throughout slow depolarizations. In contrast, the TS exemplar looked more like a lowpass filter, with a passband that rolled off around 20 Hz. Both exemplars became gradually less coherent at higher frequencies. The notch at around 35 Hz and the second peak at around 60 Hz seen in the TS spectrum were often seen in all three cell types, but the cause was not clear.

In spectra averaged across all members of each cell class (Fig. 5D), TS neurons were more coherent from 0 Hz to about 10 Hz, and PS neurons were more coherent from about 10 Hz to 30 Hz. All cells had some degree of attenuation at 0 Hz (DC), which likely reflects nonlinear f-I relationships. However, frequencies below 1 Hz were attenuated almost twice as much in PS as in TS cells. The coherence spectrum in IS neurons was similar to that in TS neurons, with a trend towards stronger lowpass attenuation. Among the cells tested with complex current injections (n = 36 cells from 29 birds), peak

coherence frequency and lowpass attenuation were both negatively correlated with response duration (Fig. 5E).

Contributions of I_{LT} and Cell Size to Step Responses and Coherence

Taken together, these results indicate that phasic excitability is associated with smaller neurons that express a 4-AP-sensitive, low-threshold outward current. To test whether these parameters are sufficient to explain the observed variation in phasicness, I constructed a single-compartment computational model for broad-spiking CM neurons (see Materials and Methods and Appendix). Given the lack of detailed data on the specific currents expressed in CM neurons and their kinetics, the goal was to replicate our main observations. With the help of my advisor, Meliza, we hand-fit the model to match the I-V curves, membrane time constants, spiking patterns, and coherence spectra. It became clear that although individual neurons varied in many parameters, adjustments to cell size and I_{LT} conductance (g_{LT}) alone were sufficient to produce the full range of observed firing patterns and coherence spectra. The responses to step currents were primarily influenced by g_{LT}. Models with low g_{LT} behaved like TS neurons, giving sustained responses to small current steps but entering depolarization block when stimulated strongly (Fig. 6A, left). Models with high g_{LT} behaved like PS neurons, with onset responses at all current levels (Fig. 6A, right). Intermediate values of g_{LT} produced IS-like behaviors, with progressively

phasic responses caused by I_{Na} inactivation when the current was strong and abruptly phasic responses caused by I_{LT} when the current was weak (Fig. 6A, middle).

With all other model parameters held constant, there was a highly nonlinear relationship between g_{LT} and *D* (Fig. 6B). From 0-6 nS, increases in g_{LT} produced modest increases in response duration, probably by helping to repolarize the membrane during the spike downstroke. Increasing g_{LT} beyond 6 nS reduced *D* because responses to weak currents became phasic, as in the middle panel of Fig. 6A. Between 10-30 nS, there was a precipitous drop in *D* as I_{LT} became strong enough to prevent repetitive firing. The critical value of g_{LT} depended on C_m, with smaller neurons tending to produce tonic responses over a broader range of g_{LT} values, and larger neurons having a larger range in which increasing g_{LT} produced a smooth decrease in duration. Further increases to g_{LT} had little effect beyond about 45 nS, the point where the model only produced onset responses.

Both g_{LT} and C_m influenced the shape of the model's coherence spectrum. The exemplar models shown in Fig. 6A,C are similar to the recorded data (Fig. 5D), with the TS neuron acting like a lowpass filter, the IS neuron showing increased attenuation at low frequencies, and the PS neurons acting like a bandpass filter. Even the notch and second peak seen in many CM neurons

were reproduced by the model, though we were unable to determine which parameters governed this effect. With all other parameters held constant, changes to g_{LT} affected the coherence at frequencies below 20 Hz (Fig. 6D). As predicted, by preventing neurons from firing to sustained depolarization, I_{LT} causes the cell to filter out low frequency inputs. Changes to cell size, on the other hand, affected coherence at higher frequencies (Fig. 6E), with smaller neurons showing increased coherence. This effect was not due to changes in τ_m, which remained constant because g_{leak} and other conductances were scaled with C_m. Instead, changes in cell size effectively scale the amplitude of the injected current, boosting coherence across the spectrum. The reason size disproportionately affects coherence at high frequencies is that I_{LT}, which has an average activation time constant in this model around 9.5 ms, counterbalances slow depolarizations.

As a consequence, the peak coherence frequency was sensitive to both g_{LT} and size (Fig. 6F). Lowpass attenuation increased approximately linearly with g_{LT} (Fig. 6G) in smaller neurons, but the relationship became non-monotonic in larger cells, because the peak of the coherence spectrum was in a range that was affected by I_{LT}.

Discussion

These results provide a first look at the intracellular physiological properties of neurons in CM, a higher-order avian auditory area in the homolog of mammalian auditory cortex (Wang et al., 2010; Jarvis et al., 2013). Extracellular recordings from CM indicate that it comprises narrow- and broad-spiking neurons with distinct functional properties (Meliza et al., 2010; Calabrese and Woolley, 2015). Our results show that CM has an even greater diversity of cell types, including some that do not appear to have a counterpart in mammalian cortex. There are at least three broad-spiking neuron types-TS, IS, and PS neurons--that produce distinct firing patterns and vary in morphology, resting potential, and expression of a low-threshold, outward-rectifying current. Differences in intrinsic dynamics are correlated with how neurons process information at different timescales.

Mechanisms of Phasic Excitability in CM

At least two different mechanisms contribute to phasic excitability in CM but operate in different voltage ranges. Depolarization block, which is caused by an accumulation of sodium channel inactivation (Venkatesan et al., 2014), is seen when TS and IS neurons are strongly stimulated and may also account for the strong accommodation observed in sustained responses (Martina et al., 1998). Because CM cells have high input resistances, depolarization block was seen with currents as small as 50-100 pA. Although this mechanism is

often assumed to be physiologically irrelevant, random activity from a few hundred synapses can produce depolarization block in CA1 models (Bianchi et al., 2012), and in intracellular recordings from starling CM, song stimuli can drive membrane voltages well above -40 mV (Perks and Gentner, 2015).

The second mechanism for phasic excitability, which is only found in a subset of neurons, is an outward current that activates about 5-10 mV below the threshold for depolarization block. Low-threshold outward rectification is seen in phasic and onset neurons of the hindbrain (Manis and Marx, 1991; Reyes et al., 1994; Rathouz and Trussell, 1998), midbrain (Peruzzi et al., 2000), and developing cortex (Locke and Nerbonne, 1997; Metherate and Aramakis, 1999). In many areas, the source of OR is I_{LT}, a 4-AP-sensitive, slowly inactivating outward current (Locke and Nerbonne, 1997; Carr and Soares, 2002; Rothman and Manis, 2003; Sivaramakrishnan and Oliver, 2001). I_{LT} activates rapidly at around the spike threshold and prevents repetitive firing by counterbalancing and shunting inward currents as early as the first spike (Rothman and Manis, 2003; Gai et al., 2010). PS and especially onset-only neurons had spikes that were shorter than average (Fig. 2C), consistent with a rapidly activating outward current. Other sources of OR that can cause phasic firing include calcium-dependent B_K-type potassium channels, seen in some cell types of the inferior colliculus (Sivaramakrishnan and Oliver, 2001), and S_K-type potassium channels, seen in RA-projecting HVC neurons (Daou

et al., 2013) and developing barrel cortex (Maravall et al., 2004). Because 4-AP caused CM neurons to become regular-spiking, decreasing the strength and rate of accommodation, I_{LT} is probably responsible for phasic firing to weak and moderate stimuli. α-dendrotoxin, a more selective blocker of low-threshold K_V1.x channels, had mixed effects on firing patterns, suggesting that multiple channel types contribute to regulation of temporal response properties in CM.

Resting potential was as much as 10 mV higher in PS neurons (Fig. 2B, 3F), which could enhance the effect of I_{LT}, as some I_{LT} channels would be active at rest and counteract excitatory synaptic currents. It is not clear why PS neurons have higher resting potentials. Any I_{LT} currents near rest would be hyperpolarizing. Sag potentials are present in many neurons, implying the presence of depolarizing I_h currents, but they are stronger in TS cells (Fig. 3E), so the predicted effect is in the wrong direction. In the caudomedial nidopallium (NCM), another pallial auditory area, phasic firing is associated with higher levels of a potassium leak conductance (Dagostin et al., 2015), but this conductance causes a decrease in resting potential, so the effect is in the opposite direction to what I observed in CM.

These observations suggest that the firing patterns of TS, IS, and PS neurons primarily reflect differences in I_{LT} expression. In a simple biophysical model,

varying g_{LT} was sufficient to reproduce TS and PS behavior. IS responses were produced over a fairly narrow range of parameters, which may account for their relative rarity in CM. Alternatively, IS neurons may express a slower low-threshold current (for example, an M-current; Jentsch, 2000). I was unable to obtain good enough voltage-clamp in slices to investigate the kinetics of low-threshold currents, so further work in primary culture or detached membrane patches is needed to determine if IS neurons have a distinct mechanism for phasicness.

Intrinsic Dynamics and Temporal Coding

The coding properties of sensory neurons are determined not only by the tuning of their inputs, but also by their intrinsic membrane dynamics, which govern how synaptic currents are integrated and transformed into patterns of spikes (Llinás, 1988; Padmanabhan and Urban, 2010). Intrinsic dynamics may be especially important in the auditory system, because acoustic signals are inherently time-varying, often on a wide range of scales (Wang et al., 2008). Indeed, a number of auditory hindbrain and midbrain nuclei contain phasic, tonic, and other cell types, and there is an extensive literature on how electrophysiological and morphological properties in these areas enable each cell type to extract different kinds of acoustic features from ascending auditory activity (Peruzzi et al., 2000; Carr and Soares, 2002; Rothman and Manis, 2003; Khurana et al., 2011). However, because phasic excitability has

not been widely reported at cortical levels, its function in more central areas has been given little attention.

To examine whether the cell types in CM might be specialized for processing acoustic features with different timescales, I recorded responses to broadband currents. Using coherence to quantify information transmission as a function of frequency (Borst and Theunissen, 1999), I found that each cell optimally encoded frequencies in a band from 0-20 Hz. Replicating this distribution in a biophysical model required coordinated variations in I_{LT} currents and cell size. Whereas I_{LT} decreased coherence at low frequencies by preventing repetitive firing to slow depolarizations (Prescott et al., 2008), smaller cells had increased coherence at high frequencies because they did not filter driving currents as strongly. I expect this effect would be even stronger if differences in dendrite length were considered. Strikingly, the distribution of peak coherence frequencies covered 80-90% of the range of temporal modulations in zebra finch song (Singh and Theunissen, 2003). CM receives ascending input from field L, which contains distinct cell groups with tuning properties that match the distribution of temporal and spectral modulations in song (Woolley et al., 2009). These results suggest that the distribution of physiological and morphological properties in CM are matched to the distribution of ascending input, and ultimately to the statistics of conspecific song.

Comparisons to Neocortex and other Pallial Areas

There were few similarities with auditory cortex in intracellular physiology. The narrow-spiking cells with high firing rates are like fast-spiking interneurons (McCormick et al., 1985; Ascoli et al., 2008), though sustained firing rates are considerably lower and adaptation more pronounced than in mouse neocortex (Erisir et al., 1999). The broad-spiking neurons that were the focus of this study may be excitatory principal neurons, but they differ from pyramidal neurons in a number of features. First, input resistances are high and capacitances are low compared to A1 in the mouse (Oswald and Reyes, 2008; Huggenberger et al., 2009), which has a comparably sized brain. These properties can be attributed to small cell bodies and compact dendritic arbors (Fig. 2G). Second, although some CM neurons produce sustained responses, they do not exhibit the exponential accommodation and consistent interspike intervals seen in regular-spiking pyramidal neurons (Holt et al., 1996;Tateno et al., 2004). Third, over 30% of broad-spiking cells in CM only produce phasic responses. In contrast, in mice of a comparable age, 90% of superficial pyramidal neurons in A1 are regular-spiking, 10% are intrinsically bursting, and phasic responses are not seen (Huggenberger et al., 2009).

Some of the differences between CM and neocortex, like cell size, may reflect an ancestral divergence: across species, birds have many more neurons per unit mass in the telencephalon than mammals (Olkowicz et al., 2016). Phasic excitability has been observed in two other pallial areas, HVC and NCM (Dutar et al., 1998; Dagostin et al., 2015), and therefore could also be a general feature of the avian forebrain. However, because small changes in the conductance of a single current type can have profound effects on firing patterns, phasic excitability can be quite plastic. Phasic cells are found in a number of cortical areas in very young rodents, during sensory critical periods (Locke and Nerbonne, 1997; Metherate and Aramakis, 1999), but this response pattern is lost through experience-dependent development (Maravall et al., 2004; Kotak et al., 2005). Thus, the diverse intrinsic dynamics in CM could be a recent adaptation to the spectrotemporal statistics of zebra finch song, or even the result of experience-dependent plasticity (Titley et al., 2017). Additional data are needed on the development of intrinsic excitability in this key brain area.

Auditory areas of the songbird pallium express many of the same layer-specific genetic markers (Dugas-Ford et al., 2012; Jarvis et al., 2013) and share key features of anatomical organization (Wang et al., 2010) with the mammalian neocortex. Our results indicate that in spite of these similarities, the caudal mesopallium is quite different from layer 2/3, its putative

homolog in cortex, in terms of morphology and intrinsic electrophysiology. An important question is how circuits with widely divergent properties in mammals and birds are able to perform many of the same computations required for cognitively complex behaviors.

Conclusions

These results show that CM contains at least three clusters of broad-spiking neurons that differ in morphological and physiological parameters, in firing patterns, and in their ability to faithfully encode rapidly modulated inputs. Phasic and tonic neurons may be specialized for encoding information on different timescales, reflecting the diverse temporal structure of zebra finch song. Further work is needed to determine the source of this intrinsic diversity. One possibility is that PS, IS, and TS neurons are distinct cell types, with different lineages and genetic markers. Such a result would be in accord with recent studies showing that excitatory neurons within layers of the neocortex comprise multiple cell classes (Harris and Shepherd, 2015). Alternatively, these groups may comprise a single cell type in different stages of development. The ages of the birds in this study span much of the sensory critical period for song production and perception (Sturdy et al., 2001; Jarvis et al., 2013; Woolley, 2012), and cellular properties may continue to mature during this period to support this learning. A third possibility is that the morphology and potassium channel complement of these cells have been

shaped by auditory experience (Dehorter et al., 2015; Titley et al., 2017). This could represent a powerful, cell-intrinsic mechanism for learning the temporal structure of sensory inputs.

Figures

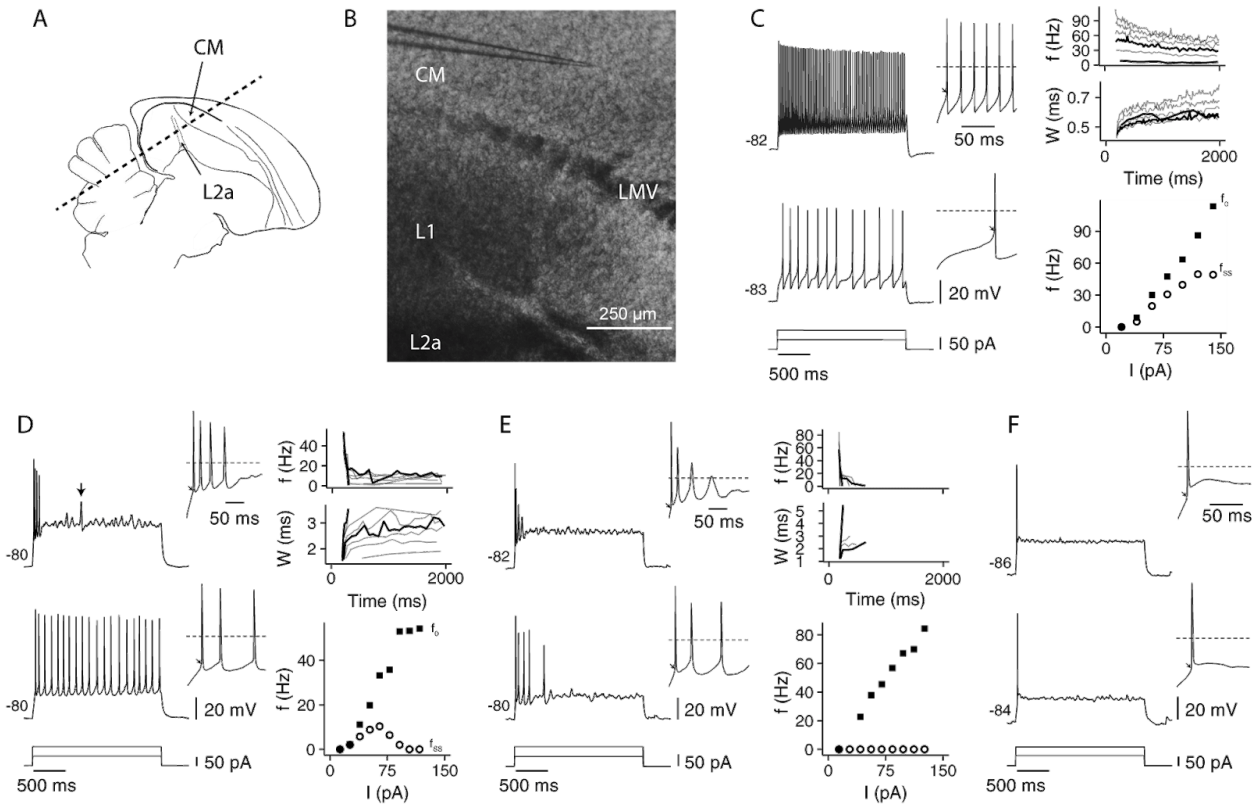

Figure 1

Spiking Response Patterns of CM Neurons.

A, Slice orientation (dashed line) is indicated on a drawing of a parasaggital section of the zebra finch brain. L2a is the primary thalamorecipient area, and CM is the area under study.

B, Low-power image of whole-cell recording from CM in zebra finch auditory pallium slice (4X, DIC, 900 nm illumination). Dark areas are heavily myelinated. LMV is a major white-matter lamina separating CM from L1 and L2a in the underlying nidopallium, which both appear dark because of

ascending thalamopallial afferents. The lighter areas in L2a and L1 may be a blood vessel.

C, A narrow-spiking (NS) neuron recorded in CM. Left panels: voltage responses to 80 pA and 40 pA step currents. Spikes are narrow with deep AHPs. Numeral indicates resting potential (mV). Insets show detail of the earliest part of the response. The small arrowhead indicates the spike takeoff point, and the dashed line indicates the spike detection threshold (see Materials and Methods) Top right panel: Instantaneous firing rate decreases over the course of the current injection. Each trace indicates response to a different current level, with the sweeps at left denoted in bold. Middle right panel: Spike width increases gradually over current injection. Bottom right panel: frequency-current (f-I) plot showing initial instantaneous rate (f_0; ▪) and steady-state rate (f_{SS}; ○).

D, A tonic-spiking neuron. Panels are as in (C). The response is sustained to low current levels (middle left panel) and phasic to stronger depolarization (top left panel). Note the irregular spike widths and rates in the sustained response, the oscillations and spikelet (arrow) following the transient response, and the non-monotonic f_{SS}- I curve.

E, A intermediate-spiking neuron. All suprathreshold current pulses resulted in phasic responses. Note that although the last, broad action potential shown in the top inset crosses the detection threshold, it was excluded because of its width and failure to exceed the threshold by at least 10 mV.

F, A phasic-spiking neuron. All suprathreshold current pulses evoked only single action potentials. The instantaneous rate is undefined.

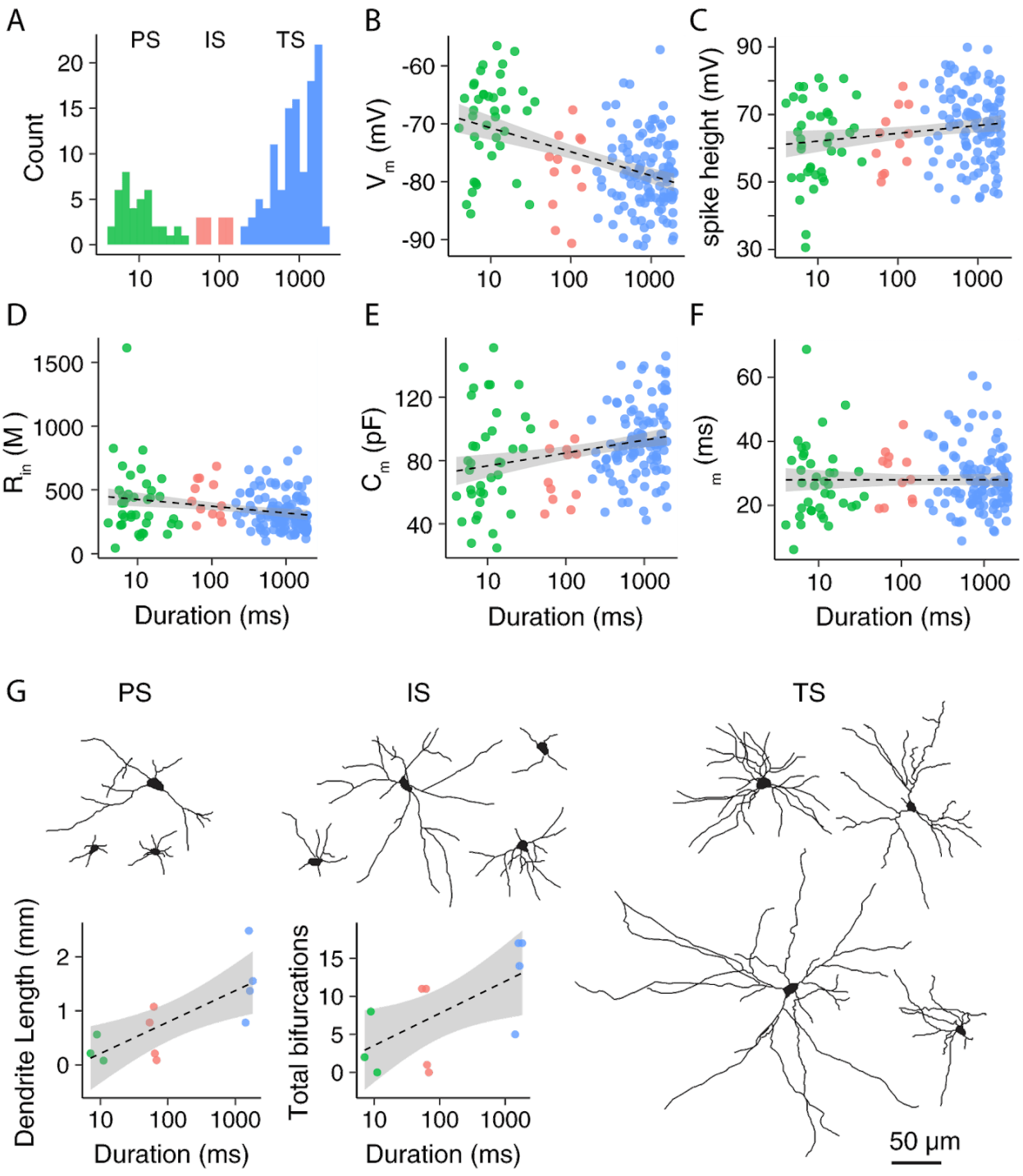

Figure 2

Physiological and Morphological Correlates of Phasic Excitability.

A, Histogram of average response duration (*D*, log scale) for broad-spiking neurons in CM. Labels and colors indicate classification based on *D*.

B, Resting potential is negatively correlated with response duration (*D*). Symbols indicate individual neurons, with color indicating classification. The dashed line and shaded area show the best linear fit and standard error. The linear relationship between V_m and *D* is significant (LMM: $t_{152} = -6.0$, $p < 0.001$).

C, The height of the first spike is positively correlated with *D* ($t_{153} = 2.3$, $p = 0.02$).

D, Input resistance was negatively correlated with *D* ($t_{153} = -2.3$, $p = 0.02$).

E, Capacitance was positively correlated with *D* ($t_{132} = 3.5$, $p = 0.001$).

F, Membrane time constant was not significantly correlated with *D* ($t_{155} = -0.02$, $p = 0.99$).

G, Camera lucida drawings of morphologically reconstructed, broad-spiking CM neurons. Drawings are oriented with the ventricle up and the midline to the right. Axons are not shown. Insets show plot of total dendritic length and total bifurcation count against *D*. The linear correlations are significant (dendrite length: $t_{5.5} = 3.6$, $p = 0.01$; bifurcations: $t_{7.3}=2.8$, $p = 0.03$).

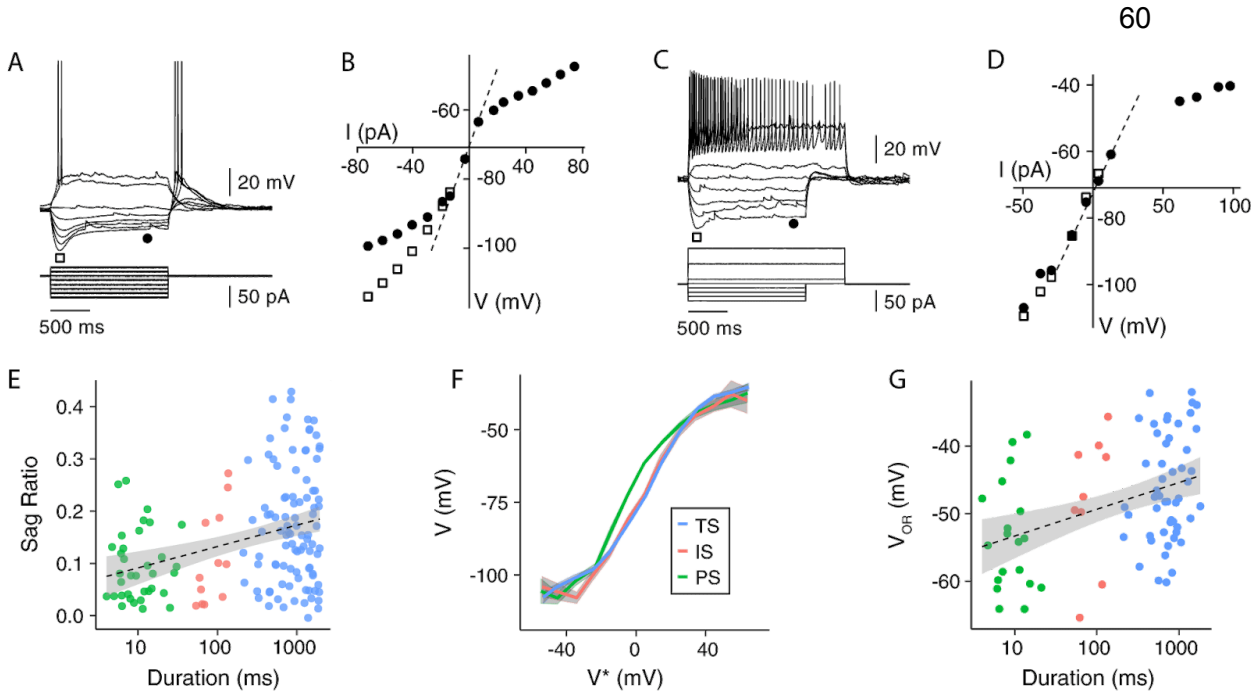

Figure 3

Current-Voltage Relationships in CM Neurons.

A, Voltage responses of a PS neuron to step currents. Note the sag currents and rebound potentials evoked by hyperpolarizing currents. Open square (☐) and solid circle (●) denote transient and steady-state deflections, respectively, and correspond to symbols in **B**.

B, Current-voltage (I-V) plot for the neuron shown in **A**. The dashed line indicates the linear portion of the steady-state (●) curve. Note that outward rectification activated around -60 mV.

C, Voltage responses of a TS neuron. Depolarizing and hyperpolarizing pulses are different durations to emphasize firing patterns.

D, I-V plot for the neuron in **C**. Points corresponding to traces with sustained firing are not shown. Outward rectification activates at a higher voltage than in **B**.

E, Sag ratio, the ratio of transient to steady-state voltage deflections for hyperpolarizing current steps, was positively correlated with *D* (LMM: t_{139} = 3.5, $p < 0.001$). Color indicates cell classification as PS, IS, or TS. The dashed line and shaded area indicate best linear fit and standard error.

F, Average I-V curves for PS (n = 20), IS (n = 10), and TS (n = 53) neurons. To correct for differences in input resistance, the abscissa shows ΔV*, the injected current scaled by the slope of the I-V curve at rest.

G, *D* (log scale) was positively correlated with V_{OR}, defined as the value of V where the slope of the I-V curve dropped below 50% of maximum. Two TS cells exhibited less than 50% outward rectification over the entire range of currents tested and were excluded. Dashed line indicates best linear fit (t_{73} = 3.4, $p = 0.001$).

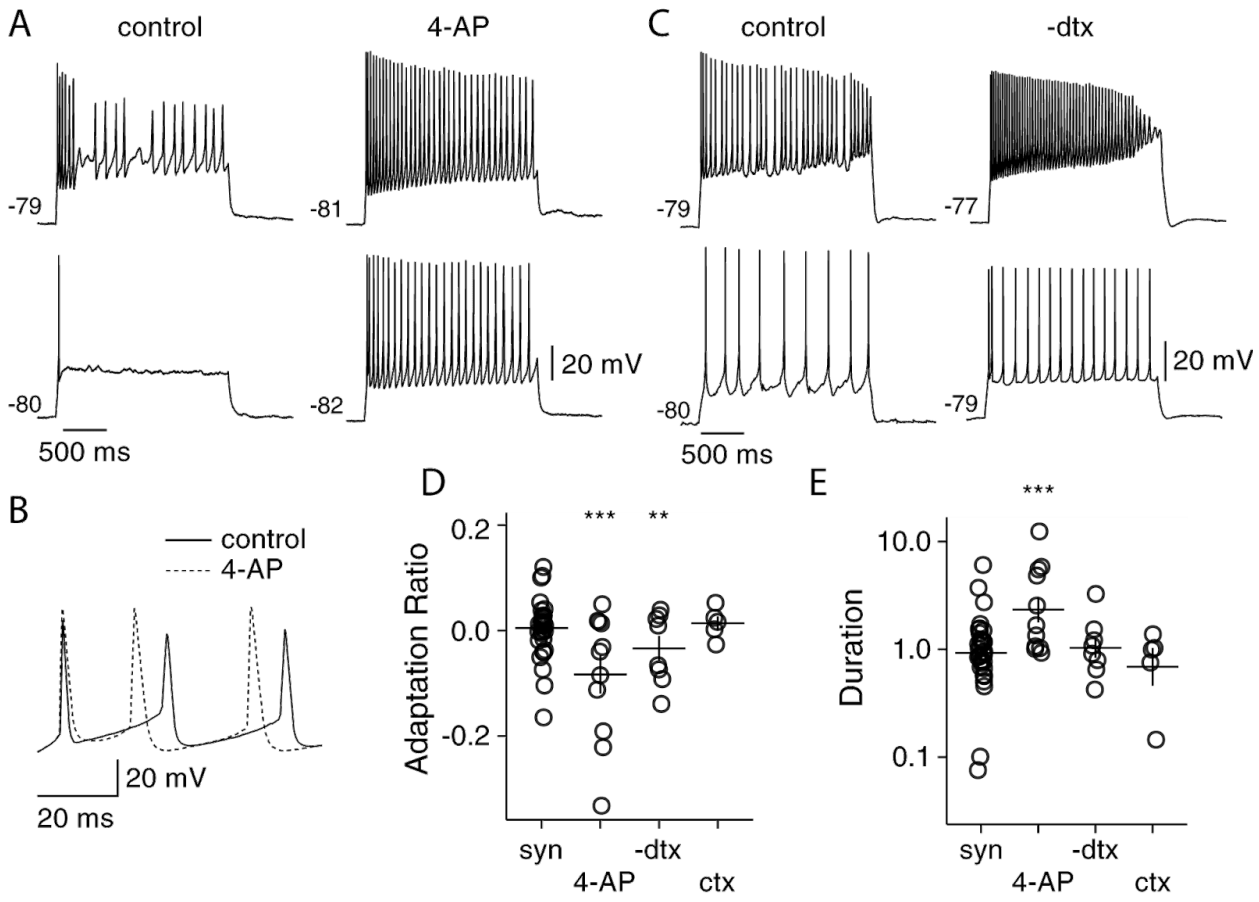

Figure 4

Phasic Spiking Depends on Potassium Currents

A, Phasic spiking in an exemplar neuron became tonic in the presence of 4-AP. Control is standard ACSF plus fast synaptic transmission blockers. Injected currents were 70 (bottom) and 140 pA (top).

B, Detail of first three spikes from A in control (solid line) and 4-AP (dashed line).

C, Tonic responses in another exemplar became more regular in the presence of α-dendrotoxin. Injected currents were 70 (bottom) and 140 pA (top).

D, Arithmetic change in adaptation ratio (A) in the presence of synaptic (syn) and potassium channel blockers (α-dtx: α-dendrotoxin; ctx: charybdotoxin). Values for synaptic blockers are relative to standard ACSF; other values are relative to ACSF plus synaptic blockers. Horizontal lines and error bars indicate mean ± SE. Stars indicate statistical significance evaluated with LMM and Tukey Test (4-AP: $z = -5.1$, $p < 0.001$; α-dtx: $z = -3.3$, $p = 0.004$).

E, Geometric change in duration D in the presence of synaptic and potassium channel blockers. Only 4-AP produced a significant change in duration ($z = 6.7$, $p < 0.001$)

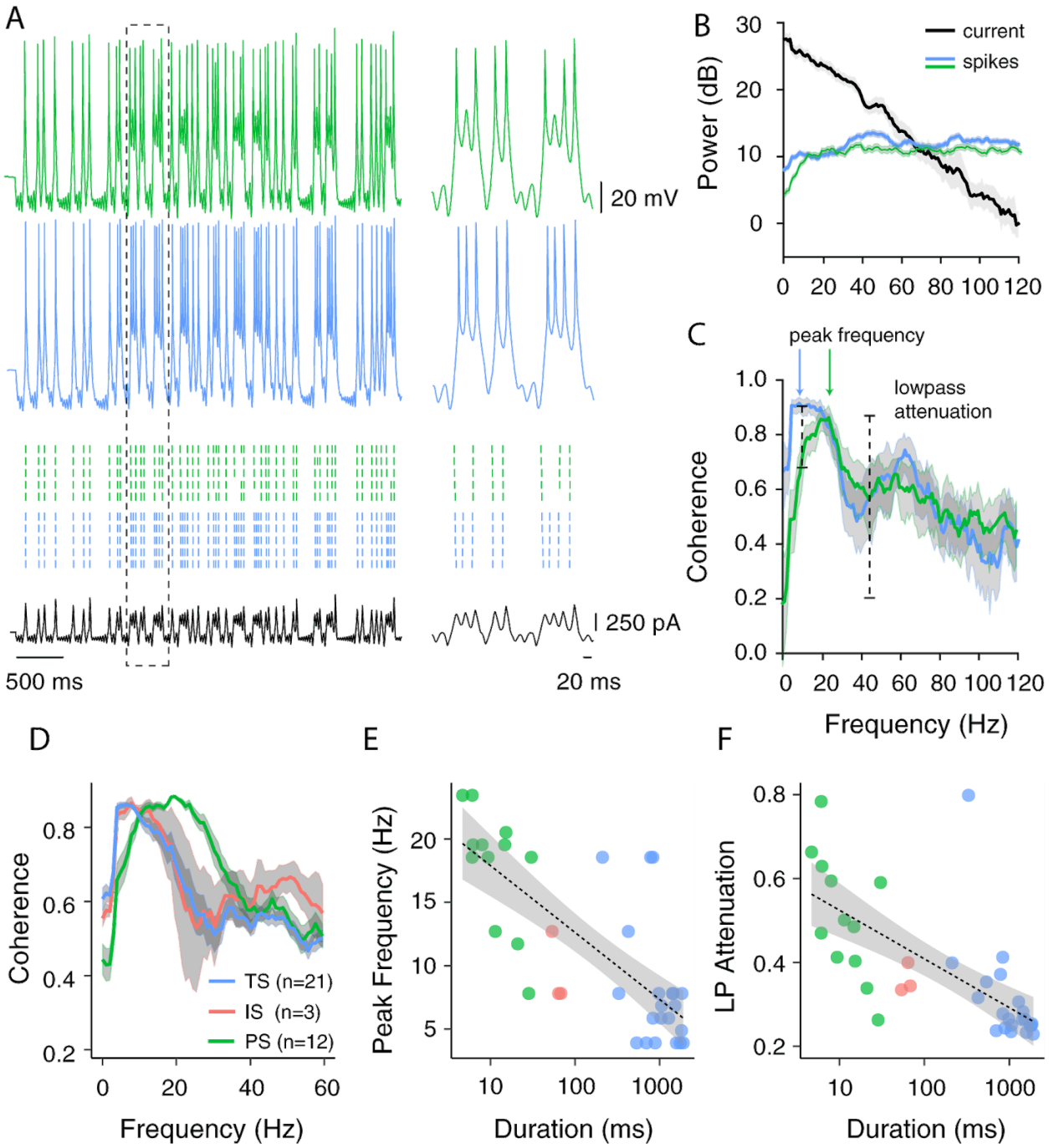

Figure 5

Frequency Response Properties of CM Neurons.

A, Responses of exemplar PS (green) and TS (blue) neurons to complex current injection. The PS neuron only produced onset responses to step currents and had an average response duration of 6 ms. Top traces show recorded voltage from one trial, raster plots show spike times for five trials, and bottom trace shows injected current. Dashed box indicates interval shown in detail at right.

B, Power spectra of injected current and spiking responses of PS and TS exemplars. Shaded regions indicate 95% confidence intervals.

C, Coherence magnitude between spiking responses and injected current for PS and TS exemplars. The TS neuron had peak coherence at low frequencies and little lowpass attenuation (ratio of coherence below 1 Hz to peak coherence), and the PS neuron had a higher peak coherence frequency and greater lowpass attenuation. Shaded regions indicate 95% confidence intervals.

D, Coherence magnitude averaged by cell type. Shaded regions indicate standard errors.

E, Response duration was correlated with peak coherence frequency (left panel) and lowpass attenuation (right panel). Each point represents an individual neuron; color represents neuron classification. Dashed line shows best linear fit for each pair of variables. Linear mixed-effects model indicated significant, independent correlations with peak coherence frequency (t_{23} =

-5.1, $p < 0.001$) and lowpass attenuation ($t_{24} = -2.8$, $p = 0.009$; total marginal $R^2 = 0.67$).

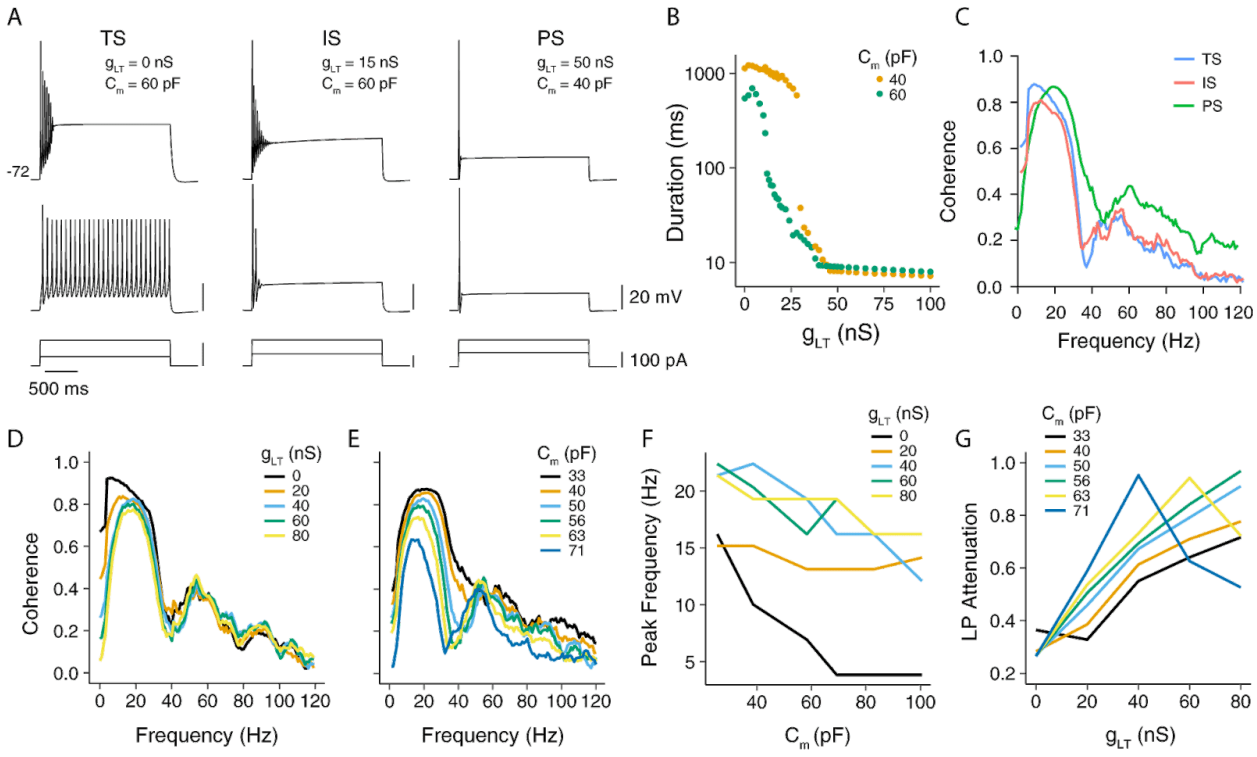

Figure 6

Step Responses and Coherence Spectra of Model CM Neurons.

A, Voltage responses to step currents by CM models with TS (left panels), IS (middle) and PS (right) parameters.

B, Average response duration *D* decreases with increasing maximal conductance of I_{LT} current g_{LT}). All model parameters were held constant except g_{LT}, which was varied between 0 nS and 100 nS in steps of 1-10 nS, and C_m, which was set to 40 or 60 pF. In the steep portion of the 60 pF curve, changes to g_{LT} as small as 1 nS caused large changes in response duration.

C, Coherence magnitude between complex current stimuli and spiking output for the TS, IS, and PS models shown in (A).

D, Coherence spectra for models with all parameters held constant (C_m = 50 pF) except g_{LT}. Increasing g_{LT} decreases coherence at low frequencies.

E, Coherence spectra for models with all parameters held constant (g_{LT} = 40 nS) except size. Size is indicated by C_m, which was scaled with conductance parameters so that density was constant.

F, Peak coherence frequency increased with g_{LT} but decreased with cell size.

G, Lowpass attenuation increased with g_{LT}, except in larger cells, where the relationship was not monotonic.

Materials and Methods

Animals

All procedures were performed according to NIH guidelines and protocols approved by the University of Virginia IACUC. Zebra finches (*Taeniopygia guttata*) were bred from our local colony, and juveniles were housed with their parents and siblings in smaller cages in the same room as the rest of the breeding colony. Experiments used slices from juveniles (n = 186 neurons from 105 birds, 22-44 days post hatch [DPH], median 36). Finches were bred in our colony from 22 different pairs. All birds received finch seed (Abba Products, Hillside NJ) and water *ad libitum* and were kept on a 16:8 h light:dark schedule in temperature- and humidity-controlled rooms (22°C).

Brain slice preparation and electrophysiology

Slices were prepared using methods adapted from (Zhao et al., 2011). Finches were administered a lethal intramuscular injection of Euthasol (pentobarbitol sodium and phenytoin sodium; 200 mg/kg; Hospira) and perfused transcardially with ice-cold cutting buffer (in mM: 92 NaCl, 2.5 KCl, 1.2 NaH_2PO_4, 30 $NaHCO_3$, 20 HEPES, 25 glucose, 5 sodium ascorbate, 2 thiourea, 3 sodium pyruvate, 10 $MgSO_4 \cdot 7H_2O$, 0.5 $CaCl_2 \cdot 2H_2O$; pH 7.3-7.4, 300-310 mmol/kg). The brain was removed from the skull, placed in ice-cold cutting buffer, and blocked in a custom 3D printed brain holder (http://3dprint.nih.gov/discover/3dpx-003953) on a dorsorostral to

ventrocaudal plane pitched 65 degrees forward of the transverse plane, so that slices through the auditory pallium would be approximately orthogonal to the ventral mesopallial lamina (LMV) and parallel to columnar axons connecting CM with field L (Fig. 1A; Wang et al., 2010). Sections were cut at 300 μm (VF-200 Compresstome; Precisionary Instruments) in room-temperature cutting buffer, transferred to 32°C cutting buffer for 5-10 min and then to room-temperature holding buffer (in mM: 92 NaCl, 2.5 KCl, 1.2 NaH_2PO_4, 30 $NaHCO_3$, 20 HEPES, 25 glucose, 5 sodium ascorbate, 2 thiourea, 3 sodium pyruvate, 2 $MgSO_4 \cdot 7H_2O$, 2 $CaCl_2 \cdot 2H_2O$; pH 7.3-7.4, 300-310 mmol/kg). Slices were allowed to recover for at least 1 h before recording. All solutions were bubbled with 95% O_2 · 5% CO_2 mixture.

Slices were transferred to a recording chamber (RC-26G; Warner Instruments) perfused with standard recording ACSF (in mM: 124 NaCl, 2.5 KCl, 1.2 NaH_2PO4, 24 $NaHCO_3$, 5 HEPES, 12.5 glucose, 2 $MgSO_4 \cdot 7H_2O$, 2 $CaCl_2 \cdot 2H_2O$; pH 7.3-7.4, 300-310 mmol/kg) at a rate of 1-2 mL/min and a temperature (at the perfusion chamber outlet) of 31.2 ± 0.4 °C (mean ± SD). This temperature is lower than normal physiological temperature of 38-44 °C (Zann, 1996), but was the highest at which slices remained healthy and recordings stable. There may be some differences in physiological properties at higher temperatures, but we note that spiking patterns did not differ qualitatively in a small number of recordings we obtained at room

temperature (not included here). Visually guided, whole-cell patch-clamp recordings were obtained under 60X infrared (900 nm) DIC optics. CM was located relative to LMV and the internal occipital capsule (CIO), which both comprise dense myelinated fibers visible as dark bands under brightfield or IR illumination (Fig. 1B). Most neurons were recorded from the lateral subdivision of CM (CLM), which is superior to CIO in this sectioning plane. Recording pipettes were pulled from filamented borosilicate glass pipettes (1.5 mm outer diameter, 1.10 mm inner diameter; Sutter Instruments) and were filled with an internal solution (in mM: 135 K-gluconate, 10 HEPES, 8 NaCl, 0.1 EGTA, 4 MgATP, 0.3 NaGTP, 10 Na-phosphocreatine; pH 7.2-7.3, 290-300 mmol/kg). In some experiments, the internal solution also contained 0.5% biocytin. Electrodes had a resistance of 3-8 MΩ in the bath. Voltages were amplified with a Multiclamp 700B amplifier (Molecular Devices Corporation) in current-clamp mode, low-pass filtered at 10 kHz, and digitized at 40 kHz with a Digidata 1440A. Pipette capacitance was neutralized, and 8-12 MΩ of series resistance was subtracted by bridge balance. Recorded voltage was corrected offline for measured liquid junction potential of 11.6 mV (at 32°C). Current injections and data collection were controlled by pClamp (version 10.4; Molecular Devices). Neurons were excluded from further analysis if the resting membrane potential was above -55 mV or if action potentials failed to cross -10 mV. Input and series resistance were monitored throughout the recording with 500-1000 ms

injections of hyperpolarizing current at two different amplitudes, and the recording was terminated once the input resistance, series resistance, or resting potential deviated by more than 20% from baseline.

At the end of many recordings, photomicrographs at 4X magnification were taken of the slice and the electrode *in situ* to allow later reconstruction of the cell location. LMV, CIO, and the ventricular surface were traced and aligned to reference images of myelin and Nissl sections cut in the same sectioning plane from two adult zebra finches. These sections were prepared by perfusing the animals with 4% paraformaldehyde in saline, storing the brain in fixative for 1-4 d prior to blocking, and cutting sections at 60 μm. Alternating sections were stained for Nissl (with cresyl violet) or myelin (with Black-Gold II). After aligning the tracings, the location of the electrode tip was recorded relative to the midline, the ventricle, and LMV. When the electrode contained biocytin, recordings were ended by slowly withdrawing the electrode from the cell until it detached and formed an outside-out patch, as evidenced by a sharp increase in resistance. The slice was allowed to rest in the recording chamber for 5-10 min and then fixed in 4% paraformaldehyde for 12 h. After fixation, slices were washed in 0.1 M PBS containing 0.3% Triton X-100 (Sigma) 3 times for 20 min, then incubated overnight on a shaker at room temperature in PBS/Triton-X containing 1.5 μg/μL of streptavidin-conjugated Alexa-Fluor 488 (Molecular Probes).

Sections were washed 3 times for 10 minutes in PBS, mounted on slides, and coverslipped with Prolong Gold Antifade Mountant (Molecular Probes). After the mounting agent cured overnight, neurons were imaged on a Nikon C2 confocal microscope and the image stacks traced using Neurolucida (version 11, MicroBrightField). A few cells were instead stained using avidin-biotinylated peroxidase (Vector ABC staining kit, Vector Labs) with 3,3-diaminobenzidine as the chromogen. These neurons were traced directly in Neurolucida on a Leica DM LB microscope and Retiga-2000R camera. In neither preparation was I able to definitively identify axons or trace their projections. There was some evidence of spines that were incompletely filled, which suggests that the biocytin did not fill the finest processes in high enough concentration to give good signal. Every effort was made to restrict analysis to processes that were clearly dendrites, with tapering diameter and Y-shaped bifurcations. However, it is possible that some of the processes were axons.

In pharmacological experiments, after establishing a baseline, the bath was perfused with standard ACSF containing a cocktail of drugs to block fast synaptic transmission: 10 μM (±)-3-(2-Carboxypiperazin-4-yl)propyl-1-phosphonic acid (CPP; Alomone Labs), 20 μM 6-Cyano-7nitroquinoaxline-2,3dione disodium salt hydrate (CNQX; Alomone Labs), and 10 μM (+)-Bicuculline (Sigma). Several minutes

after this treatment took effect, as indicated by increased input resistance and decreased variance in the membrane potential, I infused solution containing the cocktail and one of the following potassium channel blockers: 2 mM 4-aminopyridine (4-AP; Sigma), 100 nM α-dendrotoxin (Alomone Labs), or 100 nM charybdotoxin (Alomone Labs).

Signal Processing and Analysis

Action potentials often decreased in amplitude and broadened in duration over the course of stimulation, so they were detected in voltage recordings using a dual-threshold procedure. The initial detection threshold was set at 35% of the difference between the peak of the first spike in each sweep and its takeoff point (the time at which dV / dt first exceeded 10 times its standard deviation). Spikes that crossed this relatively low threshold (mean ± SD: -36 ± 5 mV) were extracted, resampled to 80 kHz, and aligned to peak time. Only spikes that peaked at least 10 mV above the detection threshold and that were less than 8 ms in width (at half-height) were kept. This procedure excluded the broad voltage oscillations observed in some neurons during prolonged depolarization. The takeoff point and detection threshold are shown in the insets of Fig. 1C-F as an example of this calculation. The following action potential shape measurements were taken from the first spike in response to a depolarizing stimulus: spike threshold was defined as the takeoff point; spike width was measured halfway between the takeoff

point and the peak; after-hyperpolarization (AHP) amplitude was measured relative to the takeoff point; and AHP time was measured relative to the peak.

The instantaneous firing rate in response to depolarizing current pulses (f_0) was defined as the reciprocal of the first interspike interval (and was therefore undefined when there was only a single spike), and the steady-state firing rate f_{SS} was calculated from the number of spikes emitted in the last 1000 ms of the pulse. Depolarizing pulses were typically 2000 ms in duration, but due to technical errors a small proportion of sweeps (7%) were 1500 or 1750 ms. Excluding these data from analysis or altering the time period over which f_{SS} was calculated did not qualitatively affect the results, presumably because adaptation tended to reach its maximum within a few hundred ms (Fig. 1D). The adaptation ratio A was defined as $(f_0 - f_{SS})/f_0$. The response duration *D* was defined as the time elapsed between the first and the last spikes of the pulse, except responses with only one pulse, which were assigned a duration equal to the width of the spike plus the AHP time. Cells were considered to be narrow-spiking (n = 17/186) and excluded from analysis if the spike width was less than 0.8 ms or the maximum f_{SS} exceeded 30 Hz. Some broad-spiking neurons (n = 6/169) produced irregular or bursting firing patterns that were not well quantified by these measures and were also excluded.

Membrane time constants (τ_m), resting input resistance (R_m), and capacitance (C_m) were estimated from hyperpolarizing step currents by fitting a sum of two exponential functions to the voltage decay (using Chebyshev polynomial regression). Neurons were excluded from this analysis if the mean squared error of the fit exceeded 0.1 mV (n = 2/163). The term with slower time constant and positive amplitude was associated with the sag current and was not further analyzed. From the faster, negative term, I calculated R_m from the amplitude, τ_m from the time constant, and C_m from the identity $C_m = \tau_m / R_m$. Current-voltage (I-V) curves were measured from voltage deflections to 1500-2000 ms current pulses. Peak and plateau values were used from negative pulses, and plateau values were used from positive pulses that evoked transient or onset responses. I-V curves were smoothed and interpolated using loess regression to estimate the minimum depolarized voltage at which input resistance was 50% of its maximum value (V_{OR}). The slope at rest was used to convert injected current values into predicted voltages (V*) so that I-V curves could be averaged across neurons.

Some neurons were stimulated with time-varying, broadband current protocols to determine their frequency response properties. Current waveforms 15 s in duration were generated from solutions to the Lorenz equations, which were chosen because the amplitude distribution is well constrained and the frequency distribution is band-limited. The pattern of

large depolarizations these currents produce is consistent with sensory-evoked and spontaneous *in vivo* intracellular recordings in starling CM (Perks and Gentner, 2015). Note that starlings, in contrast to zebra finches, have a more complex song and acquire new song motifs throughout life, but this is the only intracellular study of auditory responses conducted to date in this area. Meliza and I set the integration timestep so the period of the fastest oscillations was between 8-30 ms and then interpolated the waveform to linearly increase the mean frequency by 50% over the duration of the stimulus. For each neuron, we manually adjusted the scale of the waveform online so that there was robust spiking and hyperpolarization to around -100 mV. Coherence was calculated between the input waveform $s(t)$ and the elicited spike times $r(t)$ for 2-5 trials, using custom Python code based on Chronux (Bokil et al., 2010). Coherence is defined as $\boldsymbol{\gamma}(\omega)= (E[S(\omega)]E[R^*(\omega)])/\sqrt{|E[S(\omega)]|^2|E[R(\omega)]|^2}$ and $R(\omega)$ are the tapered Fourier transforms of $s(t)$ and $r(t)$, respectively. Note that $r(t)$ is a series of spike times; the algorithm for calculating a windowed Fourier transform of a point process is found in Chronux. E denotes the expectation calculated by averaging over tapers and trials, $||^2$ denotes the magnitude of a complex function, and * denotes the complex conjugate. In other words, the coherence is the cross-spectrum of the input and output signals normalized by the total power. The magnitude of the coherence, $|\boldsymbol{\gamma}(\omega)|^2$, ranges between

0 and 1 and indicates the degree of synchrony between the input and output as a function of frequency. Tapered Fourier transforms were estimated in sliding windows (duration 1 s, step size 50 ms), using 7 Slepian sequences with a time-bandwidth product of 3.5, and were averaged across windows, tapers, and trials. Confidence intervals for power and coherence spectra were calculated using the jacknife method (Bokil et al., 2010).

CM Somatic Model

Meliza and I constructed a conductance-based, single-compartment model for CM neurons to better understand how variation in cell size and low-threshold, voltage-gated outward currents might explain the relationship between phasicness and coherence spectra. The goal was not to create a biophysically realistic model but rather to match certain key phenomenological observations. The behaviors we sought to replicate were depolarization block to strong currents, with an equilibrium potential around -40 mV; a correlation between low-threshold outward rectification and phasic responses to weak currents; a frequency-current (f-I) curve that smoothly approaches zero firing rate (i.e., type I firing) in tonic-firing cells; and responses to complex, broadband currents that matched the coherence spectra of recorded data. The model, which was based on the ventral cochlear nucleus model of (Rothman and Manis, 2003), consisted of a single, isopotential compartment with capacitance C_m, a passive leak current I_{leak},

and the following voltage-gated currents: transient sodium (I_{Na}); A-type, rapidly inactivating potassium (I_A); high-threshold, non-inactivating potassium (I_{HT}); low-threshold, slowly inactivating potassium (I_{LT}); and hyperpolarization-activated cation (I_h). Details of the model equations are given in the Appendix.

The model was implemented using custom Python software (spyks, version 0.6.3; https://github.com/melizalab/spyks) that generates C++ code from a symbolic description of the equations of motion and parameters. The descriptor for this model is available as part of the package. The equations were integrated using a 5th-order Runge-Kutta algorithm with an adaptive error tolerance of 1×10^{-5} and an interpolated step size of 0.025 ms.

Model parameters were tuned by hand for a small number of exemplar neurons. The I-V curves, sag currents, and membrane time constants were matched by adjusting C_m, the reversal potentials, g_{leak}, and g_h. Spike shape and threshold were matched by adjusting the kinetic parameters and maximal conductances of I_{Na} and I_{HT}. As discussed by (Bianchi et al., 2012), in order for models to show depolarization block, the I_{Na} window current (i.e., the overlap between inactivation and activation curves) needed to be small, and the activation curve of the primary potassium current (I_{HT}) needed to be well above that of I_{Na}. The smoothness of the frequency-current relationships was

matched by adjusting g_A. As in the base model, the primary determinant of phasic firing to weak currents was g_{LT} (Rothman and Manis, 2003). Although the hand-tuned parameters varied from exemplar to exemplar, we found that any phasic neuron could become tonic if g_{LT} was reduced, and any tonic neuron could become phasic if g_{LT} was increased. In other words, although there were quantitative differences, the key phenomenological requirements were robust over the range of parameter values that reproduced the behavior of exemplar neurons. Therefore, for further analysis we generated a consensus model with all the parameters fixed except C_m and g_{LT}. The values of the parameters are given in the Appendix.

Coherence spectra for models were calculated from simulations using six different complex current waveforms. Each stimulus was presented 10 times. In each trial, randomly generated pink noise (1/f spectrum, band-limited to 100 Hz) with standard deviation of 20 pA was added to the driving current. The current was scaled to an RMS amplitude of 76 pA, which produced firing rates similar to what I recorded in slices.

Experimental Design and Statistical Analysis

Statistical significance of comparisons was evaluated using linear mixed-effects models (LMMs) with bird and family as random effects to account for repeated measures. Because zebra finches cannot be visually

sexed at these ages, sex was not included as a covariate in analyses. In pharmacology experiments, cell was also included as a random effect. Models were linear with a normal error assumption, except for input resistance, which did not have a normal conditional distribution and was first rank-transformed so that the test became non-parametric. Significance of fixed effects was determined using Satterthwaite approximations to estimate effective degrees of freedom, which are denoted in the text as subscripts and reflect both the sample size and within-group variances; thus, not all effects tested in a model have the same degrees of freedom. *Post-hoc* comparisons used Tukey's tests to evaluate significance. Spatial distribution of cell types within CM was tested using multivariate analysis of variation (MANOVA) with distance from midline and the proportion of distance between LMV and the ventricle as dependent measures. All statistical analyses were performed in R (version 3.4.0; RRID:SCR_001905) using the lme4 (version 1.1-13), lmerTest (version 2.0-33), and multcomp (version 1.4-6) packages. Unless otherwise stated, means are reported ± standard error.

Appendix: Model equations

The somatic CM model consists of a single, isopotential compartment with capacitance C_m. The dynamics of the voltage are described by current conservation,

$$C_m \frac{dV(t)}{dt} = I_{Na} + I_A + I_{HT} + I_{LT} + I_h + I_{leak} + I_{stim}(t) + I_{noise}(t). \quad (1)$$

Each of the currents is modeled as an ohmic conductance with zero or more gating variables. The dynamics of the gating variables obey first-order kinetics:

$$\frac{dx(t)}{dt} = \frac{x^{\infty}(V(t)) - x(t)}{\tau_x(V(t))}, \quad (2)$$

where x^{∞}(V) gives the equilibrium activation and τ_x(V) gives the time constant as functions of voltage. The equations for the currents and kinetic functions generally follow Rothman and Manis (2003b), but with some adjustments to half-activation voltages and time constants to match the spike threshold and shape in CM.

Transient Sodium

$$I_{Na} = \bar{g}_{Na} m_{Na}^3 h_{Na} (E_{Na} - V_m)$$

$$m^{\infty}(V) = [1 + \exp((-41 - V)/7)]^{-1}$$

$$\tau_m(V) = 0.077 + [0.26\exp((V + 63)/18) + 1.87\exp(-(V + 63)/25)]^{-1}$$

$$h^{\infty}(V) = [1 + \exp(-(-68 - V)/6)]^{-1}$$

$$\tau_h(V) = 1.15 + [0.036\exp((V + 63)/11) + 0.051\exp(-(V + 63)/25)]^{-1} \quad (3)$$

High-threshold Potassium

$$I_{HT} = \bar{g}_{HT}(0.85 m_{HT}^2 + 0.15 n_{HT})(E_K - V_m),$$

$$m^{\infty}(V) = [1 + \exp((-11 - V)/5)]^{-1}$$

$$\tau_m(V) = 1.35 + [0.057\exp((V + 60)/24) + 0.11\exp(-(V + 60)/23)]^{-1}$$

$$n^{\infty}(V) = [1 + \exp((-19 - V)/6)]^{-1}$$

$$\tau_h(V) = 9.65 + [0.021\exp((V + 60)/32) + 0.026\exp(-(V + 60)/22)]^{-1} \quad (4)$$

A-type Potassium

$$I_A = \bar{g}_A m_A^4 h_A c_A (E_K - V_m),$$

$$m^\infty(V) = [1 + \exp((-31 - V)/7)]^{-1/4}$$

$$\tau_m(V) = 0.193 + [0.036\exp((V + 60)/14) + 0.15\exp(-(V + 60)/24)]^{-1}$$

$$h^\infty(V) = [1 + \exp(-(-66 - V)/7)]^{-1/2}$$

$$\tau_h(V) = 1.93 + [0.0073\exp((V + 60)/27) + 0.051\exp(-(V + 60)/24)]^{-1}$$

$$c^\infty(V) = h^\infty(V)$$

$$\tau_c(V) = 19.3 + 174 * [1 + \exp(-(V + 66)/17)]^{-1} \quad (5)$$

Low-threshold Potassium

$$I_{LT} = \bar{g}_{LT} m_{LT}^4 h_{LT} (E_K - V_m),$$

$$m^\infty(V) = [1 + \exp((-48 - V)/6)]^{-1/2}$$

$$\tau_m(V) = 2.9 + [0.031\exp((V + 60)/6) + 0.083\exp(-(V + 60)/45)]^{-1}$$

$$h^\infty(V) = (1 - \zeta)[1 + \exp(-(-71 - V)/10)]^{-1} + \zeta \ (\zeta = 0.5)$$

$$\tau_h(V) = 96.5 + 1000[0.52\exp((V + 60)/20) + 0.52\exp(-(V + 60)/8)]^{-1} \quad (6)$$

Hyperpolarization-activated cation current

$$
\begin{aligned}
I_h &= \bar{g}_h h_h (E_h - V_m), \\
h^{\infty}(V) &= [1 + \exp(-(-76 - V)/7)]^{-1/2} \\
\tau_h(V) &= 48.25 + 10^5 [123 \exp((V + 60)/12) + 8.8 \exp(-(V + 60)/14)]^{-1}
\end{aligned}
\tag{7}
$$

Leak current and consensus parameters

The leak current is passive: $I_{leak} = g_{leak}(E_{leak} - V)$. In the consensus model, $\bar{g}_{Na} = 750$ nS, $E_{Na} = 40$ mV, $\bar{g}_{HT} = 95$ nS, $\bar{g}_A = 30$ nS, $E_K = -82$ mV, $\bar{g}_h = 0.5$ nS, $E_h = -43$ mV, $\bar{g}_{leak} = 1.3$ nS, and $E_{leak} = -75$ mV.

Chapter 3: Experience-dependent Development of Phasic Excitability in the Zebra Finch Auditory Caudal Mesopallium

Abstract

Sensory systems undergo experience-dependent changes during development. In songbirds, the caudal mesopallium (CM) is a cortical-level auditory area involved in learning and processing conspecific vocalizations. In juvenile zebra finches, putatively excitatory CM neurons show a diverse range of intrinsic firing patterns. Phasic-spiking neurons that fire briefly at the onset of a depolarizing current injection are better able to encode rapid modulation frequencies found in zebra finch song, whereas tonic-spiking neurons that fire sustained responses act more as low-pass filters. Here, we examined how these firing patterns emerge over development and how they depend on experience. In normally reared birds, phasic excitability transiently peaks during the sensory acquisition phase and then re-emerges in adults. However, in female-reared birds, who were not exposed to birdsong, phasic excitability was absent during the sensory acquisition phase and only emerged in adults, suggesting song experience was important for developing phasic responses. Exposing birds to the birdsong in isolation via speaker broadcasting or a male tutor did not result in a development of phasic excitability. Phasic responses only emerged after fledging, suggesting

a critical period for phasic development. Acoustic isolation of young birds after fledging resulted in an absence of phasic responses. Additionally, birds initially reared in isolation that were introduced to the colony after fledging also did not develop phasic excitability. This suggests there are multitude of environmental factors that contribute to development of normal phasic responses and other passive membrane properties, including exposure to colony acoustics, and interaction with a male tutor.

Introduction

The development of functional neural circuitry often depends on early postnatal experience (Katz and Shatz 1996; Iyengar and Bottjer, 2002). This phenomena has been studied extensively in songbirds, which require exposure to the song of an adult tutor early in life to produce a species-typical song (Doupe and Kuhl, 1999; Brainard and Doupe, 2002; London, 2017). Although much of this research has focused on how song experience forms a template that guides sensorimotor development, there is evidence that song experience also affects auditory perception more broadly, which is important not only for providing accurate feedback during vocal learning but also for the ability to use songs and other vocalizations to identify individuals and select mates (Riebel et al., 2002; Lauay et al., 2004; Woolley, 2012), often in challenging acoustic conditions.

In songbirds, the caudal mesopallium (CM) is a cortical-level auditory region (Wang et al., 2010) that is preferentially selective for familiar conspecific song (Gentner and Margoliash, 2003; Jeanne et al. 2011; Meliza and Margoliash, 2012). CM receives input from the thalamorecipient region, L2a, where neuronal responses are simple and linear (Sen et al., 2001). In contrast, the spectrotemporal receptive fields (STRFs) in CM are more complex (Sen et al., 2001), and invariance to production variability increases (Meliza and Margoliash 2012). These functional properties of CM contribute to the ability of songbirds to process birdsong for vocal learning and auditory perception.

Neurons in CM have varying intrinsic physiological properties that may play a role in their ability to process complex natural stimuli. The broad-spiking neurons in CM exhibit a diverse range of intrinsic firing patterns. Phasic-spiking (PS) patterns were defined by their short latency, only firing one or few action potentials at the onset of a depolarizing stimulus. Tonic-spiking (TS) responses were sustained in comparison, and fired continuously to depolarizing stimuli. PS dynamics are regulated by a 4-AP-sensitive low-threshold K^+ current, and are better suited to encode rapid temporal modulations. TS responses better encode slower modulations (Chen and Meliza, 2017). How this diversity emerges is currently unknown.

In rat auditory and somatosensory cortex, intrinsic phasic excitability is present in very young animals and is regulated through experience and age (Metherate and Aramakis, 1999; Maravall et al., 2004). Early auditory experience contributes to song perception in zebra finches that use song experience to form preferences for particular song features in mate selection (Woolley, 2012), and affects the response properties of midbrain and forebrain firing rates (Woolley et al., 2010). To understand how song experience impacts intrinsic response properties of CM, we first manipulated the acoustic environment by female-rearing zebra finches in sound-isolation boxes and removing the father after the first egg hatched.

Using whole-cell electrophysiology, we tracked intrinsic physiology in CM from pre-sensory learning through adulthood. We found that phasic excitability transiently emerges after fledging and peaks during the sensory acquisition phase of song learning in colony-reared birds. However, in female-reared birds, which were not exposed to birdsong but were able to hear other vocalizations such as female and juvenile calls, phasic excitability was nearly absent in juveniles. These data indicate that there are experience-dependent intrinsic physiological changes in CM neurons that could contribute to auditory processing during a critical stage in development .

Results

A transient increase in phasic excitability during sensory acquisition depends on experience

To investigate the development of phasic excitability over time, we made whole-cell recordings from CM in colony-reared (CR) animals at pre-sensory learning (18-20 dph), onset of sensory learning (25-27 dph), middle of sensory acquisition (28-33 dph), end of sensory acquisition (34-37 dph), post-sensory learning (65-70 dph), and adult crystallized (100+ dph) time points.

In a previous study, we found that a substantial proportion of broad-spiking CM neurons in juveniles between 22-44 dph gave phasic responses to depolarizing currents (Chen and Meliza). In contrast, the responses of neurons in very young animals (18–20 dph) were almost all sustained, with regular spiking intervals (Fig). Phasic firing was first seen at 25-27 dph and throughout the sensory acquisition phase (25–37 dph), but was nearly absent by 65-70 dph. There were phasic neurons in adults, but they were less prevalent than in juveniles. To quantify these changes, we measured the average spiking response duration between rheobase and 75 pA above rheobase; this range excludes phasic firing due to depolarization block. We also used a binary classification in which neurons were defined as phasic-spiking (PS) if they did not display sustained firing at any level of current stimulation. At 18-20 dph, before the onset of the sensory learning

period and immediately after fledging, almost all cells in CM were tonic-spiking and had high response durations (Fig. 1B). During the sensory acquisition phase, responses become more phasic, and the proportion of PS neurons increased, peaking between 28–33 dph. (Fig. 1C, D). The increase in intrinsic phasic excitability during the sensory acquisition period did not persist into the post-sensory phase or adulthood. Average response durations and proportion of PS cells were statistically indistinguishable from pre-sensory levels at 65-70 dph (Fig. 1C, D). There was a slight increase in phasic excitability in adult birds. This effect was not significant in response duration, but the proportion of PS cells was greater than pre-sensory levels (Fig. 1C, D).

The emergence of phasic excitability in juveniles coincided with the onset and offset of the sensory acquisition period, which suggested that it might be related to vocal development. However, there was no evidence for any difference between adult males and females. We did not sex juveniles due to the lack of visible plumage differences, but subjects were chosen at random and likely included approximately equal numbers of males and females. Because bird identity was included as a random effect in statistical analyses, we were able to estimate the variance between individuals, which was low (0.09) compared to the effect size (1.07), but we were unable to definitively determine whether there are sex differences in juveniles. In older animals,

plumage differences allowed males and females to be analyzed separately. Between 65-344 dph, both males and females showed similar levels of phasic excitability (Fig. 1E). Taken together, these data indicate that the development of phasic excitability is not sex-specific.

The emergence of phasic firing just after fledging suggested that it could depend on auditory experience. Male zebra finches do not sing in the nest (Zann, 1996), so fledging represents the first time when juveniles are exposed to song in the context of social interactions. To determine the effects of early experience on the intrinsic physiology of CM neurons, we recorded in brain slices from animals that were not exposed to song. Zebra finch pairs were placed in sound boxes to nest; once the first egg of the clutch hatched, the father was removed from the sound box. In contrast to the colony-reared birds, spiking responses in these female-reared (FR) animals were nearly all tonic (Fig. 1B). The proportion of phasic cells remained relatively low, but some PS neurons were seen at 65 dph onwards, though the change in average response duration at these time points was not statistically significant (Fig. 1C,D).

Because female-reared males will still produce song, albeit with many abnormal features (Morrison and Nottebohm, 1993; Brainard and Doupe, 2002), the males and females in this condition were separated after

becoming independent (about 35 dph) to avoid exposing FR females to any kind of song. There was a trend for FR males to have more phasic responses compared to FR females (Fig. 1F), but the difference was not statistically significant. These results demonstrate that impoverishing the acoustic environment through female-rearing prevents the normal development of phasic excitability just prior to and throughout the sensory acquisition phase.

Hearing song is not sufficient for the development of phasic excitability

In addition to removing birdsong from the acoustic environment, female-rearing requires clutches to be housed in visual and acoustic isolation from other finch families and removes any potential social interaction with a tutor. These factors could also be necessary for phasic firing to develop. To test this hypothesis, we attempted to rescue phasic excitability by selectively exposing juveniles to song using two conditions. The pair-rearing (PR) condition was identical to the female-rearing condition, except the sire was not removed. In the broadcast-rearing (BR) condition, the sire was removed, but the recorded song of an individual male was played through computer speakers at random intervals with the same average rate sung by a male living with his family (once per 310 seconds). We cut slices from these animals at 30-37 dph (median = 36 dph), the age when phasic firing peaked in normal conditions. Neurons from these slices were almost all tonic-firing,

and there was no significant difference compared to female-reared birds in either condition (Fig. 2C, D).

Exposure to colony conditions after initial deprivation does not restore phasic excitability

Phasic excitability emerged during the sensory-learning period in CR birds shortly after fledging around 18 dph, suggesting that a critical period may exist during this window. To test if experience after fledging is required for developing phasic excitability, we moved birds from the colony to sound isolation boxes after fledging, and made whole-cell recordings at 30-37 dph (median = 34 dph). In these deprivation-reared (DR) birds, almost all neurons were tonically firing (Fig. 3B), and there was no difference compared to female-reared birds (Fig. 3C, D).

Conversely, we predicted that phasic responses may develop in birds raised in isolation if exposed to colony conditions after fledging. We raised clutches in isolation boxes until 18 dph, and then introduced them into the colony for exposure-rearing (ER). The father was not moved back in with the clutch, as we were concerned if the father would attack the fledglings because they were unfamiliar. An opaque barrier was placed on the walls of the cage to avoid any social or learning interaction with adult males. Almost all neurons

were tonic-spiking (Fig. 3B, C), with no significant difference compared to female-reared birds (Fig. 3D).

Taken together, the results of these experiments support our hypothesis that auditory experience after fledging is important for developing phasic responses, but also indicate that experience before fledging is also important.

Passive membrane properties are altered in female-reared birds

Phasic responses did not develop in birds exposed to colony-conditions after fledging, suggesting that experience even before fledging can impact the development of intrinsic dynamics. To determine if there was an early trace of experience before the emergence of phasic firing, we analyzed passive membrane properties of CR and FR birds during the first time point (18–20 dph). Although firing patterns were indistinguishable between these groups at this age, resting membrane potential and input resistance were already lower in FR compared to CR birds (Fig. 4A,B) by this time. Membrane capacitance was slightly higher in FR birds, but this difference was not statistically significant (Fig. 4C). As previously shown in older juveniles, phasic excitability is associated with higher resting potential, higher input resistance, and lower membrane capacitance (Chen and Meliza, 2017), so these results suggest that the auditory environment birds experience while

still in the nest has already begun to determine the physiological properties of neurons during sensory acquisition.

Discussion

In this study, we investigated the experience-dependent development of phasic excitability in CM. Phasic excitability transiently emerged after fledging during the sensory acquisition phase of song learning, and diminished after it ended. Female-reared birds, who were raised in acoustic isolation boxes and did not experience birdsong, failed to develop phasic excitability during this period, indicating that this form of intrinsic plasticity depends on experience. Exposing birds raised in acoustic isolation boxes to song through playback or interaction with a male tutor failed to rescue phasic firing, and neither did introducing isolated birds to colony conditions after fledging. These results suggest that early colony auditory experience is necessary for normal development of intrinsic physiological properties in CM during a critical developmental period.

Experimental Limitations

In our experimental rearing conditions, we attempted to cover as many factors of colony-rearing conditions as possible, but were not able to recapitulate all aspects. Colony-reared birds are exposed to birdsong and calls from dozens of other birds, all interacting with each other. We were

unable to restore phasic firing in any of our experimental rearing conditions, but this may be because we did not cover the entire gamut of colony-rearing qualities. Further work is needed to determine what aspects of the colony-rearing experience are necessary for the emergence of phasic excitability. It is still unclear to what extent male tutor interaction contributes to developing phasic responses, though it is known that social interaction is an important aspect of developing auditory perception (Sturdy et al., 2001; Lauay et al., 2004; Chen et al., 2016), and for closing the sensory acquisition period (Morrison and Nottebohm, 1993). We have not yet investigated the effects of a combination of colony acoustics and birdsong without social interaction. Rearing birds in the colony without a male tutor would fill this gap. Likewise, pair-rearing birds in isolation with sound-level calibrated broadcasted or yoked colony noise would replicate almost all the colony-rearing conditions, except inter-clutch visual and social interactions. This condition should be able to recapitulate the phasic excitability seen in colony-reared animals. Additionally, more investigation into the when and if a critical period exists for the auditory system is required, as this question is still open.

Rearing in sound isolation boxes limited the number of birds in the environment to a single-pair and their offspring at most, limiting visual interaction with other birds in the colony. These conditions possess the

same acoustic qualities such as birdsong and calls as colony condition, but in greatly reduced quantity. The disparity in number of birds present these rearing environments could result in differences in overall sound levels. In pair-rearing conditions, young birds were only able to socially interact with one male tutor, whereas in the colony, many males are singing concurrently. It is possible that male tutors will sing louder in the presence of competing birdsongs to allow their songs to be more salient to mates or tutees, and that this environmental pressure is absent in sound boxes, leading to a decrease in overall sound level and auditory drive. Whole-cell recordings were only able to sample a small number of neurons in CM, which may not give a completely accurate assessment of population spiking dynamics. Additionally, sampling may be biased by cell body morphology, which we have previously shown is correlated with phasic excitability (Chen and Meliza, 2017).

Auditory perceptual behavior depends on experience

Auditory discrimination behavior is important for songbirds to identify conspecifics. Song experience aids in forming preferences for conspecific song over heterospecific song (Braaten and Reynolds, 1999), and is also important in forming preferences for high-quality courtship songs (Chen et al., 2017). Specifically, auditory experience helps tighten perceptual discrimination of song features such as absolute and relative pitch, and

identifying individual song notes (Sturdy et al., 2001). Birds reared in the absence of birdsong fail to behaviorally distinguish between normal song and isolate songs (Lauay et al., 2004), and are diminished in their ability to discriminate pitch (Sturdy et al., 2001). Early auditory experience is important for development of auditory perception, though the neural substrate that underlies these perceptual behaviors is not well understood.

Experience-dependent changes in auditory functional properties

Functional changes can occur in response to experience, contributing to the processing capabilities of the auditory system. The statistics of early auditory experience can yield persistent effects on the functional properties of primary auditory areas in birds and mammals. In songbirds, the development of neural selectivity for song features in the primary auditory region, Field L, is dependent on song exposure (Cousillas et al., 2004), colony acoustics and social experience (Amin et al., 2013). Experience-dependent changes in functional properties are also seen in mammalian auditory midbrain and cortex that representative of experienced acoustic qualities (Clopton and Winfield, 1976; Poon and Chen, 1992; Zhang et al., 2001; Zhou and Merzenich, 2008; Kim and Bao, 2009). Most of the manipulations used in mammalian studies exposed animals to unnatural, artificial stimuli, making the findings of these experiments difficult to generalize in the context of naturally-occurring auditory signals.

The results of this study demonstrate that CM is plastic to early auditory experience with ethological auditory signals, similar to Field L. Rearing birds in isolation led to loss of phasic excitability that was normally prevalent during the sensory acquisition period. Female-rearing deprived birds of birdsong, direct tutor interaction, and colony acoustics, and prevented the development of phasic responses (Fig. 1). Introducing birdsong and/or tutor interaction to isolate birds was also unable to restore phasic firing, implying that a combination of these components that is present in colony conditions is necessary. Our findings indicate that the structure of the auditory environment is important for the development of the auditory system, but exact components and their interactions still required further investigation.

Intrinsic plasticity

The main underlying mechanism for experience-dependent plasticity during development is primarily thought to be synaptic, but our findings here present a clear effect of experience on intrinsic properties. Intrinsic plasticity is characterized by modifications to inherent physiological properties of individual neurons (Schulz, 2006), and often manifests as changes in overall neuronal excitability (Zhang and Linden, 2003; Turrigiano, 2011). In many cases, intrinsic excitability increases in response to sensory deprivation (Desai et al., 1999; Aizenman et al., 2002; Kotak et al., 2005; Xu et

al., 2007; Mowery et al., 2015). Experience-dependent development of diverse firing patterns have also been noted in mammalian cortical regions. In rodent somatosensory and auditory cortex, phasic responses are found in very young animals during early development periods and are thought to be present only in immature neurons, but dissipate with age and experience (Metherate and Aramakis, 1999; Maravall et al., 2004).

Birds reared in the absence of birdsong showed a loss of phasic excitability, suggesting that experience is required for the development of phasic responses. However, our study did not completely prevent birds from hearing, and only removed one particular salient natural communication signal during female-rearing. In contrast to mammalian auditory and somatosensory cortex, phasic firing is near absent in birds reared in isolation, indicating that phasic responses in CM are not a property of immature neuronal development. Interestingly, introducing birdsong to environment of isolate birds in the form of broadcasted song or a male tutor was not sufficient to induce phasic response development (Fig. 2). We initially hypothesized that exposure to the temporal statistics of birdsong could act as an instructive signal for developing phasic responses that can process rapid temporal modulations present in birdsong, but this is not the case. The findings of this study indicate that the structure of the acoustic

environment is important for shaping intrinsic properties of CM neurons, but their contributions to behavior is still an open question.

Implications of experience-dependent intrinsic plasticity in CM

The emergence of phasic excitability coincides with the sensory acquisition phase of song learning, suggesting it is associated with formation of the tutor template. But phasic excitability appears to be present in both sexes (Fig. 1), so this also implies it is important for broader auditory perception, and may correlate with song preference formation and perceptual discrimination. It is possible that abnormal songs produced by isolate males may be the result of distorted auditory feedback and processing during self-practice due to improper auditory development in addition to disruption in formation of tutor song memory. The decrease in phasic excitability in older animals suggests it is associated with the closure of the sensory acquisition phase. Finches typically form a template of tutor song at this time, and birds that have been raised in visual isolation from adult tutors or in complete isolation are still able to modify their songs in adulthood when the bird's own song is normally crystallized and non-modifiable (Morrison and Nottebohm, 1993), indicating that this window of plasticity has not closed. The absence of phasic responses in our isolate conditions may be correlated with the failure to close the sensory acquisition period.

Persistent auditory perceptual deficits are seen in songbirds reared without developmental song exposure (Sturdy et al., 2001; Chen et al., 2017), suggesting that a critical period for auditory perception and processing may exist. In the mammalian auditory system, experience-dependent changes in intrinsic excitability caused by induced hearing loss occurred during an early development critical period (Kotak et al., 2005; Xu et al., 2007; Mowery et al., 2015). We posited that experience-dependent changes in intrinsic physiology similarly occur during a critical period early in life to develop the auditory system and form a memory of song before the onset of the sensory acquisition period. Seeing that phasic excitability emerged shortly after fledging, we hypothesized that fledging was the start of this critical period. However, we were unable to accurately identify a specific window of time for this intrinsic plasticity, noting that colony experience before and after fledging is important for the emergence of phasic excitability during the sensory acquisition phase (Fig. 3).

Early experience affected intrinsic spiking dynamics in CM, but also led to changes in passive membrane properties. Lowered auditory drive in birds reared without the full complement of colony experience could lead to changes in the expression of voltage-gated and/or background currents, as seen in the activity-dependent regulation of voltage-gated ion channels in interneurons of the somatosensory cortex via transcription factor Er81

(Dehorter et al., 2015) and pyramidal neurons in layer V of motor cortex (Paz et al., 2009), and background K^+ currents in LE neurons of *Aplysia* (Antonov et al., 2001). Transcriptional regulation of ion channels may be a mechanism for intrinsic plasticity in CM. Female-reared birds had more negative resting potential and lower input resistance compared to colony-reared birds before the age when phasic responses typically emerged (Fig. 4), which is consistent with more tonic neuron properties (Chen and Meliza, 2017). Intrinsic plasticity in CM not only modifies low-threshold voltage-gated potassium channels, but also background conductances such as potassium leak currents.

Conclusions

Our findings suggest that early auditory experience shapes the intrinsic dynamics of CM neurons. Normal development of phasic excitability in CM requires a multitude of factors involving early experience with birdsong, social interaction and a rich acoustic environment comprised of natural communication signals produced by a large number of individuals. This may hold larger implications for investigating the effects of early auditory experience in language acquisition in humans, who similarly rely on early exposure to speech to develop language skills. Neuronal specializations formed through experience-dependent changes in physiology and

morphology early in life may help further our understanding of how language and speech is processed in the auditory system.

Figures

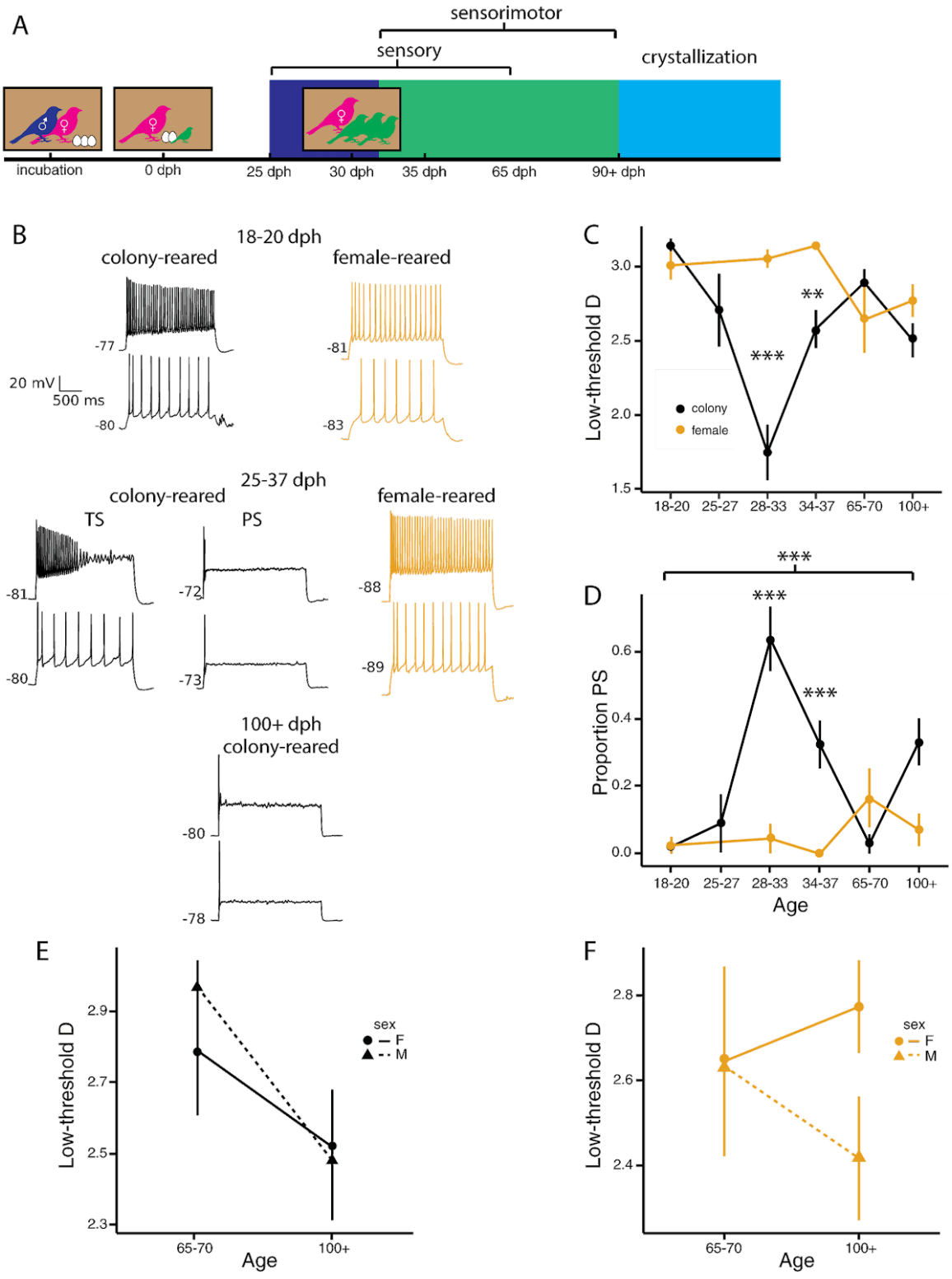
A
sensorimotor
sensory
crystallization
incubation
0 dph
25 dph
30 dph
35 dph
65 dph
90+ dph
B
18-20 dph
colony-reared
female-reared
-77
-80
-81
-83
20 mV
500 ms
25-37 dph
colony-reared
TS
PS
female-reared
-81
-80
-72
-73
-88
-89
100+ dph
colony-reared
-80
-78
C
Low-threshold D
3.0
2.5
2.0
1.5
**
***
colony
female
18-20
25-27
28-33
34-37
65-70
100+
D
***
***
***
Proportion PS
0.6
0.4
0.2
0.0
18-20
25-27
28-33
34-37
65-70
100+
Age
E
Low-threshold D
2.9
2.7
2.5
2.3
sex
F
M
65-70
100+
Age
F
Low-threshold D
2.8
2.6
2.4
sex
F
M
65-70
100+
Age

Figure 1

Female-rearing reduces phasic excitability typically found in juvenile zebra finches.

A, Female-rearing paradigm. Brown rectangle indicates housing in sound isolation boxes.

B, Example traces of whole-cell current clamp electrophysiology.

C, Comparison of response duration (logged response duration, D) across developmental time points between CR and FR birds (28-33 dph, LMM: t_{82} = 4.38, $p < 0.001$; 34-37 dph, LMM: t_{54} = 2.99, $p < 0.01$).

D, Comparison of proportion of PS cells in CR and FR birds across developmental time points (28-33 dph, two proportion z-test: $p < 0.001$; 34-37 dph, two proportion z-test: $p < 0.001$). Proportion of PS cells between 18-20 dph and 100+ dph in CR birds is significantly different (two proportion z-test: $p < 0.001$).

E, Sex differences in duration of firing responses post-sensory learning in CR birds (65-70 dph, LMM: t_{23} = 0.157, $p = 0.877$; 100+ dph, LMM: t_{32}, $p = 0.958$)

F, Sex differences in duration of firing responses post-sensory learning in FR birds (65-70 dph, LMM: t_{23} = 0.602, $p = 0.877$; 100+ dph, LMM: t_{26} = 1.051, $p = 0.303$)

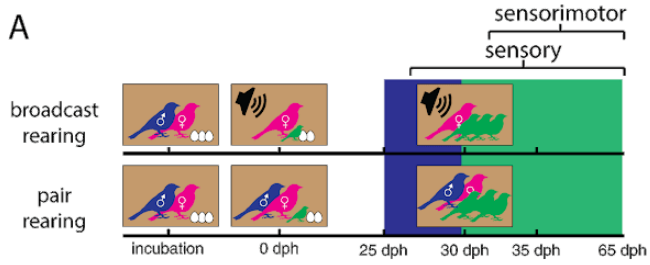
A
sensorimotor
sensory
broadcast rearing
pair rearing
incubation
0 dph
25 dph
30 dph
35 dph
65 dph

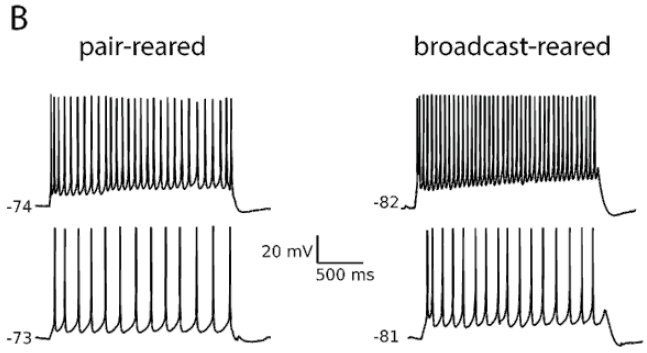
B
pair-reared
broadcast-reared
-74
-73
-82
-81
20 mV
500 ms

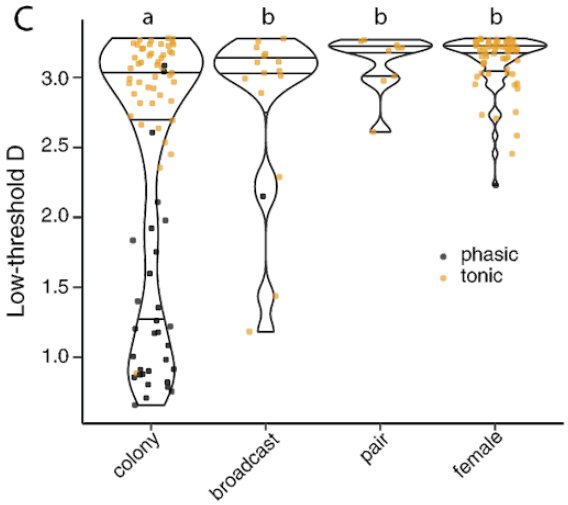
C
a
b
b
b
Low-threshold D
3.0
2.5
2.0
1.5
1.0
phasic
tonic
colony
broadcast
pair
female

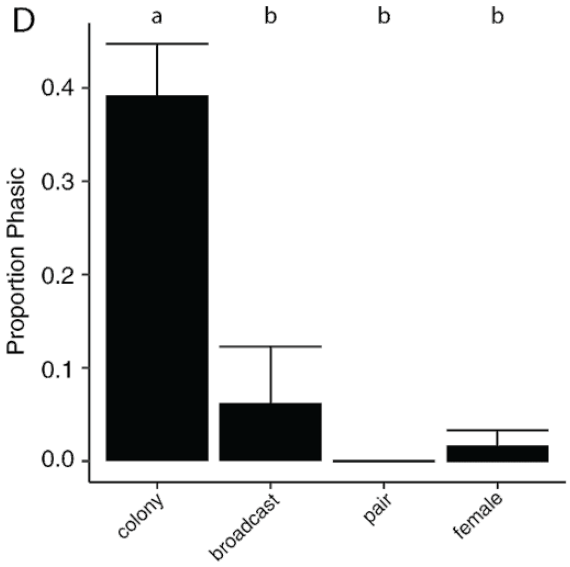
D
a
b
b
b
Proportion Phasic
0.4
0.3
0.2
0.1
0.0
colony
broadcast
pair
female

Figure 2

Broadcast- and pair-rearing does not increase phasic excitability to CR levels during the sensory acquisition period.

A, Broadcast- and pair-rearing paradigms.

B, Example traces of tonic-spiking cells in birds of both rearing conditions.

C, Violin plots showing comparisons of low-threshold D in BR and PR groups relative to FR during the sensory acquisition period (25-37 dph). Same letters between groups indicate non-significance. Bars indicate 25, 50, and 75 quartiles. Levels of phasic excitability did not differ between BR and FR (LMM: $t_{40} = 12.19$, $p = 0.22$). Levels of phasic excitability did not differ between PR and FR (LMM: $t_{48} = 0.99$, $p = 0.33$).

D, Bar plot indicating proportion of PS cells between groups (between FR and CR, two proportion z-test: $p < 0.001$).

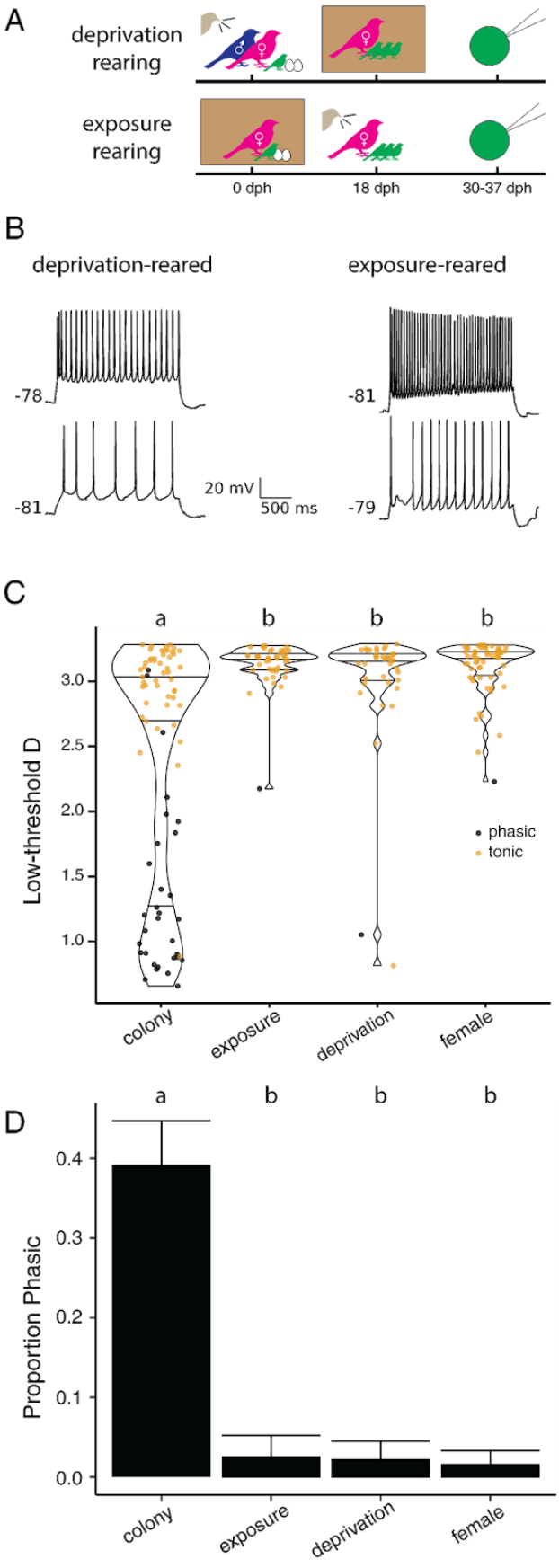
A
deprivation rearing
exposure rearing
0 dph
18 dph
30-37 dph
B
deprivation-reared
exposure-reared
-78
-81
20 mV
500 ms
-81
-79
C
a
b
b
b
Low-threshold D
3.0
2.5
2.0
1.5
1.0
phasic
tonic
colony
exposure
deprivation
female
D
a
b
b
b
Proportion Phasic
0.4
0.3
0.2
0.1
0.0
colony
exposure
deprivation
female

Figure 3

Deprivation- and exposure- rearing does not increase phasic excitability to CR levels in birds during the sensory acquisition phase.

A, Deprivation- and exposure- rearing paradigms.

B, Example traces of TS cells in birds in DR and ER conditions.

C, Violin plots showing comparisons of low-threshold D in DR and ER groups relative to FR during the sensory acquisition period (25-37 dph). Same letters between groups indicate non-significance. Levels of phasic excitability did not differ between DR and FR (LMM: $t_{49} = -0.287$, $p = 0.77$). Levels of phasic excitability did not differ between ER and FR (LMM: $t_{48} = -0.625$, $p = 0.53$).

D, Bar plot indicating proportion of PS cells between groups (between FR and CR, two proportion z-test: $p < 0.001$).

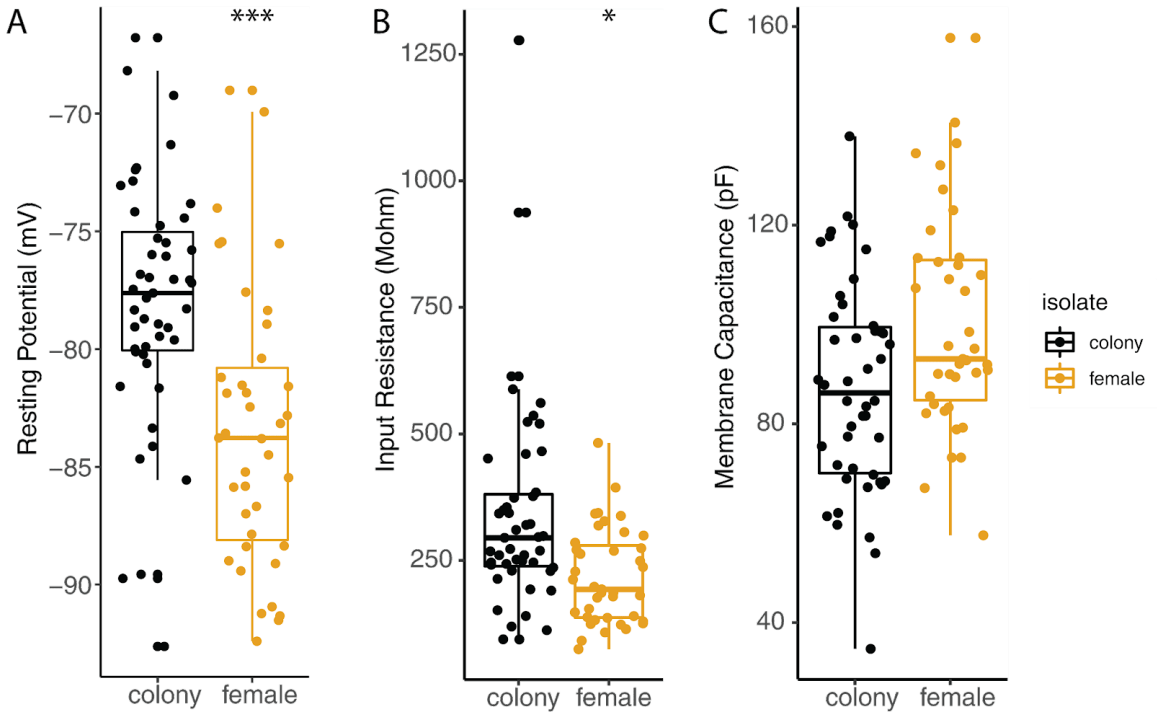

Figure 4

Comparison of passive membrane properties in FR and CR birds prior to the sensory learning phase of song acquisition.

A, Resting potential is lower in FR than CR at 18-20 dph (Tukey's Test: $z = -4.182$, $p < 0.001$).

B, Input resistance is decreased in FR birds (Tukey's Test: $z = -2.554$, $p < 0.05$)

C, Membrane capacitance shows a non-significant increase in FR birds (Tukey's Test: $z = 0.174$, $p = 0.86$).

Materials and Methods

Animals

All procedures were performed according to NIH guidelines and protocols approved by the University of Virginia IACUC. Zebra finches (*Taeniopygia guttata*) were bred from our local colony. All birds received finch seed (Abba Products, Hillside NJ) and water *ad libitum* and were kept on a 16:8 h light:dark schedule in temperature- and humidity-controlled rooms 22-24°C.

Experimental rearing conditions

In colony-reared conditions, juveniles were housed with their parents and siblings in smaller cages in the same room as the rest of the breeding colony in CR conditions (90 birds, n = 205). Of these data, 53 birds and 79 cells were previously reported in Chen and Meliza (2017). Juveniles were separated from parents around 35 dph and moved into large aviaries with the rest of the colony. Female-reared (FR) birds (34 birds, n = 202) were raised in sound isolation boxes; once the first egg in a clutch has hatched, the father was removed and placed in an separate cage in the breeding colony. In some cases, an unrelated surrogate mother was introduced into the FR cage to control for level of care, but chick survival seemed to be unaffected by this. In broadcast-reared (BR) (3 birds, n = 16) conditions, the paradigm was followed with the exception of the placement of a computer speaker into the sound box which would play pre-recorded zebra finch song. Songs were

acquired using an Audio-Technica PRO 70 cardioid condenser lavalier microphone that recorded a male and female zebra finch pair in a sound isolation box. 333 total song bouts were counted in 1740 minutes of daytime singing. Birdsong was broadcasted using a Sony PCVA-SP2 speaker during the zebra finches' daylight hours at the same bout frequency as the recorded song (1 song per 5.22 minutes). Pair-reared (PR) birds (2 birds, n = 9) were raised by both a sire and dam in sound isolation boxes. In deprivation-reared (DR) conditions (6 birds, n = 44), once a CR clutch reached 17-18 dph, the father was removed while the clutch and mother were moved into a sound isolation box. In exposure-reared (ER) conditions (6 birds, n = 38), a FR clutch was moved into the colony room at 17-18 dph and remained independently housed in a separate cage. Opaque barriers were placed on the sides of the cage to prevent visual interaction with males in neighboring cages.

Brain slice preparation and electrophysiology

Acute brain slices were prepared using methods from Chen and Meliza (2017) and adapted from Ting et al (2018). Zebra finches were administered a lethal intramuscular injection of Euthasol (pentobarbitol sodium and phenytoin sodium; 200 mg/kg; Hospira) and perfused transcardially with ice-cold HEPES (in mM: 92 NaCl, 2.5 KCl, 1.2 NaH_2PO_4, 30 $NaHCO_3$, 20 HEPES, 25 glucose, 5 sodium ascorbate, 2 thiourea, 3 sodium pyruvate, 10 $MgSO_4 \cdot 7H_2O$, 0.5 $CaCl_2 \cdot 2H_2O$; pH 7.3-7.4, 300-310 mmol/kg) or NMDG (in mM: 93 NMDG,

2.5 KCl, 1.2 NaH_2PO_4, 30 $NaHCO_3$, 20 HEPES, 25 glucose, 5 sodium ascorbate, 2 thiourea, 3 sodium pyruvate, 10 $MgSO_4 \cdot 7H_2O$, 0.5 $CaCl_2 \cdot 2H_2O$; pH 7.3-7.4, 300-310 mmol/kg) cutting buffer. The brain was blocked using a custom 3D printed brain holder (http://3dprint.nih.gov/discover/3dpx-003953). 300 µm sections were cut in ice-cold cutting buffer on a VF-200 Compresstome (Precisionary Instruments), and then transferred to 32°C cutting buffer for 10-15 min for initial recovery. Sections were then transferred to room-temperature holding buffer (in mM: 92 NaCl, 2.5 KCl, 1.2 NaH_2PO_4, 30 $NaHCO_3$, 20 HEPES, 25 glucose, 5 sodium ascorbate, 2 thiourea, 3 sodium pyruvate, 2 $MgSO_4 \cdot 7H_2O$, 2 $CaCl_2 \cdot 2H_2O$; pH 7.3-7.4, 300-310 mmol/kg) to recover for at least 1 h before use in recordings. All solutions were bubbled with 95% O_2 · 5% CO_2 mixture at least 10 minutes prior to use.

Slice recordings were conducted in a RC-26G recording chamber (Warner Instruments) perfused with standard recording ACSF (in mM: 124 NaCl, 2.5 KCl, 1.2 NaH_2PO4, 24 $NaHCO_3$, 5 HEPES, 12.5 glucose, 2 $MgSO_4 \cdot 7H_2O$, 2 $CaCl_2 \cdot 2H_2O$; pH 7.3-7.4, 300-310 mmol/kg) at a rate of 1-2 mL/min at 32°C, which was the highest and closest to physiological temperatures at which slices remained healthy and recordings stable. Whole-cell patch-clamp recordings were obtained under 60X infrared (900 nm) DIC optics. CM was located relative to LMV and the internal occipital capsule (CIO), which both comprise dense myelinated fibers visible as dark bands under brightfield or

IR illumination. Most neurons were recorded from the lateral subdivision of CM (CLM), which is superior to CIO in this sectioning plane. Recording pipettes were pulled from filamented borosilicate glass pipettes (1.5 mm outer diameter, 1.10 mm inner diameter; Sutter Instruments) using a P-1000 Micropipette Puller (Sutter Instruments) and were filled with internal solution (in mM: 135 K-gluconate, 10 HEPES, 8 NaCl, 0.1 EGTA, 4 MgATP, 0.3 NaGTP, 10 Na-phosphocreatine; pH 7.2-7.3, 290-300 mmol/kg). For some recordings, ACSF solutions were adjusted to 345-355 mmol/kg, and internal solutions were adjusted to 335-345 osmolarity to attempt to improve slice health and quality (Bottjer, 2005). No noticeable differences in slice health or quality were observed with these higher osmolarity solutions.

Electrodes had a resistance of 3-8 MΩ in the bath. Measured voltages were amplified with a Multiclamp 700B amplifier (Molecular Devices Corporation) in current-clamp mode, low-pass filtered at 10 kHz, and digitized at 40 kHz with a Digidata 1440A. Pipette capacitance was neutralized, and 8-12 MΩ of series resistance was subtracted by bridge balance. Recorded voltage was corrected offline for measured liquid junction potential of 11.6 mV at 32°C. Current injections and data collection were controlled by pClamp (version 10.4; Molecular Devices). Neurons were excluded from further analysis if the resting membrane potential was above -55 mV or if action potentials failed to cross -10 mV. Two hyperpolarizing current injections at different amplitudes

(500-1000 ms) were used to monitor input and series resistance. Recording sweeps were excluded if the input resistance, series resistance, or resting potential deviated by more than 20% from baseline.

Signal Processing and Analysis

Analysis of current-clamp recording data followed the same procedures detailed in Chen and Meliza (2017). In brief, the response duration *D* was defined as the time elapsed (log-transformed) between the first and the last spikes of the pulse, except responses with only one pulse, which were assigned a duration equal to the width of the spike plus the AHP time. Because phasic responses in CM neurons appears to be governed by both a low-threshold potassium current and a high-threshold depolarization block mechanism (Chen and Meliza, 2017), we analyzed average spiking response duration (log scale, *D*) to quantify phasic excitability at low currents (< 75 pA above rheobase) and high currents (>75 pA above rheobase), and averaged across all current sweeps. Cells were classified as narrow-spiking if the spike width was <0.8 ms or if maximum steady state spike rate was greater than 30 Hz, and were excluded from analysis. Resting input resistance (R_m), and capacitance (C_m) were estimated from hyperpolarizing step currents by fitting a sum of two exponential functions to the voltage decay (using Chebyshev polynomial regression).

Statistical Analysis

Linear mixed-effects models (LMMs) were used for comparisons of statistical significance, with bird and family as random effects to account for repeated measures. Significance of fixed effects was determined using Satterthwaite approximations to estimate effective degrees of freedom, denoted as subscripts and reflect the sample size and within-group variances; thus, not all effects tested in a model have the same degrees of freedom. Tukey's HSD tests were used to evaluate significance *post-hoc*. Analyses were performed in R (version 3.5.1) using the lme4 (version 1.1-18-1), lmerTest (version 3.0-1), and multcomp (version 1.4-8) packages. Unless otherwise stated, means are reported ± standard error.

Chapter 4: Conclusions and Future Directions

The combined results of the work presented in this dissertation have provided insight into the contributions of cell-intrinsic mechanisms to auditory processing. Utilizing songbirds as a model organism for auditory processing gives us a unique translational perspective on this task due to their ability to process spectrotemporally complex natural auditory stimuli. CM is an excellent model for teasing apart the kinds of mechanisms that are necessary for the brain to decipher the world around it, being a crucial node in the auditory pathway for beginning to form higher level schemas for categorical discrimination. This quality is made possible by the feedforward inputs of more raw, unprocessed information and top-down factors that convey behavioral salience.

The intrinsic physiology of neurons help determine the functional dynamics of a particular region. In the hindbrain, cellular specializations allow neurons to accurately encode a time-code for coincidence detection in ITD sound localization. This is enabled by the compact electrical morphology and expression of voltage-gated potassium conductances that result in quick firing dynamics. These morphological and physiological properties determine the neuron's ability to fire precisely and accurately to an auditory stimulus (Carr et al., 2006), allowing an organism to use this information in relevant

behaviors. Neurons in CM show a diversity in selectivity to particular, familiar motifs of birdsong, as well as spike shape (Meliza et al., 2010, Meliza and Margoliash, 2012). People affected by dyslexia have phoneme-processing problems which impacts reading ability. Mutations in the gene KIAA0319 are associated with dyslexia, and reducing the expression of this gene in rats through RNA interference results in reduced neural discrimination to speech sounds in primary auditory cortical A1 neurons. Intrinsic properties were also altered when *Kiaa0319* expression is reduced. Intracellular recordings in A1 revealed that onset latencies increased, as well as higher membrane input resistance, spontaneous activity, and overall firing rates (Centanni et al., 2014). We sought to investigate what cell-intrinsic mechanisms underlie the ability of CM to process complex, natural auditory information, and by extension, piece together a further understanding of cortical-level auditory processing through the contributions of individual neurons.

CM contains neurons with a diversity of spiking patterns. These spiking patterns are also correlated with various passive electrical and morphological properties. Phasic, onset spiking patterns are associated with higher membrane potentials and input resistance, while having lower membrane capacitance, consistent with their smaller cell bodies and compact dendritic arbors. Tonic firing was associated with lower membrane potential and input resistance, and higher membrane capacitance which

match their large dendritic fields. These physiological and morphological specializations also give rise to specific functionality in auditory processing. Specifically, the intrinsic spiking dynamics of PS neurons allow them to entrain to fast modulation frequencies found in zebra finch song while TS cells behave more like low-pass filters. This functional quality of CM PS neurons is most likely one of the traits that ties into CM's reliable selectivity to conspecific song. Because PS cells seemed to be specially tuned to the temporal statistics of zebra finch song, this suggested that an experience-dependent intrinsic plasticity mechanism was responsible for tuning them to the modulations of birdsong.

Decoding acoustic signals for communications is a hallmark function of the auditory system in songbirds and humans alike. This capacity is a result of both neural plasticity and exposure to song/speech in the environment. Experiential factors are a necessity in the acquisition of song and speech, demonstrated by the malformation of birdsong in isolated birds (Brainard and Doupe, 2002), and by the inability of Japanese speakers to distinguish the phonemes for English "r" and "l". The brain also needs to be malleable to these experiences, accomplishing this through adaptive synaptic and intrinsic plasticity mechanisms. In the case of Japanese speakers, lack of experience with the auditory features of the English "r" and "l" early in life prevents them from forming distinct categories for the two phonemes

(Rauschecker, 1999), only possessing the singular liquid phoneme of a Japanese “r”. One can hypothesize that through early experience, auditory neurons in English speakers may become specially tuned to identifying and processing the spectrotemporal phonetic difference between the rhotic “r” and lateral “l”. Synaptic mechanisms involved in learning and memory have been studied thoroughly in sensory systems (Turrigiano, 2008), but the role and experiential regulation of intrinsic plasticity in processing spectrotemporally complex auditory objects is less understood in this capacity. We were able to use songbirds to investigate how auditory experience and experience-dependent changes in intrinsic physiology give rise to neuronal specializations that are relevant for processing natural communication signals.

Qualitatively modifying rearing conditions led to profound alterations in intrinsic physiology of CM neurons, including the loss of phasic responses when birds were female-reared. This suggested that the intrinsic plasticity of CM neurons can modify their temporal response properties to the temporal structure of the acoustic environment. Introducing birdsong or a male tutor to these impoverished conditions was unable to recapitulate the same level of phasic excitability seen in CR birds, suggesting other factors are also necessary. The question of whether or not this intrinsic plasticity relies on sensory experience during an early sensitive period still remains open. We

initially hypothesized that phasic excitability was dependent on experience after fledging, as we saw the emergence and peak of phasic excitability shortly after fledging. Depriving birds of colony experience after fledging led to an abolishment of phasic excitability, consistent with this hypothesis. However, exposing birds to colony conditions only after fledging did not yield the expected result of developing phasic excitability from this experience. Our results indicated that experience after nest fledging is important for developing phasic responses, but so is experience before. The exact time frame for a potential critical or sensitive period for developing phasic excitability still requires investigation. These results led us to investigate the passive membrane properties of birds raised in isolation before the period for the emergence of phasic excitability. Resting membrane potential, input resistance, and membrane capacitance were already altered in FR birds before fledging, and reflected lower levels of phasic excitability despite the lack of phasic responses in both FR and CR birds. This indicates a latent change in physiology that may prime CM neurons in CR birds to develop phasic excitability.

These physiological distinctions between phasic- and tonic-spiking are regulated by the conductances of various ion channels, but the mechanism of this intrinsic plasticity still requires further investigation. Previously, I identified that low-threshold potassium currents give rise to the marked

outward rectification and onset firing behavior of PS neurons. Application of α-dendrotoxin changed phasic firing to tonic in our pharmacological experiments. α-dendrotoxin blocks $K_V1.1$, $K_V1.2$, and $K_V1.6$ channels (Harvey, 1997) though it is unknown which of these channels is the main factor or if a combination of the three contribute to phasic excitability.

Experience-dependent intrinsic plasticity generally induces changes in the expression of voltage-gated potassium channels, which leads to shifts in physiological properties such as action potential threshold or spike rates (Zhang and Linden, 2003). Following up my electrophysiological experiments presented in Chapter 3 with a focus on quantitatively determining the developmental regulation of these channels should be the next priority. *In situ* data has shown that KCNA1 and KCNA6, the genes the encode $K_V1.1$ and $K_V1.6$ respectively, are prominently expressed in CM (Fig. 1). In conjunction with the pharmacological data from Chapter 2, this provides strong reasoning to focus on these two channels. Monitoring the expression of $K_V1.1$ and $K_V1.6$ would be a strong avenue to tracking the development of phasicness over time. If phasic excitability is reliant on the experience-dependent expression or upregulation of $K_V1.1$ and $K_V1.6$, then female-rearing should ostensibly reveal a correlative decrease in expression of these two channels in tandem with a decrease in phasicness.

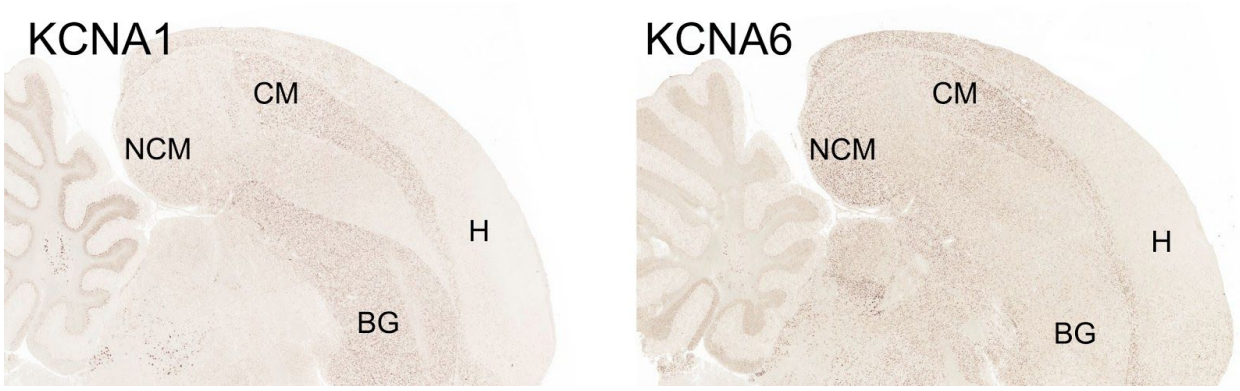

Figure 1: Sagittal ISH sections from the zebra finch brain atlas of KCNA1 (left) and KCNA6 (right), showing prominent staining for their respective genes in CM, as well as varying levels in other reference regions (Zebra Finch Expression Brain Atlas, 2018)

Real-time quantitative PCR has been accomplished in zebra finches and other songbird species (Olias et al., 2014), with a number of robust housekeeping genes available. Ideally, tissue samples of CM and other control regions such as hyperpallium, basal ganglia, and NCM would be collected from FR and CR birds and analyzed via qPCR at timepoints similar to the ones detailed in Chapter 3. A potential challenge that may arise from this approach however, is the lack of a documented methodology for precisely and cleanly extracting sections of CM for use in qPCR. Its irregular shape would make it difficult to obtain tissue punches without contamination from other regions. Expression levels of KCNA1 and KCNA6

should decrease in CM for FR birds relative to CR, correlating to a decrease in overall phasicness.

Additionally, analyzing protein expression of the candidate channels through immunohistochemistry or Western blotting would help bolster the results of the qPCR. This experiment would also provide concrete evidence for levels of channel expression. Transcription does not correlate directly with protein translation (Vogel and Marcotte, 2012), as post-transcriptional, translational, and degradation regulation also play a large role in determining protein abundance. The difficulty, however, lies in the lack of robust protein antibodies for birds. Thus, although immunohistochemical staining and Western blotting analyses would provide more convincing evidence for regulation of low-threshold channels, qPCR is more reliable and more quantitative.

Another convincing avenue would be to knock-out the genes of interest. Hypothetically, knocking out $K_V1.1$ and $K_V1.6$ would lead to a profound loss of phasicness even in CR birds. However, this is made difficult by the fact that development of transgenic zebra finches is still in its infancy. Attempts to use lentiviruses and AAVs to transfect cells in songbirds have also yielded highly variable efficacy (Heston and White, 2017) with some success in developing a germline transgenic zebra finch (Liu et al., 2015). Recently, a more robust

methodology for gene manipulation was developed for use in posthatch zebra finches (Ahmadianterhani and London, 2017). Using *in vivo* electroporation, it is possible to delivery genes for CRISPR/Cas9 gene editing. Plasmid solution can be injected into the lateral ventricle of P3 zebra finch chicks, and coerced into the region of interest by electroporating the plasmid solution with electric paddles. This approach could definitively identify which low-threshold channels are necessary for phasic firing.

The complex task of auditory categorical discrimination that CM performs is linked to its diverse intrinsic physiology and neuronal intrinsic plasticity. The previously presented data inform us that the brain does not exist in a vacuum. To fully understand the brain and sensory processing, we need to take into account the structure of experience and stimulation that the brain processes which ultimately molds to the world around it through fundamental adaptive changes in its building blocks.

References

Aizenman CD, Akerman CJ, Jensen KR, Cline HT. 2003. Visually driven regulation of intrinsic neuronal excitability improves stimulus detection in vivo. *Neuron* **39**:831–842.

Aizenman CD, Muñoz-Elías G, Cline HT. 2002. Visually driven modulation of glutamatergic synaptic transmission is mediated by the regulation of intracellular polyamines. *Neuron* **34**:623–634.

Akutagawa E, Konishi M. 2010. New brain pathways found in the vocal control system of a songbird. *The Journal of Comparative Neurology* **518**:3086–3100. doi:10.1002/cne.22383

Amin N, Gastpar M, Theunissen FE. 2013. Selective and Efficient Neural Coding of Communication Signals Depends on Early Acoustic and Social Environment. *PLOS ONE* **8**:e61417. doi:10.1371/journal.pone.0061417

Amin N, Gill P, Theunissen FE. 2010. Role of the Zebra Finch Auditory Thalamus in Generating Complex Representations for Natural Sounds. *Journal of Neurophysiology* **104**:784–798. doi:10.1152/jn.00128.2010

Amin N, Grace JA, Theunissen FE. 2004. Neural response to bird?s own song and tutor song in the zebra finch field L and caudal mesopallium. *Journal of Comparative Physiology A: Sensory, Neural, and Behavioral Physiology* **190**:469–489. doi:10.1007/s00359-004-0511-x

Antonov I, Antonova I, Kandel ER, Hawkins RD. 2001. The Contribution of Activity-Dependent Synaptic Plasticity to Classical Conditioning in Aplysia. *J Neurosci* **21**:6413–6422. doi:10.1523/JNEUROSCI.21-16-06413.2001

Antunes FM, Malmierca MS. 2014. An Overview of Stimulus-Specific Adaptation in the Auditory Thalamus. *Brain Topography* **27**:480–499. doi:10.1007/s10548-013-0342-6

Ascoli GA, Petilla Interneuron Nomenclature Group, Alonso-Nanclares L, Anderson SA, Barrionuevo G, Benavides-Piccione R, Burkhalter A, Buzsáki G, Cauli B, Defelipe J, Fairén A, Feldmeyer D, Fishell G, Fregnac Y, Freund TF, Gardner D, Gardner EP, Goldberg JH, Helmstaedter M, Hestrin S, Karube F, Kisvárday ZF, Lambolez B, Lewis DA, Marin O, Markram H, Muñoz A, Packer A, Petersen CCH, Rockland KS, Rossier J, Rudy B, Somogyi P, Staiger JF, Tamas G, Thomson AM, Toledo-Rodriguez M, Wang Y, West DC, Yuste R. 2008. Petilla

terminology: nomenclature of features of GABAergic interneurons of the cerebral cortex. *Nat Rev Neurosci* **9**:557–568. doi:10.1038/nrn2402

Atoji Y, Karim MR. 2014. Homology of the mesopallium in the adult chicken identified by gene expression of the neocortical marker cholecystokinin. *Neuroscience Letters* **562**:85–89. doi:10.1016/j.neulet.2014.01.011

Avermann M, Tomm C, Mateo C, Gerstner W, Petersen CCH. 2012. Microcircuits of excitatory and inhibitory neurons in layer 2/3 of mouse barrel cortex. *Journal of Neurophysiology* **107**:3116–3134. doi:10.1152/jn.00917.2011

Beck H, Yaari Y. 2008. Plasticity of intrinsic neuronal properties in CNS disorders. *Nature Reviews Neuroscience* **9**:357–369. doi:10.1038/nrn2371

Belmeguenai A, Hosy E, Bengtsson F, Pedroarena C, Piochon C, Teuling E, He Q, Ohtsuki G, De Jeu MTG, Elgersma Y, De Zeeuw CI, Jörntell H, Hansel C. 2010. Intrinsic plasticity complements LTP in parallel fiber input gain control in cerebellar Purkinje cells. *J Neurosci* **30**:13630–13643. doi:10.1523/JNEUROSCI.3226-10.2010

Benito E, Barco A. 2010. CREB's control of intrinsic and synaptic plasticity: implications for CREB-dependent memory models. *Trends in Neurosciences* **33**:230–240. doi:10.1016/j.tins.2010.02.001

Berwick RC, Beckers GJL, Okanoya K, Bolhuis JJ. 2012. A Bird's Eye View of Human Language Evolution. *Frontiers in Evolutionary Neuroscience* **4**. doi:10.3389/fnevo.2012.00005

Bianchi D, Marasco A, Limongiello A, Marchetti C, Marie H, Tirozzi B, Migliore M. 2012. On the mechanisms underlying the depolarization block in the spiking dynamics of CA1 pyramidal neurons. *Journal of Computational Neuroscience* **33**:207–225. doi:10.1007/s10827-012-0383-y

Bizley JK, Cohen YE. 2013. The what, where and how of auditory-object perception. *Nature Reviews Neuroscience* **14**:693–707. doi:10.1038/nrn3565

Blundon JA, Roy NC, Teubner BJW, Yu J, Eom T-Y, Sample KJ, Pani A, Smeyne RJ, Han SB, Kerekes RA, Rose DC, Hackett TA, Vuppala PK, Freeman BB, Zakharenko SS. 2017. Restoring auditory cortex plasticity in adult mice by restricting thalamic adenosine signaling. *Science* **356**:1352–1356. doi:10.1126/science.aaf4612

Bokil H, Andrews P, Kulkarni JE, Mehta S, Mitra PP. 2010. Chronux: a platform for analyzing neural signals. *J Neurosci Methods* **192**:146–151. doi:10.1016/j.jneumeth.2010.06.020

Boogert NJ, Giraldeau L-A, Lefebvre L. 2008. Song complexity correlates with learning ability in zebra finch males. *Animal Behaviour* **76**:1735–1741. doi:10.1016/j.anbehav.2008.08.009

Borst A, Theunissen FE. 1999. Information theory and neural coding. *Nat Neurosci* **2**:947–957. doi:10.1038/14731

Bottjer SW. 2005. Silent synapses in a thalamo-cortical circuit necessary for song learning in zebra finches. *J Neurophysiol* **94**:3698–3707. doi:10.1152/jn.00282.2005

Braaten RF, Reynolds K. 1999. Auditory preference for conspecific song in isolation-reared zebra finches. *Animal Behaviour* **58**:105–111. doi:10.1006/anbe.1999.1134

Brager DH, Johnston D. 2007. Plasticity of Intrinsic Excitability during Long-Term Depression Is Mediated through mGluR-Dependent Changes in Ih in Hippocampal CA1 Pyramidal Neurons. *J Neurosci* **27**:13926–13937. doi:10.1523/JNEUROSCI.3520-07.2007

Brainard MS, Doupe AJ. 2013. Translating Birdsong: Songbirds as a Model for Basic and Applied Medical Research. *Annual Review of Neuroscience* **36**:489–517. doi:10.1146/annurev-neuro-060909-152826

Brainard MS, Doupe AJ. 2002. What songbirds teach us about learning. *Nature* **417**:351.

Breton J-D, Stuart GJ. 2009. Loss of sensory input increases the intrinsic excitability of layer 5 pyramidal neurons in rat barrel cortex. *The Journal of Physiology* **587**:5107–5119. doi:10.1113/jphysiol.2009.180943

Brew HM, Hallows JL, Tempel BL. 2003. Hyperexcitability and reduced low threshold potassium currents in auditory neurons of mice lacking the channel subunit Kv1.1. *J Physiol* **548**:1–20. doi:10.1113/jphysiol.2002.035568

Brons JF, Woody CD. 1980. Long-term changes in excitability of cortical neurons after Pavlovian conditioning and extinction. *J Neurophysiol* **44**:605–615. doi:10.1152/jn.1980.44.3.605

Bryan Kolb, Ian Q. Whishaw. n.d. An Introduction to Brain and Behavior, 2nd ed. Worth Publishers.

Bustin SA. 2000. Absolute quantification of mRNA using real-time reverse transcription polymerase chain reaction assays. *J Mol Endocrinol* **25**:169–193.

Butler AB, Reiner A, Karten HJ. 2011. Evolution of the amniote pallium and the origins of mammalian neocortex: Butler et al. *Annals of the New York Academy of Sciences* **1225**:14–27. doi:10.1111/j.1749-6632.2011.06006.x

Calabrese A, Woolley SMN. 2015. Coding principles of the canonical cortical microcircuit in the avian brain. *Proceedings of the National Academy of Sciences* **112**:3517–3522. doi:10.1073/pnas.1408545112

Campbell DLM, Hauber ME. 2009. Cross-fostering diminishes song discrimination in zebra finches (Taeniopygia guttata). *Anim Cogn* **12**:481–490. doi:10.1007/s10071-008-0209-5

Caras ML, O'Brien M, Brenowitz EA, Rubel EW. 2012. Estradiol Selectively Enhances Auditory Function in Avian Forebrain Neurons. *J Neurosci* **32**:17597–17611. doi:10.1523/JNEUROSCI.3938-12.2012

Carr CE, Iyer S, Soares D, Kalluri S, Simon JZ. 2006. Are Neurons Adapted for Specific Computations? Examples from Temporal Coding in the Auditory System. Oxford University Press.

Carr CE, Soares D. 2002. Evolutionary Convergence and Shared Computational Principles in the Auditory System. *BBE* **59**:294–311. doi:10.1159/000063565

Carroll BJ, Bertram R, Hyson RL. 2018. Intrinsic physiology of inhibitory neurons changes over auditory development. *J Neurophysiol* **119**:290–304. doi:10.1152/jn.00447.2017

Centanni TM, Booker AB, Sloan AM, Chen F, Maher BJ, Carraway RS, Khodaparast N, Rennaker R, LoTurco JJ, Kilgard MP. 2014. Knockdown of the dyslexia-associated gene Kiaa0319 impairs temporal responses to speech stimuli in rat primary auditory cortex. *Cereb Cortex* **24**:1753–1766. doi:10.1093/cercor/bht028

Chen AN, Meliza CD. 2017. Phasic and Tonic Cell Types in the Zebra Finch Auditory Caudal Mesopallium. *J Neurophysiol*. doi:10.1152/jn.00694.2017

Chen Y, Clark O, Woolley SC. 2017. Courtship song preferences in female zebra finches are shaped by developmental auditory experience. *Proc R Soc B* **284**:20170054. doi:10.1098/rspb.2017.0054

Chen Y, Matheson LE, Sakata JT. 2016. Mechanisms underlying the social enhancement of vocal learning in songbirds. *PNAS* **113**:6641–6646. doi:10.1073/pnas.1522306113

Clopton BM, Winfield JA. 1976. Effect of early exposure to patterned sound on unit activity in rat inferior colliculus. *J Neurophysiol* **39**:1081–1089. doi:10.1152/jn.1976.39.5.1081

Coetzee WA, Amarillo Y, Chiu J, Chow A, Lau D, McCORMACK TOM, Morena H, Nadal MS, Ozaita A, Pountney D, Saganich M, Miera EV-SD, Rudy B. 1999. Molecular Diversity of K+ Channels. *Annals of the New York Academy of Sciences* **868**:233–255. doi:10.1111/j.1749-6632.1999.tb11293.x

Coulter DA, Lo Turco JJ, Kubota M, Disterhoft JF, Moore JW, Alkon DL. 1989. Classical conditioning reduces amplitude and duration of calcium-dependent afterhyperpolarization in rabbit hippocampal pyramidal cells. *J Neurophysiol* **61**:971–981. doi:10.1152/jn.1989.61.5.971

Cousillas H, George I, Henry L, Richard J-P, Hausberger M. 2008. Linking Social and Vocal Brains: Could Social Segregation Prevent a Proper Development of a Central Auditory Area in a Female Songbird? *PLOS ONE* **3**:e2194. doi:10.1371/journal.pone.0002194

Cousillas H, Richard J-P, Mathelier M, Henry L, George I, Hausberger M. 2004. Experience-dependent neuronal specialization and functional organization in the central auditory area of a songbird. *European Journal of Neuroscience* **19**:3343–3352. doi:10.1111/j.0953-816X.2004.03376.x

Dagostin AA, Lovell PV, Hilscher MM, Mello CV, Leão RM. 2015. Control of Phasic Firing by a Background Leak Current in Avian Forebrain Auditory Neurons. *Front Cell Neurosci* **9**:471. doi:10.3389/fncel.2015.00471

Daou A, Ross MT, Johnson F, Hyson RL, Bertram R. 2013. Electrophysiological characterization and computational models of HVC neurons in the zebra finch. *Journal of Neurophysiology* **110**:1227–1245. doi:10.1152/jn.00162.2013

de Jonge MC, Black J, Deyo RA, Disterhoft JF. 1990. Learning-induced afterhyperpolarization reductions in hippocampus are specific for cell type and potassium conductance. *Exp Brain Res* **80**:456–462.

de Villers-Sidani E, Merzenich MM. 2011. Lifelong plasticity in the rat auditory cortex: basic mechanisms and role of sensory experience. *Prog Brain Res* **191**:119–131. doi:10.1016/B978-0-444-53752-2.00009-6

Dehorter N, Ciceri G, Bartolini G, Lim L, del Pino I, Marín O. 2015. Tuning of fast-spiking interneuron properties by an activity-dependent transcriptional switch. *Science* **349**:1216–1220. doi:10.1126/science.aab3415

Desai NS, Rutherford LC, Turrigiano GG. 1999. Plasticity in the intrinsic excitability of cortical pyramidal neurons. *Nature Neuroscience* **2**:515–520. doi:10.1038/9165

Disterhoft JF, Coulter DA, Alkon DL. 1986. Conditioning-specific membrane changes of rabbit hippocampal neurons measured in vitro. *Proc Natl Acad Sci USA* **83**:2733–2737.

Disterhoft JF, Oh MM. 2007. Alterations in intrinsic neuronal excitability during normal aging. *Aging Cell* **6**:327–336. doi:10.1111/j.1474-9726.2007.00297.x

Douglas RJ, Martin KAC. 2004. NEURONAL CIRCUITS OF THE NEOCORTEX. *Annual Review of Neuroscience* **27**:419–451. doi:10.1146/annurev.neuro.27.070203.144152

Doupe AJ, Kuhl PK. 1999. Birdsong and human speech: common themes and mechanisms. *Annual review of neuroscience* **22**:567–631.

Dugas-Ford J, Ragsdale CW. 2015. Levels of homology and the problem of neocortex. *Annu Rev Neurosci* **38**:351–368. doi:10.1146/annurev-neuro-071714-033911

Dugas-Ford J, Rowell JJ, Ragsdale CW. 2012. Cell-type homologies and the origins of the neocortex. *Proceedings of the National Academy of Sciences* **109**:16974–16979. doi:10.1073/pnas.1204773109

Dunning JL, Maze SE, Atwood EJ, Prather JF. n.d. Caudal mesopallial neurons in female songbirds bridge sensory and motor brain regions. *Journal of Comparative Neurology* **0**. doi:10.1002/cne.24440

Dutar P, Vu HM, Perkel DJ. 1998. Multiple cell types distinguished by physiological, pharmacological, and anatomic properties in nucleus HVc of the adult zebra finch. *J Neurophysiol* **80**:1828–1838. doi:10.1152/jn.1998.80.4.1828

Elie JE, Theunissen FE. 2016. The vocal repertoire of the domesticated zebra finch: a data-driven approach to decipher the information-bearing acoustic features of communication signals. *Animal Cognition* **19**:285–315. doi:10.1007/s10071-015-0933-6

Erisir A, Lau D, Rudy B, Leonard CS. 1999. Function of specific K(+) channels in sustained high-frequency firing of fast-spiking neocortical interneurons. *J Neurophysiol* **82**:2476–2489. doi:10.1152/jn.1999.82.5.2476

Fan Y, Fricker D, Brager DH, Chen X, Lu H-C, Chitwood RA, Johnston D. 2005. Activity-dependent decrease of excitability in rat hippocampal neurons through increases in I_h. *Nature Neuroscience* **8**:1542–1551. doi:10.1038/nn1568

Farine DR, Spencer KA, Boogert NJ. 2015. Early-Life Stress Triggers Juvenile Zebra Finches to Switch Social Learning Strategies. *Current Biology* **25**:2184–2188. doi:10.1016/j.cub.2015.06.071

Fortune ES, Margoliash D. 1992. Cytoarchitectonic organization and morphology of cells of the field L complex in male zebra finches (Taenopygia guttata). *Journal of Comparative Neurology* **325**:388–404.

Fox K, Wong ROL. 2005. A Comparison of Experience-Dependent Plasticity in the Visual and Somatosensory Systems. *Neuron* **48**:465–477. doi:10.1016/j.neuron.2005.10.013

Freedman DJ. 2005. Experience-Dependent Sharpening of Visual Shape Selectivity in Inferior Temporal Cortex. *Cerebral Cortex* **16**:1631–1644. doi:10.1093/cercor/bhj100

Fu M, Zuo Y. 2011. Experience-dependent Structural Plasticity in the Cortex. *Trends Neurosci* **34**:177–187. doi:10.1016/j.tins.2011.02.001

Gai Y, Doiron B, Rinzel J. 2010. Slope-based stochastic resonance: how noise enables phasic neurons to encode slow signals. *PLoS Comput Biol* **6**:e1000825. doi:10.1371/journal.pcbi.1000825

Gainutdinov KL, Andrianov VV, Gainutdinova TK, Tarasova EA. 2000. The electrical characteristics of command and motor neurons during acquisition of a conditioned defensive reflex and formation of long-term sensitization in snails. *Neurosci Behav Physiol* **30**:81–88.

Gainutdinov KL, Chekmarev LJ, Gainutdinova TH. 1998. Excitability increase in withdrawal interneurons after conditioning in snail. *Neuroreport* **9**:517–520.

Gao E, Suga N. 2000. Experience-dependent plasticity in the auditory cortex and the inferior colliculus of bats: Role of the corticofugal system. *PNAS* **97**:8081–8086. doi:10.1073/pnas.97.14.8081

Ge R, Chen N, Wang J-H. 2009. Real-time neuronal homeostasis by coordinating VGSC intrinsic properties. *Biochemical and Biophysical Research Communications* **387**:585–589. doi:10.1016/j.bbrc.2009.07.066

Gentner TQ, Hulse SH, Ball GF. 2004. Functional differences in forebrain auditory regions during learned vocal recognition in songbirds. *Journal of Comparative Physiology* A **190**:1001–1010. doi:10.1007/s00359-004-0556-x

Gentner TQ, Margoliash D. 2003. Neuronal populations and single cells representing learned auditory objects. *Nature* **424**:669.

George I, Alcaix S, Henry L, Richard J-P, Cousillas H, Hausberger M. 2010. Neural Correlates of Experience-Induced Deficits in Learned Vocal Communication. *PLoS ONE* **5**:e14347. doi:10.1371/journal.pone.0014347

Gobes SMH, Jennings RB, Maeda RK. 2017. The sensitive period for auditory-vocal learning in the zebra finch: Consequences of limited-model availability and multiple-tutor paradigms on song imitation. *Behavioural Processes*. doi:10.1016/j.beproc.2017.07.007

Gray CM, McCormick DA. 1996. Chattering cells: superficial pyramidal neurons contributing to the generation of synchronous oscillations in the visual cortex. *Science* **274**:109–113.

Grosse G, Draguhn A, Höhne L, Tapp R, Veh RW, Ahnert-Hilger G. 2000. Expression of Kv1 potassium channels in mouse hippocampal primary cultures: development and activity-dependent regulation. *Journal of Neuroscience* **20**:1869–1882.

Guan D, Lee JCF, Higgs MH, Spain WJ, Foehring RC. 2007. Functional roles of Kv1 channels in neocortical pyramidal neurons. *J Neurophysiol* **97**:1931–1940. doi:10.1152/jn.00933.2006

Haedo RJ, Golowasch J. 2006. Ionic Mechanism Underlying Recovery of Rhythmic Activity in Adult Isolated Neurons. *Journal of Neurophysiology* **96**:1860–1876. doi:10.1152/jn.00385.2006

Hammerschmidt K, Schreiweis C, Minge C, Pääbo S, Fischer J, Enard W. 2015. A humanized version of Foxp2 does not affect ultrasonic vocalization in adult mice. *Genes, Brain and Behavior* **14**:583–590. doi:10.1111/gbb.12237

Harris KD, Mrsic-Flogel TD. 2013. Cortical connectivity and sensory coding. *Nature* **503**:51–58. doi:10.1038/nature12654

Harris KD, Shepherd GMG. 2015. The neocortical circuit: themes and variations. *Nature Neuroscience* **18**:170–181. doi:10.1038/nn.3917

Harvey AL. 2001. Twenty years of dendrotoxins. *Toxicon* **39**:15–26.

Harvey AL. 1997. Recent studies on dendrotoxins and potassium ion channels. *General Pharmacology: The Vascular System* **28**:7–12. doi:10.1016/S0306-3623(96)00173-5

Hauber ME, Campbell DLM, Woolley SMN. 2010. The functional role and female perception of male song in Zebra Finches. *Emu - Austral Ornithology* **110**:209–218. doi:10.1071/MU10003

Hauber ME, Woolley SMN, Cassey P, Theunissen FE. 2013. Experience dependence of neural responses to different classes of male songs in

the primary auditory forebrain of female songbirds. *Behavioural Brain Research* **243**:184–190. doi:10.1016/j.bbr.2013.01.007

Heil P, Scheich H. 1991. Functional organization of the avian auditory cortex analogue. I. Topographic representation of isointensity bandwidth. *Brain research* **539**:110–120.

Heston JB, White SA. 2017. To transduce a zebra finch: interrogating behavioral mechanisms in a model system for speech. *J Comp Physiol A Neuroethol Sens Neural Behav Physiol* **203**:691–706. doi:10.1007/s00359-017-1153-0

Hisey E, Kearney MG, Mooney R. 2018. A common neural circuit mechanism for internally guided and externally reinforced forms of motor learning. *Nature Neuroscience* **21**:589–597. doi:10.1038/s41593-018-0092-6

Hölscher C. 1999. Synaptic plasticity and learning and memory: LTP and beyond. *Journal of Neuroscience Research* **58**:62–75. doi:10.1002/(SICI)1097-4547(19991001)58:1<62::AID-JNR7>3.0.CO;2-G

Holt GR, Softky WR, Koch C, Douglas RJ. 1996. Comparison of discharge variability in vitro and in vivo in cat visual cortex neurons. *J Neurophysiol* **75**:1806–1814. doi:10.1152/jn.1996.75.5.1806

Holtmaat A, Svoboda K. 2009. Experience-dependent structural synaptic plasticity in the mammalian brain. *Nature Reviews Neuroscience* **10**:647–658. doi:10.1038/nrn2699

Huggenberger S, Vater M, Deisz RA. 2009. Interlaminar differences of intrinsic properties of pyramidal neurons in the auditory cortex of mice. *Cereb Cortex* **19**:1008–1018. doi:10.1093/cercor/bhn143

Huguet G, Meng X, Rinzel J. 2017. Phasic Firing and Coincidence Detection by Subthreshold Negative Feedback: Divisive or Subtractive or, Better, Both. *Front Comput Neurosci* **11**. doi:10.3389/fncom.2017.00003

Iwasaki S, Chihara Y, Komuta Y, Ito K, Sahara Y. 2008. Low-Voltage-Activated Potassium Channels Underlie the Regulation of Intrinsic Firing Properties of Rat Vestibular Ganglion Cells. *Journal of Neurophysiology* **100**:2192–2204. doi:10.1152/jn.01240.2007

Iwasaki S, Nakajima T, Chihara Y, Inoue A, Fujimoto C, Yamasoba T. 2012. Developmental changes in the expression of Kv1 potassium channels in rat vestibular ganglion cells. *Brain Research* **1429**:29–35. doi:10.1016/j.brainres.2011.10.015

Iyengar S, Bottjer SW. 2002. The Role of Auditory Experience in the Formation of Neural Circuits Underlying Vocal Learning in Zebra

Finches. *J Neurosci* **22**:946–958. doi:10.1523/JNEUROSCI.22-03-00946.2002

Janata P, Margoliash D. 1999. Gradual Emergence of Song Selectivity in Sensorimotor Structures of the Male Zebra Finch Song System. *The Journal of Neuroscience* **19**:5108–5118. doi:10.1523/JNEUROSCI.19-12-05108.1999

Jarvis ED, Scharff C, Grossman MR, Ramos JA, Nottebohm F. 1998. For Whom The Bird Sings: Context-Dependent Gene Expression. *Neuron* **21**:775–788. doi:10.1016/S0896-6273(00)80594-2

Jarvis ED, Yu J, Rivas MV, Horita H, Feenders G, Whitney O, Jarvis SC, Jarvis ER, Kubikova L, Puck AEP, Siang-Bakshi C, Martin S, McElroy M, Hara E, Howard J, Pfenning A, Mouritsen H, Chen C-C, Wada K. 2013. Global view of the functional molecular organization of the avian cerebrum: mirror images and functional columns. *J Comp Neurol* **521**:3614–3665. doi:10.1002/cne.23404

Jeanne JM, Thompson JV, Sharpee TO, Gentner TQ. 2011. Emergence of Learned Categorical Representations within an Auditory Forebrain Circuit. *Journal of Neuroscience* **31**:2595–2606. doi:10.1523/JNEUROSCI.3930-10.2011

Jentsch TJ. 2000. Neuronal KCNQ potassium channels: physiology and role in disease. *Nat Rev Neurosci* **1**:21–30. doi:10.1038/35036198

Johansson F, Jirenhed D-A, Rasmussen A, Zucca R, Hesslow G. 2014. Memory trace and timing mechanism localized to cerebellar Purkinje cells. *PNAS* **111**:14930–14934. doi:10.1073/pnas.1415371111

Jung S-C, Hoffman DA. 2009. Biphasic Somatic A-Type K+ Channel Downregulation Mediates Intrinsic Plasticity in Hippocampal CA1 Pyramidal Neurons. *PLOS ONE* **4**:e6549. doi:10.1371/journal.pone.0006549

Karcz A, Rübsamen R, Kopp-Scheinpflug C. 2012. Low-threshold potassium currents stabilize IID-sensitivity in the inferior colliculus. *Front Neural Circuits* **6**. doi:10.3389/fncir.2012.00060

Karmarkar UR, Buonomano DV. 2006. Different forms of homeostatic plasticity are engaged with distinct temporal profiles. *European Journal of Neuroscience* **23**:1575–1584. doi:10.1111/j.1460-9568.2006.04692.x

Karten HJ. 1967. The organization of the ascending auditory pathway in the pigeon (Columba livia) I. Diencephalic projections of the inferior

colliculus (nucleus mesencephali lateralis, pars dorsalis). *Brain Research* **6**:409–427. doi:10.1016/0006-8993(67)90055-8

Katz LC, Shatz CJ. 1996. Synaptic Activity and the Construction of Cortical Circuits. *Science* **274**:1133–1138. doi:10.1126/science.274.5290.1133

Kelly TK, Ahmadiantehrani S, Blattler A, London SE. 2018. Epigenetic regulation of transcriptional plasticity associated with developmental song learning. *Proc R Soc B* **285**:20180160. doi:10.1098/rspb.2018.0160

Khurana S, Remme MWH, Rinzel J, Golding NL. 2011. Dynamic interaction of Ih and IK-LVA during trains of synaptic potentials in principal neurons of the medial superior olive. *J Neurosci* **31**:8936–8947. doi:10.1523/JNEUROSCI.1079-11.2011

Kim G, Doupe A. 2011. Organized Representation of Spectrotemporal Features in Songbird Auditory Forebrain. *Journal of Neuroscience* **31**:16977–16990. doi:10.1523/JNEUROSCI.2003-11.2011

Kim H, Bao S. 2013. Experience-dependent overrepresentation of ultrasonic vocalization frequencies in the rat primary auditory cortex. *Journal of Neurophysiology* **110**:1087–1096. doi:10.1152/jn.00230.2013

Kim H, Bao S. 2009. Selective Increase in Representations of Sounds Repeated at an Ethological Rate. *J Neurosci* **29**:5163–5169. doi:10.1523/JNEUROSCI.0365-09.2009

Klug A, Bauer EE, Hanson JT, Hurley L, Meitzen J, Pollak GD. 2002. Response Selectivity for Species-Specific Calls in the Inferior Colliculus of Mexican Free-Tailed Bats is Generated by Inhibition. *Journal of Neurophysiology* **88**:1941–1954. doi:10.1152/jn.2002.88.4.1941

Kobatake E, Wang G, Tanaka K. 1998. Effects of Shape-Discrimination Training on the Selectivity of Inferotemporal Cells in Adult Monkeys. *Journal of Neurophysiology* **80**:324–330. doi:10.1152/jn.1998.80.1.324

Konishi M. 1973. How the Owl Tracks Its Prey: Experiments with trained barn owls reveal how their acute sense of hearing enables them to catch prey in the dark. *American Scientist* **61**:414–424.

Kotak VC, Fujisawa S, Lee FA, Karthikeyan O, Aoki C, Sanes DH. 2005. Hearing Loss Raises Excitability in the Auditory Cortex. *J Neurosci* **25**:3908–3918. doi:10.1523/JNEUROSCI.5169-04.2005

Lauay C, Gerlach NM, Adkins-Regan E, DeVoogd TJ. 2004. Female zebra finches require early song exposure to prefer high-quality song as adults. *Animal Behaviour* **68**:1249–1255. doi:10.1016/j.anbehav.2003.12.025

Le Vay S, Wiesel TN, Hubel DH. 1980. The development of ocular dominance columns in normal and visually deprived monkeys. *Journal of Comparative Neurology* **191**:1–51. doi:10.1002/cne.901910102

Levelt CN, Hübener M. 2012. Critical-Period Plasticity in the Visual Cortex. *Annual Review of Neuroscience* **35**:309–330. doi:10.1146/annurev-neuro-061010-113813

Li L, Ji X, Liang F, Li Y, Xiao Z, Tao HW, Zhang LI. 2014. A Feedforward Inhibitory Circuit Mediates Lateral Refinement of Sensory Representation in Upper Layer 2/3 of Mouse Primary Auditory Cortex. *The Journal of Neuroscience* **34**:13670–13683. doi:10.1523/JNEUROSCI.1516-14.2014

Li X, Yu K, Zhang Z, Sun W, Yang Z, Feng J, Chen X, Liu C-H, Wang H, Guo YP, He J. 2014. Cholecystokinin from the entorhinal cortex enables neural plasticity in the auditory cortex. *Cell Research* **24**:307–330. doi:10.1038/cr.2013.164

Lim Y, Lagoy R, Shinn-Cunningham BG, Gardner TJ. 2016. Transformation of temporal sequences in the zebra finch auditory system. *eLife* **5**:e18205. doi:10.7554/eLife.18205

Llinás RR. 1988. The intrinsic electrophysiological properties of mammalian neurons: insights into central nervous system function. *Science* **242**:1654–1664.

Locke RE, Nerbonne JM. 1997. Role of voltage-gated K+ currents in mediating the regular-spiking phenotype of callosal-projecting rat visual cortical neurons. *J Neurophysiol* **78**:2321–2335. doi:10.1152/jn.1997.78.5.2321

London SE. 2017. Developmental song learning as a model to understand neural mechanisms that limit and promote the ability to learn. *Behavioural Processes*. doi:10.1016/j.beproc.2017.11.008

Lu K, Vicario DS. 2014. Statistical learning of recurring sound patterns encodes auditory objects in songbird forebrain. *Proceedings of the National Academy of Sciences* **111**:14553–14558. doi:10.1073/pnas.1412109111

Maffei A, Nelson SB, Turrigiano GG. 2004. Selective reconfiguration of layer 4 visual cortical circuitry by visual deprivation. *Nature Neuroscience* **7**:1353–1359. doi:10.1038/nn1351

Manis PB, Marx SO. 1991. Outward currents in isolated ventral cochlear nucleus neurons. *J Neurosci* **11**:2865–2880.

Maravall M, Stern EA, Svoboda K. 2004. Development of Intrinsic Properties and Excitability of Layer 2/3 Pyramidal Neurons During a Critical

Period for Sensory Maps in Rat Barrel Cortex. *Journal of Neurophysiology* **92**:144–156. doi:10.1152/jn.00598.2003

Marler P, Peters S. 1977. Selective vocal learning in a sparrow. *Science* **198**:519–521. doi:10.1126/science.198.4316.519

Marsh RA, Nataraj K, Gans D, Portfors CV, Wenstrup JJ. 2006. Auditory Responses in the Cochlear Nucleus of Awake Mustached Bats: Precursors to Spectral Integration in the Auditory Midbrain. *Journal of Neurophysiology* **95**:88–105. doi:10.1152/jn.00634.2005

Martina M, Schultz JH, Ehmke H, Monyer H, Jonas P. 1998. Functional and molecular differences between voltage-gated K+ channels of fast-spiking interneurons and pyramidal neurons of rat hippocampus. *J Neurosci* **18**:8111–8125.

Maul KK, Voss HU, Parra LC, Salgado-Commissariat D, Ballon D, Tchernichovski O, Helekar SA. 2009. The development of stimulus-specific auditory responses requires song exposure in male but not female zebra finches. *Developmental Neurobiology* NA-NA. doi:10.1002/dneu.20751

Mayko ZM, Roberts PD, Portfors CV. 2012. Inhibition shapes selectivity to vocalizations in the inferior colliculus of awake mice. *Frontiers in Neural Circuits* **6**. doi:10.3389/fncir.2012.00073

McCormick DA, Connors BW, Lighthall JW, Prince DA. 1985. Comparative electrophysiology of pyramidal and sparsely spiny stellate neurons of the neocortex. *J Neurophysiol* **54**:782–806. doi:10.1152/jn.1985.54.4.782

Medini P. 2014. Experience-dependent plasticity of visual cortical microcircuits. *Neuroscience* **278**:367–384. doi:10.1016/j.neuroscience.2014.08.022

Meliza CD, Chi Z, Margoliash D. 2010. Representations of Conspecific Song by Starling Secondary Forebrain Auditory Neurons: Toward a Hierarchical Framework. *Journal of Neurophysiology* **103**:1195–1208. doi:10.1152/jn.00464.2009

Meliza CD, Margoliash D. 2012. Emergence of Selectivity and Tolerance in the Avian Auditory Cortex. *Journal of Neuroscience* **32**:15158–15168. doi:10.1523/JNEUROSCI.0845-12.2012

Metherate R, Aramakis VB. 1999. Intrinsic electrophysiology of neurons in thalamorecipient layers of developing rat auditory cortex. *Developmental Brain Research* **115**:131–144. doi:10.1016/S0165-3806(99)00058-9

Mori C, Wada K. 2015. Songbird: a unique animal model for studying the molecular basis of disorders of vocal development and communication. *Exp Anim* **64**:221–230. doi:10.1538/expanim.15-0008

Morrison RG, Nottebohm F. 1993. Role of a telencephalic nucleus in the delayed song learning of socially isolated zebra finches. *J Neurobiol* **24**:1045–1064. doi:10.1002/neu.480240805

Mowery TM, Kotak VC, Sanes DH. 2015. Transient Hearing Loss Within a Critical Period Causes Persistent Changes to Cellular Properties in Adult Auditory Cortex. *Cereb Cortex* **25**:2083–2094. doi:10.1093/cercor/bhu013

Mozzachiodi R, Byrne JH. 2010. More than synaptic plasticity: role of nonsynaptic plasticity in learning and memory. *Trends in Neurosciences* **33**:17–26. doi:10.1016/j.tins.2009.10.001

Oertel D. 1999. The Role of Timing in the Brain Stem Auditory Nuclei of Vertebrates. *Annual Review of Physiology* **61**:497–519. doi:10.1146/annurev.physiol.61.1.497

Olias P, Adam I, Meyer A, Scharff C, Gruber AD. 2014. Reference Genes for Quantitative Gene Expression Studies in Multiple Avian Species. *PLoS ONE* **9**:e99678. doi:10.1371/journal.pone.0099678

Olkowicz S, Kocourek M, Lučan RK, Porteš M, Fitch WT, Herculano-Houzel S, Němec P. 2016. Birds have primate-like numbers of neurons in the forebrain. *Proc Natl Acad Sci USA* **113**:7255–7260. doi:10.1073/pnas.1517131113

Oswald A-MM, Reyes AD. 2008. Maturation of Intrinsic and Synaptic Properties of Layer 2/3 Pyramidal Neurons in Mouse Auditory Cortex. *Journal of Neurophysiology* **99**:2998–3008. doi:10.1152/jn.01160.2007

Padmanabhan K, Urban NN. 2010. Intrinsic biophysical diversity decorrelates neuronal firing while increasing information content. *Nat Neurosci* **13**:1276–1282. doi:10.1038/nn.2630

Pathak D, Guan D, Foehring RC. 2016. Roles of specific K_v channel types in repolarization of the action potential in genetically identified subclasses of pyramidal neurons in mouse neocortex. *Journal of Neurophysiology* **115**:2317–2329. doi:10.1152/jn.01028.2015

Paz JT, Mahon S, Tiret P, Genet S, Delord B, Charpier S. 2009. Multiple forms of activity-dependent intrinsic plasticity in layer V cortical neurones in vivo. *The Journal of Physiology* **587**:3189–3205. doi:10.1113/jphysiol.2009.169334

Perks KE, Gentner TQ. 2015. Subthreshold membrane responses underlying sparse spiking to natural vocal signals in auditory cortex. *Eur J Neurosci* **41**:725–733. doi:10.1111/ejn.12831

Peruzzi D, Sivaramakrishnan S, Oliver DL. 2000. Identification of cell types in brain slices of the inferior colliculus. *Neuroscience* **101**:403–416.

Pollak GD, Burger RM, Klug A. 2003. Dissecting the circuitry of the auditory system. *Trends in Neurosciences* **26**:33–39. doi:10.1016/S0166-2236(02)00009-7

Poon PWF, Chen X. 1992. Postnatal exposure to tones alters the tuning characteristics of inferior collicular neurons in the rat. *Brain Research* **585**:391–394. doi:10.1016/0006-8993(92)91243-8

Power JM, Wu WW, Sametsky E, Oh MM, Disterhoft JF. 2002. Age-related enhancement of the slow outward calcium-activated potassium current in hippocampal CA1 pyramidal neurons in vitro. *J Neurosci* **22**:7234–7243. doi:20026641

Prather JF. 2013. Auditory signal processing in communication: Perception and performance of vocal sounds. *Hearing Research* **305**:144–155. doi:10.1016/j.heares.2013.06.007

Prescott SA, De Koninck Y, Sejnowski TJ. 2008. Biophysical basis for three distinct dynamical mechanisms of action potential initiation. *PLoS Comput Biol* **4**:e1000198. doi:10.1371/journal.pcbi.1000198

Prinz AA, Bucher D, Marder E. 2004. Similar network activity from disparate circuit parameters. *Nat Neurosci* **7**:1345–1352. doi:10.1038/nn1352

Pytte CL, Parent C, Wildstein S, Varghese C, Oberlander S. 2010. Deafening decreases neuronal incorporation in the zebra finch caudomedial nidopallium (NCM). *Behavioural Brain Research* **211**:141–147. doi:10.1016/j.bbr.2010.03.029

Rao D, Basura GJ, Roche J, Daniels S, Mancilla JG, Manis PB. 2010. Hearing Loss Alters Serotonergic Modulation of Intrinsic Excitability in Auditory Cortex. *Journal of Neurophysiology* **104**:2693–2703. doi:10.1152/jn.01092.2009

Rathouz M, Trussell L. 1998. Characterization of outward currents in neurons of the avian nucleus magnocellularis. *J Neurophysiol* **80**:2824–2835. doi:10.1152/jn.1998.80.6.2824

Rauschecker JP. 1999. Auditory cortical plasticity: a comparison with other sensory systems. *Trends in Neurosciences* **22**:74–80. doi:10.1016/S0166-2236(98)01303-4

Reiner A, Perkel DJ, Mello CV, Jarvis ED. 2004. Songbirds and the Revised Avian Brain Nomenclature. *Annals of the New York Academy of Sciences* **1016**:77–108. doi:10.1196/annals.1298.013

Reyes AD, Rubel EW, Spain WJ. 1994. Membrane properties underlying the firing of neurons in the avian cochlear nucleus. *J Neurosci* **14**:5352–5364.

Riebel K, Smallegange IM, Terpstra NJ, Bolhuis JJ. 2002. Sexual equality in zebra finch song preference: evidence for a dissociation between song recognition and production learning. *Proceedings of the Royal Society of London B: Biological Sciences* **269**:729–733. doi:10.1098/rspb.2001.1930

Roberts TF, Hisey E, Tanaka M, Kearney MG, Chattree G, Yang CF, Shah NM, Mooney R. 2017. Identification of a motor-to-auditory pathway important for vocal learning. *Nature Neuroscience* **20**:978–986. doi:10.1038/nn.4563

Ross MT, Flores D, Bertram R, Johnson F, Hyson RL. 2017. Neuronal Intrinsic Physiology Changes During Development of a Learned Behavior. *eNeuro* **4**. doi:10.1523/ENEURO.0297-17.2017

Rothman JS, Manis PB. 2003a. Differential Expression of Three Distinct Potassium Currents in the Ventral Cochlear Nucleus. *Journal of Neurophysiology* **89**:3070–3082. doi:10.1152/jn.00125.2002

Rothman JS, Manis PB. 2003b. The Roles Potassium Currents Play in Regulating the Electrical Activity of Ventral Cochlear Nucleus Neurons. *Journal of Neurophysiology* **89**:3097–3113. doi:10.1152/jn.00127.2002

Saar D, Grossman Y, Barkai E. 2001. Long-lasting cholinergic modulation underlies rule learning in rats. *J Neurosci* **21**:1385–1392.

Saar D, Grossman Y, Barkai E. 1998. Reduced after-hyperpolarization in rat piriform cortex pyramidal neurons is associated with increased learning capability during operant conditioning. *Eur J Neurosci* **10**:1518–1523.

Sanchez-Andres JV, Alkon DL. 1991. Voltage-clamp analysis of the effects of classical conditioning on the hippocampus. *J Neurophysiol* **65**:796–807. doi:10.1152/jn.1991.65.4.796

Sanes DH, Constantine-Paton M. 1983. Altered activity patterns during development reduce neural tuning. *Science* **221**:1183–1185.

Schneider DM, Woolley SMN. 2011. Extra-Classical Tuning Predicts Stimulus-Dependent Receptive Fields in Auditory Neurons. *Journal of Neuroscience* **31**:11867–11878. doi:10.1523/JNEUROSCI.5790-10.2011

Schneider DM, Woolley SMN. 2010. Discrimination of Communication Vocalizations by Single Neurons and Groups of Neurons in the Auditory Midbrain. *Journal of Neurophysiology* **103**:3248–3265. doi:10.1152/jn.01131.2009

Schulz DJ. 2006. Plasticity and stability in neuronal output via changes in intrinsic excitability: it's what's inside that counts. *Journal of Experimental Biology* **209**:4821–4827. doi:10.1242/jeb.02567

Sen K, Theunissen FE, Doupe AJ. 2001. Feature Analysis of Natural Sounds in the Songbird Auditory Forebrain. *Journal of Neurophysiology* **86**:1445–1458. doi:10.1152/jn.2001.86.3.1445

Seroussi Y, Brosh I, Barkai E. 2002. Learning-induced reduction in post-burst after-hyperpolarization (AHP) is mediated by activation of PKC. *Eur J Neurosci* **16**:965–969.

Sharpee TO, Atencio CA, Schreiner CE. 2011. Hierarchical representations in the auditory cortex. *Current Opinion in Neurobiology* **21**:761–767. doi:10.1016/j.conb.2011.05.027

Shim HG, Lee Y-S, Kim SJ. 2018. The Emerging Concept of Intrinsic Plasticity: Activity-dependent Modulation of Intrinsic Excitability in Cerebellar Purkinje Cells and Motor Learning. *Exp Neurobiol* **27**:139–154. doi:10.5607/en.2018.27.3.139

Singh NC, Theunissen FE. 2003. Modulation spectra of natural sounds and ethological theories of auditory processing. *J Acoust Soc Am* **114**:3394–3411.

Sivaramakrishnan S, Oliver DL. 2001. Distinct K currents result in physiologically distinct cell types in the inferior colliculus of the rat. *J Neurosci* **21**:2861–2877.

Soares D, Chitwood RA, Hyson RL, Carr CE. 2002. Intrinsic Neuronal Properties of the Chick Nucleus Angularis. *Journal of Neurophysiology* **88**:152–162. doi:10.1152/jn.2002.88.1.152

Sturdy CB, Phillmore LS, Sartor JJ, Weisman RG. 2001. Reduced social contact causes auditory perceptual deficits in zebra finches, Taeniopygia guttata. *Animal Behaviour* **62**:1207–1218. doi:10.1006/anbe.2001.1864

Suga N, O'Neill WE, Kujirai K, Manabe T. 1983. Specificity of combination-sensitive neurons for processing of complex biosonar signals in auditory cortex of the mustached bat. *Journal of Neurophysiology* **49**:1573–1626. doi:10.1152/jn.1983.49.6.1573

Sullivan WE, Konishi M. 1984. Segregation of stimulus phase and intensity coding in the cochlear nucleus of the barn owl. *J Neurosci* **4**:1787–1799.

Sun Q-Q. 2009. Experience-Dependent Intrinsic Plasticity in Interneurons of Barrel Cortex Layer IV. *Journal of Neurophysiology* **102**:2955–2973. doi:10.1152/jn.00562.2009

Svirskis G, Kotak V, Sanes DH, Rinzel J. 2004. Sodium Along With Low-Threshold Potassium Currents Enhance Coincidence Detection of Subthreshold Noisy Signals in MSO Neurons. *Journal of Neurophysiology* **91**:2465–2473. doi:10.1152/jn.00717.2003

Tateno T, Harsch A, Robinson HPC. 2004. Threshold firing frequency-current relationships of neurons in rat somatosensory cortex: type 1 and type 2 dynamics. *J Neurophysiol* **92**:2283–2294. doi:10.1152/jn.00109.2004

Tchernichovski O, Lints TJ, Derégnaucourt S, Cimenser A, Mitra PP. 2004. Studying the Song Development Process: Rationale and Methods. *Annals of the New York Academy of Sciences* **1016**:348–363. doi:10.1196/annals.1298.031

Theunissen FE, Amin N, Shaevitz SS, Woolley SMN, Fremouw T, Hauber ME. 2004. Song Selectivity in the Song System and in the Auditory Forebrain. *Annals of the New York Academy of Sciences* **1016**:222–245. doi:10.1196/annals.1298.023

Theunissen FE, Sen K, Doupe AJ. 2000. Spectral-Temporal Receptive Fields of Nonlinear Auditory Neurons Obtained Using Natural Sounds. *The Journal of Neuroscience* **20**:2315–2331. doi:10.1523/JNEUROSCI.20-06-02315.2000

Theunissen FE, Shaevitz SS. 2006. Auditory processing of vocal sounds in birds. *Current Opinion in Neurobiology* **16**:400–407. doi:10.1016/j.conb.2006.07.003

Thompson JV, Gentner TQ. 2010. Song Recognition Learning and Stimulus-Specific Weakening of Neural Responses in the Avian Auditory Forebrain. *Journal of Neurophysiology* **103**:1785–1797. doi:10.1152/jn.00885.2009

Titley HK, Brunel N, Hansel C. 2017. Toward a Neurocentric View of Learning. *Neuron* **95**:19–32. doi:10.1016/j.neuron.2017.05.021

Tucker KR, Huertas MA, Horn JP, Canavier CC, Levitan ES. 2012. Pacemaker rate and depolarization block in nigral dopamine neurons: a somatic sodium channel balancing act. *J Neurosci* **32**:14519–14531. doi:10.1523/JNEUROSCI.1251-12.2012

Turrigiano G. 2011. Too Many Cooks? Intrinsic and Synaptic Homeostatic Mechanisms in Cortical Circuit Refinement. *Annual Review of Neuroscience* **34**:89–103. doi:10.1146/annurev-neuro-060909-153238

Turrigiano GG. 2008. The Self-Tuning Neuron: Synaptic Scaling of Excitatory Synapses. *Cell* **135**:422–435. doi:10.1016/j.cell.2008.10.008

Turrigiano GG. 1999. Homeostatic plasticity in neuronal networks: the more things change, the more they stay the same. *Trends in Neurosciences* **22**:221–227. doi:10.1016/S0166-2236(98)01341-1

Vates GE, Broome BM, Mello CV, Nottebohm F. 1996. Auditory pathways of caudal telencephalon and their relation to the song system of adult male zebra finches (Taenopygia guttata). *Journal of Comparative Neurology* **366**:613–642.

Venkatesan K, Liu Y, Goldfarb M. 2014. Fast-onset long-term open-state block of sodium channels by A-type FHFs mediates classical spike accommodation in hippocampal pyramidal neurons. *J Neurosci* **34**:16126–16139. doi:10.1523/JNEUROSCI.1271-14.2014

Vogel C, Marcotte EM. 2012. Insights into the regulation of protein abundance from proteomic and transcriptomic analyses. *Nature Reviews Genetics* **13**:227–232. doi:10.1038/nrg3185

Walters MJ, Collado D, Harding CF. 1991. Oestrogenic modulation of singing in male zebra finches: differential effects on directed and undirected songs. *Animal Behaviour* **42**:445–452. doi:10.1016/S0003-3472(05)80043-0

Wang X. 2013. The harmonic organization of auditory cortex. *Frontiers in Systems Neuroscience* **7**. doi:10.3389/fnsys.2013.00114

Wang X, Lu T, Bendor D, Bartlett E. 2008. Neural coding of temporal information in auditory thalamus and cortex. *Neuroscience* **157**:484–494.

Wang Y, Brzozowska-Prechtl A, Karten HJ. 2010. Laminar and columnar auditory cortex in avian brain. *Proceedings of the National Academy of Sciences* **107**:12676–12681.

Wiener L. 1986. Song learning in birds: Possible models for human language acquisition. *WORD* **37**:159–175. doi:10.1080/00437956.1986.11435775

Woolley SMN. 2012. Early experience shapes vocal neural coding and perception in songbirds. *Developmental Psychobiology* **54**:612–631. doi:10.1002/dev.21014

Woolley SMN, Fremouw TE, Hsu A, Theunissen FE. 2005. Tuning for spectro-temporal modulations as a mechanism for auditory discrimination of natural sounds. *Nat Neurosci* **8**:1371–1379. doi:10.1038/nn1536

Woolley SMN, Gill PR, Fremouw T, Theunissen FE. 2009. Functional Groups in the Avian Auditory System. *Journal of Neuroscience* **29**:2780–2793. doi:10.1523/JNEUROSCI.2042-08.2009

Woolley SMN, Hauber ME, Theunissen FE. 2010. Developmental experience alters information coding in auditory midbrain and forebrain neurons. *Developmental Neurobiology* **70**:235–252. doi:10.1002/dneu.20783

Woolley SMN, Portfors CV. 2013. Conserved mechanisms of vocalization coding in mammalian and songbird auditory midbrain. *Hearing Research* **305**:45–56. doi:10.1016/j.heares.2013.05.005

Xie R, Meitzen J, Pollak GD. 2005. Differing Roles of Inhibition in Hierarchical Processing of Species-Specific Calls in Auditory Brainstem Nuclei. *Journal of Neurophysiology* **94**:4019–4037. doi:10.1152/jn.00688.2005

Xu H, Kotak VC, Sanes DH. 2007. Conductive Hearing Loss Disrupts Synaptic and Spike Adaptation in Developing Auditory Cortex. *Journal of Neuroscience* **27**:9417–9426. doi:10.1523/JNEUROSCI.1992-07.2007

Yanagihara S, Yazaki-Sugiyama Y. 2018. Social interaction with a tutor modulates responsiveness of specific auditory neurons in juvenile zebra finches. *Behavioural Processes*. doi:10.1016/j.beproc.2018.04.003

Zann R. 1996. The Zebra Finch: A Synthesis of Field and Laboratory Studies. Oxford: Oxford University Press.

Zaretsky MD, Konishi M. 1976. Tonotopic organization in the avian telencephalon. *Brain Research* **111**:167–171. doi:10.1016/0006-8993(76)91058-1

Zebra Finch Expression Brain Atlas. n.d. http://www.zebrafinchatlas.org/

Zhang LI, Bao S, Merzenich MM. 2001. Persistent and specific influences of early acoustic environments on primary auditory cortex. *Nature Neuroscience* **4**:1123–1130. doi:10.1038/nn745

Zhang W, Linden DJ. 2003. The other side of the engram: experience-driven changes in neuronal intrinsic excitability. *Nature Reviews Neuroscience* **4**:885–900. doi:10.1038/nrn1248

Zhao S, Ting JT, Atallah HE, Qiu L, Tan J, Gloss B, Augustine GJ, Deisseroth K, Luo M, Graybiel AM, Feng G. 2011. Cell type–specific channelrhodopsin-2 transgenic mice for optogenetic dissection of neural circuitry function. *Nat Methods* **8**:745–752.

Zhou X, Merzenich MM. 2008. Enduring effects of early structured noise exposure on temporal modulation in the primary auditory cortex. PNAS **105**:4423–4428. doi:10.1073/pnas.0800009105

Zhou X, Nagarajan N, Mossop BJ, Merzenich MM. 2008. Influences of un-modulated acoustic inputs on functional maturation and critical-period plasticity of the primary auditory cortex. *Neuroscience*, From Cochlea to Cortex: Recent Advances in Auditory Neuroscience **154**:390–396. doi:10.1016/j.neuroscience.2008.01.026